Proteomics of early embryonic development of zebrafish (*Danio rerio*)

Purushothaman Kathiresan

FACULTY OF BIOSCIENCES AND AQUACULTURE

NORD
University

www.nord.no

Proteomics of early embryonic development of zebrafish (*Danio rerio*)

Purushothaman Kathiresan

A thesis for the degree of
Philosophiae Doctor (PhD)

PhD in Aquatic Biosciences no. 38 (2021)
Faculty of Biosciences and Aquaculture

Purushothaman Kathiresan
Proteomics of early embryonic development of zebrafish (Danio rerio)

Preface

The thesis is submitted in fulfilment of the requirements for the degree of Philosophiae Doctor (PhD) at the faculty of Biosciences and Aquaculture (FBA), Nord University. The different studies complied in this dissertation are original research performed at Nord University, Bodø and National University of Singapore, Singapore over a period of three years. The studies were funded by the Research Council of Norway, InnControl project (grant #275786) and Nord University scholarship.

The project team consisted of the following members:

Kathiresan Purushothaman, MSc, FBA, Nord University: PhD Student

Prof. Igor Babiak, Professor, FBA, Nord University: primary supervisor

Dr. Lin Qingsong, Senior Research Fellow, DBS, National University of Singapore: co-supervisor

Prof. Steinar Johansen, Professor, FBA, Nord University: co- supervisor

Dr. Christopher Presslauer, Postdoctoral researcher, FBA, Nord University: co- supervisor

Acknowledgement

The 3 years of my PhD has been a memorable and eventful journey. It has put me through still waters and tropical thunderstorms alike. Was it worth? I think it absolutely was. A lot of people deserve to be acknowledged for helping in the successful completion of this thesis.

First and foremost, praises and thanks to the God and my parents, the Almighty, for them showering me with blessings throughout my research work.

I express my sincere gratitude to my main supervisor, Professor Igor Babiak for his continuous support during my PhD study and research. His motivation, enthusiasm, and immense knowledge has guided me during my study period; his guidance helped me in research and writing of research articles and this thesis.

My heartfelt thanks to my co-supervisor Dr. Lin Qingsong, National University of Singapore, who allowed me to work in his lab. His valuable advices and inputs cannot be thanked with words. He has helped me a lot in the preparation of manuscripts and thesis. Also, he taught me modern proteomics technics in his lab.

Gratitude should also be extended to my co-supervisor Professor Steinar Daae Johansen for his valuable suggestions and inputs to make my manuscript and thesis publication ready.

I would like to thank my co-supervisor Dr. Christopher Edward Presslauer, who has supported me during my initial days and for his help in conducting my experiments.

My sincere and humble thanks to Mr. Lim Teck Kwang, National University of Singapore, who helped me to run the experiments. His

support even during the weekends should be praised. He has supported me during my stay in Singapore.

I express my thanks to Dr. Prem Prakash Das, National University of Singapore, for his inputs during analysis and manuscript writing.

I also thank Dr. Terhi Kärpänen who helped me to revise my thesis.

I also thank Dr. Joanna Babiak and Dr. Tor Erik Jørgensen for their kind help during my laboratory works.

I am thankful to all the FBA technical staff for their assistance over the years. In particular, I would thank to Heidi Ludviksen and Cesilie Amundsen for their assistance in the lab and zebrafish facility.

Thank you to all the FBA administrative staff, especially Jarle Jørgensen, Jeanett Stegen, Irene Stork, Ann Merete Sivertsen and Kristine Vevik for their assistance over the years.

My most sincere gratitude to Dr. Shubha Vij, my guiding light and the spark that fuelled my drive. Without your persuasion I would not have taken this PhD journey. My career would have lost this massive leap of progress without your advice, and hence I wish that our collaboration thrives during my future career also. Thank you for all your support and good wishes.

Very few people have the ability to unconditionally support their spouse. Bhuvana Sathya my beloved wife is second to none. She has put up with more adversities and challenges through my PhD study period. Her support has driven me to the successful completion of my PhD. During my long absences she took the total responsibility of the well-being of our children and a lot more that I am probably not even aware of. Words are not enough to express how much I have depended on your unwavering support and unconditional love. I thank you with every fiber of my being - this PhD is

Dedication

I would like to dedicate this dissertation to my family members who were with me whenever I needed them: Kathiresan, Vasanthal, Malaimegu, Ramu, Rajammal (always with your memories), Chettal, Ram Gopal, Nagakanni, Ram Shanmugam, Sundarambal, ASG. Krishnan, ASG. Shanmugam, Prithvirajan, Pandurangan, Devaki, Rengamathi, Raja Kumaran Sethupathi, M. Pictai Manickam, M. Ramakrishnan, Kayalvizhi, ASGK. Sundaraja Pandiyan, ASGS. Parthasarathy, Rathiga, Karunakaran, Bala Kajendran, Shanthini, Nithya (always with us), Jai Megul, Monishka, Neha, Dhanvesh Ram and Velan.

Table of contents

List of figures

List of tables

List of papers

Paper I   **Purushothaman K**, Das PP, Presslauer C, Lim TK, Johansen SD, Lin Q, Babiak I. (2019). Proteomics analysis of early developmental stages of zebrafish embryos. International Journal of Molecular Sciences, 20 (24), 6359.

Paper II   **Purushothaman K**, Das PP, Lim TK, Shijie T, Johansen SD, Lin Q, Babiak I. Vegetal embryonic proteome in cleavage-stage zebrafish. Manuscript.

Paper III   **Purushothaman K**, Das PP, Yeoh SM, Lim TK, Johansen SD, Lin Q, Babiak I. Unravelling the proteome dynamics during the early developmental stages of zebrafish. Manuscript.

List of abbreviations

- 2D-DIGE - two-dimensional difference gel electrophoresis
- 2-DE - two-dimensional gel electrophoresis
- 2D-LC-MS/MS - two-dimensional liquid chromatography coupled to tandem mass spectrometry
- Ago - Argonaute
- AP axis - anterior-posterior axis
- Apo - Apolipoprotein
- AV axis - animal-vegetal axis
- Bb - Balbiani body
- Bmp - Bone morphogenetic protein
- Buc- Bucky ball
- CA - cortical alveoli
- Ca - Calcium
- Cfl1 - Cofilin 1
- Cldnd - Claudin
- Cry - Cryptochromes
- Dazl - Deleted in azoospermia-like
- DDA - data-dependent acquisition
- DEL - deep cell layer
- DIA - data-independent acquisition
- 2D-DIGE - two-dimensional difference gel electrophoresis
- dpf - day post-fertilization
- dph - day post-hatching
- DV axis - dorso-ventral axis
- ec - ectoplasm
- EGT - early gastrula transition
- emPAI - exponentially modified protein abundance index
- en - endoplasm

- EVL - enveloping layer
- eYSL - external yolk syncytial layer
- FFA - free fatty acids
- Fgf - Fibroblast growth factor
- hpf - hours post-fertilization
- Hsp- Heat shock protein
- ICAT - Isotope-coded affinity tags
- Igf2bp3- Insulin-like growth factor-2 mRNA binding proteins 3
- IHC - immunohistochemistry
- iTRAQ - isobaric tags for relative and absolute quantification
- iYSL - internal yolk syncytial layer
- Khdrbs1a - KH domain-containing, RNA-binding, signal transduction-associated 1a
- Krt - Keratin
- LC/MS - liquid chromatography/ mass spectrometry
- LD - lipid droplets
- LV - Lipovitellin
- M phase - mitotic division phase
- m6A - N6-methyladenosine
- Macf1 - Microtubule actin crosslinking factor 1
- MALDI-TOF - matrix-assisted laser desorption/ionization time-of-flight tandem mass spectrometry
- Mapkap2 - Mitogen activated protein kinase activated protein kinase 2
- MBT - mid blastula transition
- miRNA - micro RNA
- MRM - multiple reaction monitoring
- MS - mass spectrometry
- MudPIT - multidimensional protein identification
- MZT - maternal-to-zygotic transition
- ORFs - open reading frames

- PAI - protein abundance index

- Pcg - polycomb group

- PGC - Primordial germ cell

- Plk1 - Polo-like kinase 1

- PV - Phosvitin

- RBPs - RNA-binding proteins

- RP-HPLC - Reverse-phase high-performance liquid chromatography

- S phase - synthesis phase

- SILAC- stable isotopic labelling with amino acids in cell culture

- SMRT-Seq - single-molecule real-time sequencing

- SRM - single reaction monitoring

- SWATH - sequential window acquisition of all theoretical mass spectra

- TGF-β - Transforming growth factor beta

- TMT - tandem mass tag

- Tpp1 - Tripeptidyl-peptidase I

- Vrtn - Vertnin

- Vtg - Vitellogenin

- YCL - yolk cytoplasmic layer

- Yg - Yolk granules

- Ym - Yolk membrane

- YSL - Yolk syncytial layer

- YSN - Yolk syncytial nuclei

- ZGA - Zygotic genome activation

Abstract

Genome and proteome of zebrafish (*Danio rerio*), a freshwater fish, have high similarity to the human genome and proteome, which makes the zebrafish an attractive model to study human biology-related aspects, such as diseases. In addition, due to its quick cell cycle, synchronous embryonic development, high fecundity and embryo transparency, zebrafish is an excellent model for developmental biology studies that aim to disclose mechanisms of maternal regulation of development. This regulation occurs in the earliest stages of development, before an embryo gains control of its own development through transcription of its own genes. The process of shifting the developmental regulation from parentally (mostly, maternally), provided regulatory elements to those embryonic ones, is termed maternal-to-zygotic transition (MZT). In mammals, it starts early in the development, usually with the first cleavage of the zygote. In contrast, MZT in fish occurs much later, after several rounds of cell divisions. Therefore, fish seem to be a good model to study maternal phase of developmental regulation.

There is ample literature on transcriptomics associated with early zebrafish embryonic development, whereas data on the proteome are scarce, especially those linked to the pre-MZT stages. This is due to the high molecular weight of embryonic yolk proteins that masks the presence of low molecular weight proteins. The general objective of this PhD study was to identify and characterize the proteome of zebrafish embryos during early embryonic developmental stages. The specific objectives were: 1) To develop an efficient procedure for reducing the amount of yolk in early zebrafish embryos to enable liquid chromatography mass spectrometry-based proteomics, 2) To identify the proteome of vegetal part of embryos during the early development of zebrafish, 3) To map protein dynamics during early development of zebrafish embryos. The major methods used in this study were: Isobaric tag for relative and absolute quantitation (iTRAQ), shotgun, Liquid chromatography–mass spectrometry (LC–MS/MS) and Sequential window acquisition of all theoretical mass spectra (SWATH. Quantification of proteins was done using iTRAQ.

This study for the first time reports proteomic analysis of early embryos (pre-MBT stage) of zebrafish. The improved deyolking protocol yielded approximately 3 times more unique proteins than those identified in non-deyolked counterparts. Also, the protocol enabled to reduce the vitellogenin (36- 58-fold) and increase the concentration of non-vitellogenin proteins (2-6-fold). Over 5000 proteins from 10 embryonic stages of the zebrafish embryos were identified across the early development from unfertilized eggs to bud stage (onset of somitogenesis).

This study also characterized vegetal proteome, that is the proteome located in the vegetal, non-blastodisc part of the early embryo. Identified proteins were involved in translation, post-translational modifications, protein processing, carbon metabolism, lysosomal degradation and axis specification. Immunohistochemical analysis has disclosed the localization of chosen proteins: ribosomal protein small subunit 16 (RPS16), eukaryotic translation elongation factor 2 (eEF2), and a chaperone heat shock protein 90- beta (HSP90β) in the vegetal cytoplasm, suggesting translational and protein processing activity out of early blastomeres.

Among the discovered maternally loaded proteins, there were transcription factors, proteins involved in microRNA biogenesis and regulation, methylation of nucleic acids, blue-light photoreceptors, proteins associated with cell divisions, maternal products clearance, translation, animal-vegetal axis coordinates, cytoskeleton establishment, epiboly formation and lens development—that are vital during zebrafish embryogenesis. This suggest that the maternal control of the early development is executed through not only translation of transcripts of maternal-effect genes, but also intricated, native maternal proteome.

Genomic information alone cannot provide accurate and comprehensive knowledge of physiological processes because proteins are the architects of the majority of the biological functions. This study contributes to the understanding of the regulation of vertebrate early embryogenesis. The information on zebrafish embryonic proteome supplements the genomic and transcriptomic information. Another generic outcome is

the method for effective deyolking, applicable to other polylecithial animals such as fish, reptiles, amphibians and birds.

Abstract in Norwegian – Sammendrag på norsk

Genomer og proteomer fra sebrafisk (*Danio rerio*; en ferskvannsfisk) og menneske har mange likhetstrekk. Dette gjør sebrafisk til et attraktivt modellsystem for studier av sykdom og andre biologisk-relaterte forhold hos mennesket. Faktorer som rask cellesyklus, synkron embryoutvikling, høy fruktbarhet, og transparente embryo bidrar også til at sebrafisk er en svært god modellorganisme i studier av utviklingsbiologi, hvor målet har vært å avdekke maternale regulatoriske mekanismer. Denne reguleringen skjer i de tidligste utviklingsstadier, før embryoet får kontroll over sin egen utvikling gjennom transkripsjon av egne gener. Prosessen som fører til et skifte i utviklingsregulering fra parental (hovedsakelig maternal) til embryonal kalles den "maternal til zygotisk overgangen" (MZT). I pattedyr starter prosessen tidlig i utviklingen, og vanligvis før første deling av zygoten. MZT i fisk derimot skjer mye senere, og først etter mange runder med celledeling. Av denne grunn synes fisk å være et meget gunstig modellsystem i studier av maternale faser av utviklingsregulering.

Det er rikelig med vitenskapelig litteratur innen transkriptomikk på tidlig embryonal utvikling i sebrafisk, men tilsvarende informasjon om proteomet er mer sjelden, og da spesielt for pre-MZT stadier. En viktig årsak her kan tilskrives yolk ("eggeplomme") proteiner av høymolekylær vekt som maskerer tilstedeværelsen av lav-molekylære proteiner. Hovedhensikten med denne doktorgradsstudien var å identifisere og karakterisere proteomet hos sebrafisk embryoer i tidlige embryonale utviklingsstadier. Mer spesifikke mål var å: 1) Utvikle en effektiv prosedyre for å få redusert mengden av yolk ("deyolking") i tidlig embryonal utvikling i sebrafisk, 2) Identifisere proteomet i vegetative deler i tidlig embryonal utvikling i sebrafisk, og 3) Kartlegge dynamikken i proteinsammensetning i tidlig embryonal utvikling i sebrafisk. De viktigste metodene som ble anvendt var: iTRAQ ("isobaric Tag for Relative and Absolute Quantitation"), shotgun, LC-MS/MS ("Liquid Chromatography-Mass Spectrometry"), og SWATH ("Sequential Window Acquisition of all THeoretical mass spectra"). Kvantitering av proteiner ble utført ved hjelp av iTRAQ.

Denne studien rapporterer for første gang en omfattende proteomikkanalyse av tidlige embryoer i sebrafisk. Den anvendte deyolking-protokollen resulterte i omlag 3 ganger mer av unike proteiner sammenlignet med tilsvarende protokoll uten deyolking. Protokollen resulterte i 36-58 gangers reduksjon av vitellogenin og 2-6 gangers økning av non-vitellogenin proteiner. Over 5000 proteiner fra 10 embryonale stadier av sebrafisk embryoer ble identifisert i løpet av tidlig utvikling, fra ubefruktede egg til starten av somitogenesen.

Videre karakteriserte denne studien også det vegetative proteomet, det vil si proteomet lokalisert i den vegetative, non-blastodisk delen av tidlig embryo. Her var proteiner involverte i prosesser som translasjon, post-translasjon modifikasjon, protein prosessering, karbonmetabolisme, lysosomal degradering, og akse-spesifisering. Immunohistokjemiske analyser avdekket lokalisasjon av utvalgte proteiner (som RPS16, eEF2, HSP90β) i vegetativt cytoplasma, noe som kan tyde på aktiv translasjon og protein prosessering ut i tidlig blastom.

Blant de maternale proteiner som ble påvist i studien var transkripsjonsfaktorer, proteiner involvert i miRNA biogenese og regulering, proteiner involvert i nukleinsyremetylering, blått-lys fotoreseptorer, proteiner assosiert med celledeling og opprenskning av maternale produkter, translasjon, koordinering av den animale-vegetale akse, etablering av cytoskjelett, dannelse av epiboly, og utvikling av linse, - aktiviteter som er sentrale i embryogenesen hos sebrafisk. Dette tyder på at maternal kontroll i tidlig utvikling utføres ikke bare av translasjon av transkripter av maternal-effekt genes, men også av det native maternalte proteom.

Informasjon basert på genom alene kan ikke alltid bidra med presis kunnskap av fysiologiske prosesser, dette fordi proteiner ofte er arkitektene bak de fleste biologiske funksjonene. Doktorgradsstudiet bidrar til å bedre forstå hvordan tidlig embryoutvikling hos vertebrater blir regulert. Ny kunnskap av det embryonale proteom i sebrafisk vil derfor utfylle informasjon basert på genom og transkriptom. Et annet viktig moment fra studien er at metoden for effektiv deyolking også synes å være anvendbar på andre polylecitinale dyr som fisk, reptiler, amfibier og fugler.

1. Introduction

1.1. Maternal control of early embryogenesis

Zygote formation marks the initiation of the embryogenesis process. It involves the fusion of the female and the male pronuclei resulting in a single zygotic genome endowed with genes from both the parents. Scientific research conducted over the years have been attempting to unravel the underlying mechanisms that lead to the zygote formation (Laubichler & Davidson 2008). The sea urchin (*Echinus melo*) model has been the most common choice to elucidate the principles governing organism development processes, and the relationship between cellular components and heredity (Ernst 1997, Laubichler & Davidson 2008). The advantage of the sea urchin model has been related to its availability and synchrony in the early developmental processes (Ettensohn 2017). The earliest effort based on the sea urchin model has been made by Dubosse, Derbes and von Baer in 1847 who first described the *in vitro* fertilization and development of sea urchin embryos (Briggs & Wessel 2006). In 1875, the research work of Hertwig (1875) revealed that the chromosomes and the nucleus have a central role in the heredity and development. Later in the nineteenth century, Theodor Boveri came up with the concept of non-equivalence of the chromosomes (Baltzer 1964). The study revealed that the cross-fertilization of gametes from different species yielded larvae characterized by features of both parents. Initially, it was presumed that the nuclear material of the sperm cells contributed towards the development of the genetic determinants. However, further experiments involving mechanical processes to develop eggs devoid of any nucleus revealed the presence of some hybrid characteristics. These observations are the basis of evidence for the involvement of maternal cytoplasm in the development of the genetic characteristics (Laubichler & Davidson 2008). This groundwork was then exploited further leading to the modern-day understanding of early embryogenesis in animals.

Transcriptional quiescence is one of the important characteristics of the early embryo. Its development in the initial stages is solely directed by the parentally (mainly maternally) derived proteins and RNAs from the egg cytoplasm (Deshpande et al. 2004,

Tintori et al. 2016). The gradual activation of the embryonic genome is accompanied by degradation of the maternal factors. This leads to the initiation of the maternal-to-zygotic transition (MZT) phase, wherein the developmental control is handed over from the maternal factors to the products of the activated nuclear genome. The two primary events of the MZT include maternal clearance and initiation of zygotic transcription (Tadros & Lipshitz 2009).

1.1.1 Maternal control of early embryogenesis in invertebrates

In the context of unravelling the early embryonic development in invertebrates, the majority of the studies have been conducted in fruit fly, *Drosophila melanogaster* (Avilés-Pagán & Orr-Weaver 2018). The studies revealed that the early embryonic development before MZT is controlled by maternal proteins and RNAs deposited in the egg during oogenesis (Gouw et al. 2009). In *Drosophila melanogaster*, 13 synchronic nuclear divisions occur at the early stages of embryo development without any cell division. The early mitotic divisions occurs after partial nuclear envelope breakdown (Avilés-Pagán & Orr-Weaver 2018). These early cycles of cell division vary significantly from the conventional ones as they consist only of the DNA synthesis phase (S phase) and the mitotic division phase, M phase (Shermoen et al. 2010). Absence of the cytokinesis further enhances the speed of the division thus enabling 13 cycles of nuclei divisions within a span of 2-hour time. These rapid S-M divisions in the *D. melanogaster* embryo remain under the maternal control and are followed by three post-blastoderm divisions. The pace is however slowed down with the 14th nuclear division as it additionally involves the G2 gap phase. The independent divisions of blastoderm extending from the 14th to 16th cycle remain under the control of *String cdc25 phosphatase*, a product of the zygotic genome expression. Once the blastoderm cycle completes, the epidermal cells exit the cell cycle. The G1 phase is then added to the cell cycle of the cells in the differentiating larval organs. These cells thereafter enter the endocycle and the transcriptional induction of the genes required for S phase marks the initiation of the G1-S transition. The mitotic divisions continue to develop the nervous system and other major tissues and organs (Unhavaithaya et al. 2013, Blythe & Wieschaus 2015, Harrison & Eisen 2015).

1.1.2 Maternal control of early embryogenesis in vertebrates

The period between the production and fertilization of the egg and activation of the zygotic genome has been considered important during the embryogenesis in the vertebrates. Multicellular organisms develop from single cells, which have the capability of generating various cells, and this is a signalling pathway-directed process (Marlow 2010). The embryo grows into a mature adult which can produce the cells required for the future development. Animal eggs contain all the nutrients required for an embryo to develop until it can acquire food on its own. The eggs of the vertebrates consist of mRNAs and proteins during oogenesis (Tong et al. 2000, Bourc'his et al. 2001). The maternal mRNA and proteins regulate embryonic developmental events such as meiosis, fertilization, transitions between meiotic and mitotic cell cycles, and the shift from the use of maternal gene products to the embryo's own gene products during zygotic genome activation, ZGA (Dosch et al. 2004). Various stages of oocyte development and egg production in vertebrates are conserved. Hence, specifically oocyte quality determines the early embryogenesis in vertebrates due to high dependency of MZT (Howley & Ho 2000, Payer et al. 2003). Important developmental changes such as the maternal mRNA transcripts degradation, epigenetic reprogramming/chromatin remodelling, and activation of the freshly produced embryonic genome take place during the MZT (Bettegowda et al. 2007).

The fundamental processes that the maternally derived factors execute during the vertebrate embryogenesis include fertilization, activation of the egg, nutrition, mediation of the first cell division, and the ZGA (Marlow 2010). The maternal factors are also responsible for determining the body axes. During the oogenesis, development of the animal-vegetal axis (AV) also referred to as the prospective anterior-posterior axis in the amphibians and fish, is also mediated by the maternally-derived factors (Suzuki et al. 2000). The development of the dorsal-ventral axis during early embryonic cleavage stages is also driven by the maternal gene products (De Robertis et al. 2000, Schier 2001). In lower vertebrates, the maternal factors thus have been identified to lay the foundation for the overall embryonic development.

In vertebrates, histone modification and DNA methylation are the most significant epigenetic modifications during early embryonic development. DNA demethylation might be either active or passive. The independent replication of DNA is restricted to the male genome which is being considered as an active form, while the passive form occurs in female genome and is dependent on DNA replication (Zhang & Smith 2015). Li et al. (2010) found that the maternal-effect genes were responsible for the effective orchestration of the events that followed fertilization until successful preimplantation in the early mouse development (Figure 1). The importance of the maternal factors in the early development could be gauged from the multiple studies. Mutations in maternal-effect genes interrupt the early embryogenic development (Burns et al. 2003, Payer et al. 2003, Wu et al. 2003).
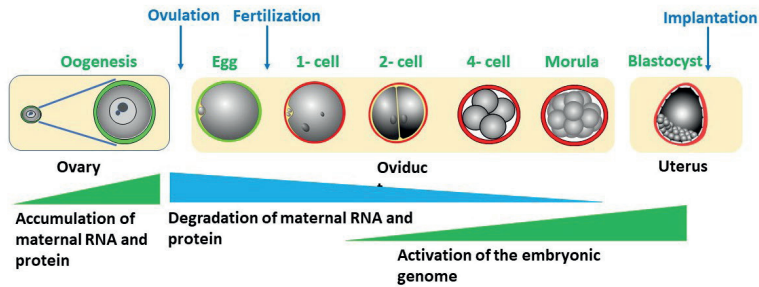
Figure 1. Mouse preimplantation embryonic development. This schematic diagram shows the dynamics of accumulation and degradation of maternal mRNA and proteins as well as the activation of embryonic genome. (Source: Li et al. 2010).

1.2 Zebrafish as a model for developmental biology

Zebrafish (*Danio rerio*) is a freshwater fish. The species thrives in the rivers of tropical Asia, including India, Nepal, Bangladesh and Pakistan (Talwar 1991). Zebrafish is not a food fish but rather a valued ornamental fish (Gerhard & Cheng 2002, Nelson et al. 2016). The zebrafish genome has a high genetic similarity to the human genome, consisting of 25 versus 23 pairs of chromosomes (Postlethwait et al. 2000), and containing 26,206 versus 20,479 protein-coding genes, respectively (Howe et al. 2013). Zebrafish is

commonly used as a human diseases model in studying hearing, visual, hematopoietic, skeletal, renal, neurodegenerative, and neuromuscular disorders (Dooley & Zon 2000, Keller & Keller 2018). The zebrafish model is also used for vertebrate cardiovascular development and environmental toxicology studies (Stainier & Fishman 1994) and to understand cardiac development and pathology of zebrafish that are similar to those in human (Arab et al. 2006). Several zebrafish pathogen models have been established to address human infectious diseases and develop effective vaccines (Sullivan & Kim 2008).

Zebrafish is an excellent model for developmental biology studies, to understand the mechanisms of maternal mRNA expression and gene network regulation, due to its fast cell cycle and synchronous embryonic development by the 11th division (Ikegami et al. 1999, Jukam et al. 2017). Features such as large numbers of offspring in a relatively short generation time, *ex vivo* development and optical transparency of embryos have allowed large-scale forward and reverse genetic screens in zebrafish (Haffter et al. 1996, Amsterdam et al. 1999, Moens et al. 2008, Kettleborough et al. 2013, Varshney et al. 2015), along with high-throughput drug discovery processes (Peterson et al. 2004, Murphey et al. 2006, North et al. 2007). The optical transparency combined with the fast development of zebrafish embryos permits *in vivo* visualization of cellular behavior for the duration of organogenesis (Lößner et al. 2012). The impetus for using zebrafish as a model organism enhanced since the 1990s when this organism was used by Nobel Prize winner Christiane Nüsslein-Volhard in Tubingen, Germany, and Wolfgang Driever and Mark Fishman in Boston, USA, to develop genetic mutants of zebrafish aiding various biological analyses (Khan & Alhewairini 2018).

1.3 Oogenesis in zebrafish

Oogenesis is the process of formation of a fertilizable egg from gonial precursors. Oogenesis in mammals involves the conversion of the germ cells into primary oocytes after the initiation of the meiosis. However, further progression of meiosis is arrested after chromosome replication, at the prophase I (Edson et al. 2009). Resumption of the meiosis in mammals occurs at the puberty when the secondary oocytes and the first

polar body are produced. The released ovum can either become fertilized and processed throughout the second meiotic division or it may be arrested again by entering into the metaphase II of meiosis. However, in zebrafish, the oogenesis significantly varies from that of mammals. In the leptotene stage, some of the oogonial cells enter the meiosis and transform to the primary oocytes, the rest continue their mitotic proliferation. Overall, there are six developmental stages in zebrafish oocytes, based on microscopic observation, and physiological and biochemical events (Lubzens et al. 2010). According to Selman et al. (1993) and Lubzens et al. (2010), there are primary growth (stage Ia and Ib), cortical alveolus stage (stage II), vitellogenesis (stage III), oocyte maturation (stage IV) and fully mature eggs (stage V); as shown in Figure 2.
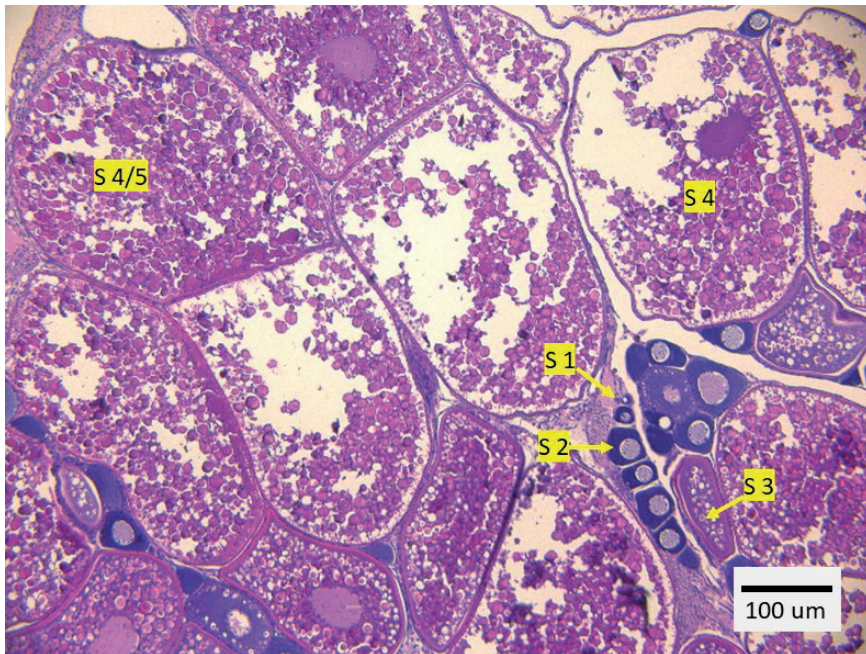
Figure 2. Organization of oocytes in the ovary of adult zebrafish, stages I, II, III, and IV are denoted as S1, S2, S3, and S4, respectively. Some of the biggest oocytes can be either in Stage IV or V. (Igor Babiak lab, unpublished*).*

The primary growth stage is separated into two phases: pre-follicle phase (stage IA) and follicle phase (stage IB). A fluid-filled sac called the ovarian follicle is made of a single oocyte. The stage IA (zygotene stage) oocytes are characterized by the coexistence of the oocytes within the nests. The oocyte at this stage contains a large nucleus with condensed chromosomes. With the progressive development, the oocytes become entirely enveloped with a sheath of pre-follicle cells. During the stage IB (diplotene stage), the formation of a definitive follicle occurs, wherein the oocyte gradually increases in size. A single layer of squamous follicle cells envelope the oocyte. In this stage, intracellular organelles proliferate and chromosome decondensation is initiated. In all known animals including zebrafish, the oocyte development is arrested during the first meiotic prophase (prophase I), with the appearance of a large nucleus called the germinal vesicle. The completion of stage I is marked by the abundance of the lamellae, mitochondria, Golgi complexes, and cisternae of rough endoplasmic reticulum in the cortical cytoplasm. Further, in between the short microvilli that extend from the oocyte surface, scattered patches of amorphous electron-dense material are observed. It can be an indicator of the initiation of vitelline envelope development (Selman et al. 1993, Lubzens et al. 2010).

The cortical alveoli (CA) or cortical vesicles are characteristic features of the stage II oogenesis. CA are the first prominent cytoplasmic structures of teleost oocytes detectable under light microscopy (Selman & Wallace 1989). They are similar to the cortical granules of other invertebrates and vertebrates. Insights into the chemical composition of CA have been crucial for identifying their functions in fertilization and early embryonic development (Hart 1990). Histochemical analysis has revealed that CA contain carbohydrates and proteins (Selman & Wallace 1986). CA in several fish species also contain lectins (Nosek et al. 1984). Later on, during activation of a mature egg, lectins and glycoproteins of CA are released into the perivitelline space, blocking polyspermy (Nosek et al. 1984, Kobayashi 1985, Ohta et al. 1990). Another notable event that occurs during stage II is the formation of a tripartite vitelline envelope. The end of stage II is marked by the surrounding oocytes with the follicle layers.

Stage III of the oogenesis in zebrafish - vitellogenesis - is defined as the process that facilitates the accumulation of the yolk within the maturing oocytes (Nicolas 1999). The vitellogenesis stage is also called the major growth stage. During the process, the oocyte becomes opaque. The size of the oocyte substantially increases from 140 to 270 μm due to the accretion of yolk, which contains primarily vitellogenins, female-specific yolk precursor proteins synthesized in the liver upon estrogen signaling, through its two components: the enzyme complex, cytochrome P450 aromatase (CYP19), which catalyses the rate-limiting step in estrogen biosynthesis and the ligand-activated transcription factor, estrogen receptors that interact with the target genes of estrogen (Callard et al. 2011, Hao et al. 2013). The oocyte also accumulates other molecules such as co-enzymes and lipids. Vitellogenin constitutes the main source of nutrients during the early stages of embryogenesis. The other characteristic events of stage III are the progressive thinning of the vitelline envelope and significant decrease in number of nucleoli near the center of the germinal vesicle. At the end of the vitellogenesis stage, the oocyte becomes competent to endure fertilization and contains maternal mRNAs, lipids, carbohydrates, proteins, vitamins and hormones that are vital for appropriate embryonic development and initiation of oocyte maturation (Selman et al. 1993).

The stage III oocytes remain arrested at the prophase I and may remain in that condition for weeks. The progress to stage IV is facilitated by the urge of the female fish to mate with the male fish (Wu et al. 2003). Once mating is destined, stage III oocytes proceed to the stage IV of the oocyte development that involves the initiation of the oocyte maturation. During this stage, meiosis resumes and the germinal vesicle moves towards the oocyte periphery. The movement is accompanied by the breakdown of the nuclear envelope. The mature oocytes complete the first meiotic division and continue to the metaphase stage of the second meiotic division wherein the further progression is arrested. It is during stage IV of the oogenesis that the oocyte becomes an egg (Selman & Wallace 1989). At the full maturation stage or the stage V of oogenesis, the translucent egg is ovulated and released to the ovarian lumen (Selman et al. 1993).

The regulation of the oocyte maturation process involves pituitary gonadotropins, sex steroids and the crosstalk that occurs between the maturing oocytes and their

surrounding somatic cells (Coticchio et al. 2015). Such an intricate regulation often justifies the inability to obtain mature oocytes of high quality (Guzel & Oktem 2017). The maternal gene products are also said to render significant influence on the early development of vertebrate embryos. Studies have revealed that any abnormality in the functioning of the maternal-effect genes could result in birth defects, and the emergence of diseases in the adult stages of life (Li et al. 2010, Huang & Sheng 2014).

1.4 The maternal-to-zygotic transition in zebrafish

The maternally inherited mRNAs and proteins guide the initial embryonic development in zebrafish owing to the absence of *de novo* transcription in the initial stages. The initial developmental phase is characterized by synchronous cell cycles devoid of any gap phases. A remarkable study concerning the embryonic development of zebrafish has been conducted by Harvey et al. (2013), who utilized RNA sequencing and single nucleotide polymorphisms to differentiate the maternal and paternal mRNAs in the developing zebrafish embryo. The study reported significant post-transcriptional regulation of the maternal mRNAs before the initiation of the zygotic transcription. In this case, the paternal mRNAs appearance was used as an indication of zygotic transcription. The post-transcriptional regulation of maternal mRNAs through cytoplasmic polyadenylation elements located at the 3' untranslated regions (UTRs) increases the embryo's transcriptional competence (Harvey et al. 2013), and Cyclin B1 is involved in cell cycle and polyadenylation of maternal mRNAs (Mendez & Richter 2001, Groisman et al. 2002).

There are three terms related to the transition from maternal to embryonic (zygotic) control of the development, which partially overlap: ZGA, MZT, and mid-blastula transition (MBT). ZGA refers to the phase wherein *de novo* transcription occurs, and during this period the zygotic genome takes control over the developmental processes. In this phase, the zygotic genome undergoes fully-fledged transcription and the initial transcripts facilitate the degradation of the maternally-derived factors that impose an inhibitory effect on the zygotic transcription process. On the hand, MZT refers to the

whole set of developmental events related to the overtake of the development by the embryo, notably including the process of degradation of maternal elements. The MZT period that expands through the transcription initiation and the ensuing cell cycle ends when the cells become prone to apoptosis. Whereas, MBT is a developmental event that occurs during the MZT. MBT is characterized by dramatic cell cycle modification, and bulk zygotic transcription (Tadros & Lipshitz 2009, Langley et al. 2014). MZT serves as the representative time phase during which the cell initiates movement and becomes apoptosis sensitive (Tadros & Lipshitz 2009, Langley et al. 2014), as depicted in Figure 3.
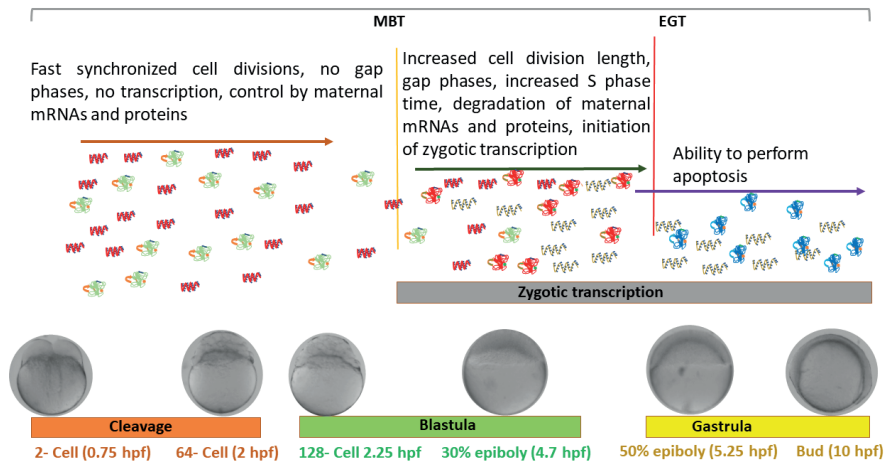
Figure 3. Maternal-to-zygotic transition during zebrafish embryonic development. maternal mRNA; maternal protein; zygotic mRNA; zygotic protein at blastula period; zygotic protein at gastrula period. MBT, mid-blastula transition and EGT, early gastrula transition (modified from Langley et al. 2014).

In zebrafish, the ZGA coincides with the events of MBT (Foe & Alberts 1983, Kane & Kimmel 1993), although its onset is earlier, starting at approximately 64-cell stage (Heyn et al. 2014). The primary events that characterize the MBT include loss of synchrony in cell divisions, cell cycle elongation, and ZGA. Wragg and Müller (2016) in their review

pointed out the lack of clarity in the molecular mechanisms that underpined the coincidental ZGA with MBT. However, the theory by Newport and Kirschner sheds some light in this regard. The preeminent theory proposes that the attainment of the threshold nucleoplasm to cytoplasm ratio mediates the initiation of the MBT. The maternally deposited factors in the early embryo are responsible for transcriptional repression of the zygotic genome (Newport & Kirschner 1982). Thus, the commencement of ZGA is largely dependent upon the maternal clearance that involves stepwise degradation of the maternal mRNAs critical in early oocyte maturation and homeostasis (Tadros & Lipshitz 2009, Barckmann & Simonelig 2013, Lee et al. 2014). In zebrafish, micro RNA (miRNA) *miR-430,* an early regulatory RNA transcript expressed in the embryo, aids the degradation of the maternal transcripts (Bazzini et al. 2012). Also, N6-methyladenosine (m6A) modifications of maternal mRNA are signatures for Ythdf2 reader protein, which directs the degradation of maternal mRNA (Zhang et al. 2020). During MZT, the RNA metabolism and turnover is also facilitated by several other unique RNA-binding proteins (Despic et al. 2017). The duration of the maternal control of embryogenesis varies between species depending on ZGA and the persistence of maternal gene products (Baroux et al. 2008, Tadros & Lipshitz 2009). The maternal clearance holds significant importance in the overall execution of the MZT as the maternally derived factors, if present, may impose deleterious effects thereby interrupting the embryonic development. Apart from maternal clearance, initiation of zygotic transcription is a vital process in the subsequent development of the embryo, as interruptions may result in the inability of the cells to undergo gastrulation (Newport & Kirschner 1982, Kane et al. 1996).

The mechanism of ZGA has been explained by two models. One of the models, above mentioned the nucleo-cytoplasmic (N/C) ratio model, states that the transcriptional repression is reversed by the accumulation of the increasing quantity of nuclear material in comparison to the cytoplasm volume that remains constant over the time encompassing the progressive cell division stages. However, the inhibitory effects of the maternally derived repressive factors on the ZGA necessitate the model to consider diminishing of such repressive factors before initiation of the transcription process. In

the case of the alternative model, the gene expression timing is determined by the maternal clock that does not remain under the influence of the number of cell divisions. The model states that for transcription to be triggered, the activities of the maternal factors are required to attain a critical level (Lee et al. 2014). Among the two models, the latter seems to be more appealing, given the evidence obtained from polysome profiling and high-throughput ribosome foot-printing that reveals an enhancement in the translational efficiency (Lee et al. 2013). Further, the prevalence of the cytoplasmic polyadenylation of the maternally provided mRNAs renders additional support for that model (Aanes et al. 2011, Harvey et al. 2013). Critical components encoded by the maternal mRNAs such as the transcription factors and chromatin modifiers were identified to be the major drivers of the ZGA process (Lee et al. 2014). The concept that the transcriptional factors mediate the ZGA has been reinstated by Schulz and Harrison (2019), in a study on the mechanisms underlying ZGA and its correlation with the zygotic chromatin architecture reprogramming. The upregulation of the translational processes post-fertilization mediates the accumulation of transcription factors, which in turn have a central role in the overall genome activation processes. The transcription factors execute their ZGA effects by mediating the chromatin remodelling which helps erase the previous cell identity followed by the creation of a new one (Schulz & Harrison 2019).

1.5 Zebrafish embryonic development

The embryonic development of the zebrafish can be subdivided into 8 major developmental stages: zygote, cleavage, blastula, gastrula, segmentation, pharyngula, hatching, and the larval period (Kimmel et al. 1995).

1.5.1 Zygote

As opposed to the process in mammals, where the activation of the egg requires contact with a spermatozoon, in most fish species a contact with water provides the necessary stimulation for egg activation. Zygote formation begins with the fusion of pronuclei. The pronuclear congression at the time of fertilization depends on microtubule asters, which are formed near the male pronucleus. Centrosomal aster

connects to the male pronucleus, and the astral microtubules help to connect to the female pronucleus. This attachment helps in the migration of female pronucleus towards the male pronucleus in a dynein/dynactin-dependent manner (Lindeman & Pelegri 2012). Upon activation, the egg swells due to water influx, and its chorion, which is the outermost membrane surrounding the embryo, elevates thus moving away from the vicinity of the fertilized egg. The blastodisc occurs on the upper side of the yolk. In the process of separation of the cytoplasm from the yolk, the major portion of the cytoplasm moves along separate yolk-free channels. The stretches of cytoplasm, "streamers", connect the eggs' inner regions with the base of blastodisc. This movement occurs for the duration of the first cell cycle and continues up to the sixth cycle (Beams et al. 1985). The time duration of the zygote period may extend up to a maximum of 0.75 h (Kimmel et al. 1995). However, a temperature of 28°C has been reported to accelerate the overall embryonic development of the zebrafish (Meyers 2018).

1.5.2 Cleavage

The cleavage period is marked by six cleavages which occur at a defined orientation. The first cleavage is followed by meroblastic division of the blastomeres at a regular interval of 15 min at 28.5˚C. Cell divisions during the cleavage period, 0.75 hours post-fertilization (hpf) to 2.25 hpf (2-cell to 64-cell stages, respectively), occur synchronously, resulting in a mound of cells that sits on the animal pole of a large yolk cell. At the 2-cell stage, the cleavage furrow appears close to the animal pole and grows quickly toward the vegetal pole. The cleavage furrow passes all the way through the blastodisc, but not the yolky zone of the embryo. One blastomere is cleaved into two equal-sized blastomeres. At the 4-cell stage, the two blastomeres do not cleave completely. Here, the cleavage happens in a single plane across the animal pole and is perpendicular to the first cleavage plane. This results in four blastomeres arranged in a 2 x 2 array. At the 8-cell stage, the cleavage is still incomplete. Here, the cleavage occurs in two different planes, producing eight blastomeres in a 2 x 4 array (Figure 4). At the onset of the 8-cell stage to 16-cell stage, some cells are completely separated from the yolk and the rest is still associated with the yolk (Kimmel et al. 1995). The cleavage occurs along two planes

and produces 4 x 4 array of cells at the 16-cell stage, and 4 x 8 array of blastomeres at the 32-cell stage (Figure 4).
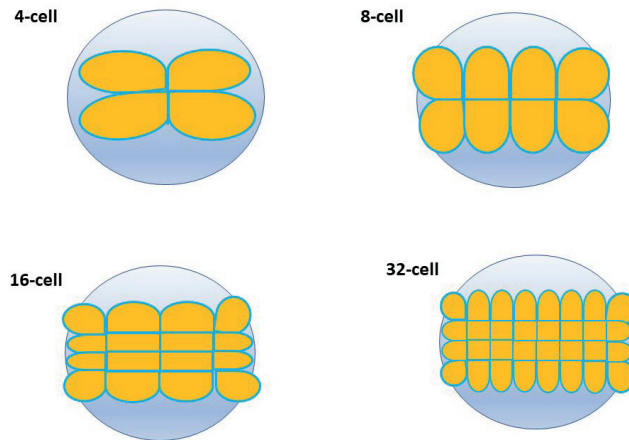
Figure 4. Diagram of animal polar views of the planes of the cleavage stages: 4-, 8-, 16- and 32-cell stages in zebrafish. 4-cell to 32-cell stages show sequential cleavages, with even-numbered ones cutting the long axis of the blastodisc. (Source: Kimmel et al.1995).

The cleavage period ends at the 64-cell stage where the array of blastomeres appears like a mould with some cells buried deeper. Each of the two daughter cells that are produced at the 32-cell stage become located to the bottom part of the blastodisc and are referred to as the buried cells, or deep cells. The remaining daughter cells are located on the upper side eventually forming the enveloping layer (EVL) surrounding the blastodisc. The EVL or the outermost single cell layer of an embryo flattens in the blastula stage and gets transformed into a periderm (Bruce 2016, Marsal & Martin-Blanco 2017).

1.5.3 Blastula

The blastula period begins at the 128-cell stage or 8th zygotic cell cycle when the blastodisc appears ball-like, and it ends at the commencement of gastrulation at the 14th

zygotic cell cycle. Three critical processes during the blastula period include MZT, the formation of the yolk syncytial layer (YSL) and the initiation of epiboly (Kimmel et al. 1995, Dhillon et al. 2019).

The synchronous divisions of the cells continue in the blastula period. The blastodisc at the end of each cell cycle is crossed by a wave, which could be defined as a pattern of cellular segregation that passes through the blastodisc obliquely, with cells close to the animal pole exposed first, followed by the marginal cells. The initiation of the MBT is marked by the lengthening of the cell cycle. Synchronous lengthening is not a general phenomenon for all the cells, some may remain in the interphase stage characterised by easily visible nuclei, while the others may enter mitosis. The differential morphology of the cells has been the direct indication of the asynchrony that exists between the blastomeres. The gradual lengthening of the interphase is accompanied by cell motility and increased RNA synthesis (Kimmel et al. 1995).

In the early blastula phase, the blastomeres located in the marginal section are destined to become the YSL (Figure 5). The number of deep cells increases from the early blastula stage until the sphere stage. During doming, the rearrangement of deep cells occurs through intercalation (Warga & Kimmel 1990, Bruce 2016). The EVL cells line up in about 5 irregular tiers between the margin and the animal pole at 128-cell stage and with seven irregular tiers at 256-cell stage. The MBT begins at the 512-cell stage, the EVL blastomere cells line up in nine irregular tiers between the animal pole and margin. The pace of cell cycles starts to slow down. At the end of this stage, the first tier of EVL cells start to lose their lower borders that indicates the starting of YSL formation. In the 1000-cell stage, 11 tiers of EVL cells are present in between the animal pole and margin. The formation of the YSL is mediated by the release of the cytoplasm and nuclei after the collapse of the marginal blastomeres against the cytoplasm of the yolk cells. The yolk syncytial nuclei (YSN) are located within the YSL. The YSL usually comprises of approximately 20 nuclei in a single ring around the blastodisc margin. First, the YSN appear in a single row, near the margin of the blastoderm, then metachronously divide three to five times, without cytokinesis, to finally become postmitotic, just before the commencement of epiboly (Kane et al. 1992, Trinkaus 1992, Kimmel et al. 1995). Thus,

the YSL can be referred to as a multinucleate layer that lays just below the cellular blastoderm. YSL can be split into the external YSL (eYSL) and the internal YSL (iYSL). The eYSL is located external to the blastodisc, while the iYSL remains beneath the blastodisc. In the course of the development of the zebrafish embryo, the YSL is identified as the extraembryonic structure that is restricted to a particular lineage (Kimmel et al. 1995).

In zebrafish, epiboly marks the ending of the blastula phase. It is referred to as the first coordinated cell movement that is observed in zebrafish. Initiation of epiboly is accompanied by certain specific modifications such as the thinning and spreading of both the YSL and the blastoderm to envelop the yolk completely. Epiboly completes when the yolk plug is closed by the blastoderm margin (Warga & Kimmel 1990, Bruce 2016, Sun et al. 2017). At the end of epiboly, the embryo has three separate cellular layers: (1) deep cell layer (DEL), which is formed during early epiboly (while blastodisc is transformed into blastoderm at dome stage). The DEL will be reorganized into epiblast and hypoblast during the development of gastrula from blastula, (2) EVL, and (3) yolk cell that contains yolk cytoplasmic layer (YCL), an array of microtubules that spread along the animal-vegetal axis to the vegetal pole of the embryo, and YSL (Zalik et al. 1999, Sakaguchi et al. 2002, Behrndt et al. 2012). The blastula phase extends from 2.25 to 5.25 h at 28.5°C.
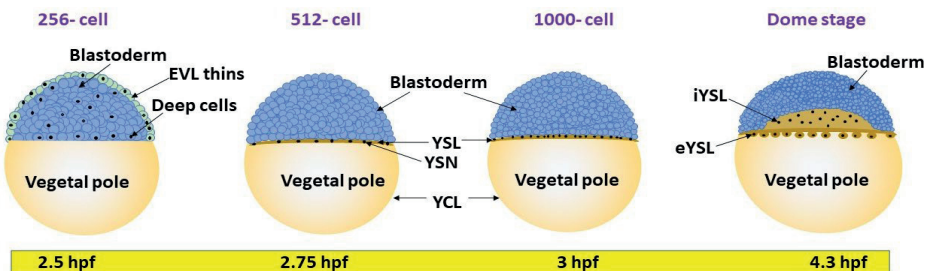
Figure 5. Structure of enveloping layer, deep cells and the formation and structure of the yolk syncytial layer in zebrafish. EVL, Enveloping layer; YCL, yolk cytoplasmic layer; YSL, yolk syncytial layer; YSN, yolk syncytial layer nuclei; iYSL, internal yolk syncytial layer; eYSL, external yolk syncytial layer (Figure modified from Carvalho & Heisenberg 2010).

Another prominent feature of the embryonic development is the primordial germ cell (PGC) formation. They are the stem cells of the gametes that are responsible for directing the transmission of the genome to future generations. The PGCs originate at a different place from the embryonic gonads. However, during development, they migrate towards the developing gonadal ridges to induce reciprocal interactions between the germ cells and somatic cells, critical for successful gonadal differentiation (Raz 2003, Kocer et al. 2009, Lesch & Page 2012, Saito et al. 2014). The cell migration is of importance owing to its significant influence on the early embryonic development, organogenesis, organ function, and homeostasis (Chisholm & Firtel 2004, Vicente-Manzanares et al. 2005).

1.5.4 Gastrula

The gastrula period begins from 50% epiboly and ends up at the bud stage. The whole embryo is surrounded by EVL, which later falls as a true epidermis that forms from the deeper cell layers (Sagerström et al. 2005). An effective reorganisation of deep layer cells that happens in the dome stage is necessary for the blastoderm to reduce its thickness from 6-8 to 2-3 cells during the gastrulation (Kimmel et al. 1995, Bensch et al. 2013, Bruce 2016). Just after 50% epiboly, the deep cell epiboly pauses until the shield stage, which highlights the transition from initiation of epiboly to progression. The deep cell epiboly starts again after the shield stage, which continues towards the completion of the gastrulation period.

During the gastrula period, the cell movement continues in a coordinated form of involution, convergence, and extension. The 50% of epiboly remains in the early shield stage and gradually increases in the late shield stage. At the shield stage, the involution continues at the entire margin of the blastoderm which in the gastrula phase has a uniform thickness. Then, the convergence commences, wherein the deep layer cells apart from moving towards the blastoderm converging to form the germ ring. The germ ring is the embryonic structure that develops at the blastoderm rim as a thickened annulus. The thickening of the germ ring results from the involution process occurring at the blastoderm margin. The involution gives rise to the epiblast and hypoblast within

the germ ring, which are cellular layers emerging as a result of the folding of the blastoderm. In the meantime, the deep cells converging towards the germ ring accumulate to give rise to the embryonic shield. This marks the 75% epiboly stage. At the embryonic shield, the involuting cells then form the axial hypoblast that continues the movement of involution to stream towards the animal pole (Kimmel et al. 1995, Dhillon et al. 2019).

At the 90% epiboly stage, the axial blastoderm thickens on the dorsal side rather than the ventral side. The establishment of anterior-posterior (AP) and dorso-ventral (DV) axes is another crucial event at the gastrulation period (Davidson 1990, Schmitz & Campos-Ortega 1994). The patterning of the AP axis occurs in two phases. During the initiation phase, the embryo is usually separated into the body and the head. In the elaboration phase, the body gradually forms toward the posterior end, establishing the trunk and tail (Woolley et al. 2000, Kimelman & Martin 2012). The mesoderm part of the head, which is a crucial signalling centre (organizer), is initially established close to the equator at the dorsal side of the embryo. During gastrulation, the organizer moves toward the animal pole, identifying the place where the brain is formed. Conversely, the mesoderm part of the body and the spinal cord are arranged. The tailbud formation is initiated. It is formed by the migration of the most posterior cells toward the vegetal pole. This facilitates alignment of the AP axis with the AV axis at the end of the gastrulation period (Myers et al. 2002, Kimelman & Martin 2012).

The gastrula period is completed at the 100% epiboly or the bud stage. At this point, the yolk plug will be fully covered by blastoderm. The caudal end of the embryonic axis grows completely into the tail bud. The cells from the tail bud are responsible for the development of the posterior trunk. The neural plate thickens along the whole embryonic axis on the dorsal side, anterior to the tail bud. The cells towards the posterior end of the neural plate contribute to the formation of the trunk spinal cord. The most prominent thickening happens close to the animal pole in the head region. The end of gastrulation period is marked by the formation of the Kupffer's vesicle. It is a small but distinctive epithelial sac that arises in the tail bud and aids the establishment of the visceral laterality. Owing to the crucial role of the vesicle in the initiation of left-

right development of the internal organs such as digestive organs, portions of the brain and heart (Essner et al. 2005, Okabe et al. 2008), the Kupffer´s vesicle is often referred to as the left-right organizer (Essner et al. 2002, Roxo-Rosa & Lopes 2019). The gastrula phase extends from 5.25 – 10.33 h post-fertilization at 28.5˚C.

1.5.5 Segmentation

This period is characterised by a variety of morphogenetic development. It marks the formation and development of somites, which appear from the pre-somitic mesoderm (Holley 2006, Szeto & Kimelman 2006, Tlili et al. 2019). They are referred to as the undifferentiated mesodermal component of either early trunk or metamere. Slow- and fast-twitch muscle fibres and different types of progenitor cells are generated from the somites before maturing into the myotome (Nguyen-Chi et al. 2012, Yin et al. 2018). Eventually, the myotome contains slow muscle fibres and multinucleated fast fibres, which have progenitors initially located near the notochord and more laterally, respectively. It is only at about 10.5 hpf that the first somites appear in a zebrafish embryo. In the segmentation period, the number of somites increases to 26 (Stickney et al. 2000).

Another significant morphogenic development of the segmentation phase is the formation of the otic placode by cavitation during the 14-19th somite stages beside the hindbrain rudiment. It gets transformed into the otic vesicle during the 20-25th somite stages, which consists of two sac-like structures (Solomon et al. 2003, Chen & Streit 2013, Baxendale & Whitfield 2014). On the dorsal side, the vesicle transforms into the semi-circular canals while on the ventral side it forms otolith organs. Although the Kupffer's vesicle originates during the gastrulation period, its extension transiently occurs during most of the segmentation period.

In the segmentation period, the origins of the primary organs become detectable. Further development involves the prominent formation of the tail bud along with elongation of the embryo. The segmentation period also marks the initiation of the first body movements. The segmentation period extends from 10.33 to 24 h post-fertilization at 28.5˚C.

1.5.6 Pharyngula

The embryo develops into a bilaterally organized organism. At the pharyngula period, the embryo possesses a notochord with a newly formed set of somites that reaches to the end of a long tail. The hollow and interiorly extended nervous system is formed with the fast-cerebellar morphogenesis of the metencephalon. The rapid development of pharyngeal arches, initial pigmentation of skin, retina and tail, the appearance of melanophores in head and yolk sac, formation of the circulatory system, beginning of heartbeats, cellular erosion at the tail end, the appearance of the liver and swim bladder and gut tract, the formation of heart chambers, development of olfactory cilia and condensed otic vesicle walls, beginning of dechorionation, are the main processes of this phase (Müller & van Leeuwen 2004, Parichy et al. 2009). The pharyngula period extends from 24 to 48 hpf at 28.5˚C.

1.5.7 Hatching

The growth rate of embryos is similar as in the previous period. Apart from the gut and associated organs, morphogenesis of most other organs becomes complete. However, the rate of morphogenesis is significantly reduced. The hatching period extends from 48 to72 hpf at 28.5˚C.

1.5.8 Larval period

During this phase, the fish body grows substantially, and by the end of the larval period, it becomes thrice its initial length. This phase is also marked by a trail of morphological changes that transform the fins, the pigment pattern, and the morphology of the body thus giving rise to the juvenile configuration (Kaushik et al. 2011). In zebrafish, the larval period extends from 72 hpf up to 30 days post-hatching (dph). The transformation from the sexually immature juvenile state to the adult with full sexual maturity may take place over about three months (Kimmel et al. 1995, Parichy et al. 2009).

1.6 Yolk organization and vital components

Teleost yolk globules are round before fertilization and they become angular once the blastodisc is formed. There is no barrier between the yolk and blastodisc. Hence, yolk globules are kept in a compressed condition so that they do not move into the blastodisc. Determinants of early development, predominantly maternal RNA and some proteins are present in the yolk-containing vegetal part of zebrafish embryos (Mizuno et al. 1999, Ober & Schulte-Merker 1999). While the majority of ooplasm is located towards the animal pole forming the blastodisc, clusters of ooplasm also remain within the yolk area. Additionally, a thin layer of ooplasm is located toward the yolk membrane (Figure 6). A group of filamentous structures of variable width is present in the cortex and endoplasmic streamers. These filamentous structures include both microfilaments and microtubules (Beams et al. 1985). This organization of yolk is important for the quality, performance and survival of the embryo because signals from the yolk, maternal hormones, immunoglobulins and mRNAs are associated with specific yolk areas (Roustaian & Litvak 2007).

In humans and rodents, there is a functional placenta and hemotrophic nutrition is active during the fetal period. Nevertheless, there are differences in early embryonic nutrition; at this stage histiotrophic nutrition prevails. Rodents do not have a maternally supplied yolk and therefore cannot rely on the existing nutrients, while humans and zebrafish have protruding yolk sac (Burton et al. 2002). However, zebrafish is a lecithotrophic animal, human embryos start as histiotrophic organism. The major protein in human yolk is Albumin, while that in zebrafish yolk is Vitellogenin (Burton et al. 2001). In both organisms, bulk proteins are cleaved after embryonic uptake. On the other hand, yolk lipids such as cholesterol and sphingomyelins are metabolized before embryonic uptake (Burton et al. 2001, Sant & Timme-Laragy 2018).
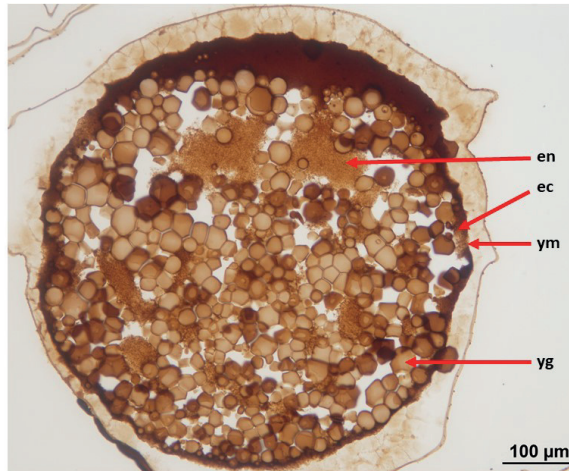
Figure 6. Micromorphology of the 32-cell stage zebrafish embryo showing both animal pole (top) and vegetal pole. yg, yolk granules; ym, yolk membrane; ec, ectoplasm; and en, endoplasm (Igor Babiak lab, unpublished).

The yolk in ovoviviparous and oviparous species is primarily made up of the yolk proteins and lipids (see *Section 1.3. Oocyte development*). Vitellogenins are the major protein part of the zebrafish egg yolk, recruited during the vitellogenesis into the developing oocyte (Zhong et al. 2014). Vitellogenins are cleaved into lipovitellin I and II (LVI and LVII) and phosvitin (PV), which serve as the most important nutritional resource for the growing embryo (Wang et al. 2005, Link et al. 2006, Ge et al. 2017). Zebrafish genome has at least 7 genes that encode for 3 Vitellogenins, namely type I (Vtg1, 4-7) LVII; type II (Vtg2) and type III (Vtg3, lacks PV and LVII) (Wang et al. 2005, Yilmaz et al. 2018).

The supply of a pool of free fatty acids (FFA) to zebrafish embryos is very critical for the generation of ATP. ATP hydrolysis drives the development process. The maternally deposited ATP is depleted relatively fast and hence the hydrolysis of lipids helps in generating ATP (Dutta & Sinha 2017). Lipid droplets (LD) are distinct structures that have been observed in many of the vertebrates including zebrafish. Studies done on the localization of lipid droplets have shown that they are enriched in blastodisc. Yolk

contains neutral lipids, diacylglycerol, triacylglycerol and cholesterol esters. A comparison of LD from the 1-cell stage to 1000-cell stage showed a decrease in the size of LD along with depletion of lipids from the yolk sac (Dutta & Sinha 2017).

Miyares et al. (2014) reported that lipids accumulated in the yolk sac were later redistributed uniformly resulting in their systemic export throughout the embryo as the development proceeded. In another study, Fraher et al. (2016) noted yolk sac lipid utilization by the embryo. In fertilized eggs, cholesterol was the most abundant lipid followed by phosphatidylcholine, di- and triacylglycerol, cholesterol esters, and sphingomyelin. Most of these lipids were depleted by 24 h of development. Though there was a depletion of maternal lipids, an increase in other classes of lipids was found, which was associated with their synthesis in the yolk sac (Fraher et al. 2016).

1.7 Some important events during embryonic development and selected molecular mechanisms underlying them

Subcellular cytoplasmic domain formation and restricted gene expression patterns regulate initial phase of oogenesis. However, the exact mechanisms that underpin the morphogenetic development within the oocyte remains unclear. One of the defining events that orchestrate the transformation from fertilization to embryonic patterning and organogenesis is the calcium (Ca^{2+}) signalling (Whitaker 2006). Studies involving maternal-effect mutants have unravelled the genetic regulation of the dynamic intracellular Ca^{2+} level. Results showed that maternal genes as the primary modulator of the organizational and translocation changes were observed within the cytoplasm. The maternal-effect genes are also responsible for maintaining the Ca^{2+} homeostasis (Mei et al. 2009, Li-Villarreal et al. 2015). Studies conducted in sea urchin and *Xenopus* eggs have revealed the significant involvement of the Ca^{2+} levels in influencing the processes that follow fertilization (Machaty et al. 2017). In both species, an increase in the intracellular Ca^{2+} level was observed immediately after the egg-sperm interaction which resulted in the establishment of an alkaline environment within the egg cytoplasm (Rees et al. 1995, Carroll et al. 2000). Addressing the relationship between ion

homeostasis and cytoplasmic segregation, Fuentes et al. (2018) have hypothesized that mutations in the maternal genes that regulate Ca^{2+} and H^+ ions may interfere with the ion balance thereby resulting in an unfavourable ionic environment that induces alteration within the oocyte.

Kaufman et al. (2018) proposed RNA-binding proteins (RBPs) as prominent regulators of the developmental processes within oocytes. The target molecules for RBPs are assembled in ribonucleoprotein granules. The RNA-binding protein of multiple splice forms 2 (Rbpms2), interacts with molecules involved in processes such as reproduction and egg patterning. Intact RNA binding domains are critical for the accumulation and localization of the Rbpms2 to the subcellular compartments. In the case of zebrafish, the C-terminal domain of the protein promotes the localization to the bipolar centrosomes/spindle (Kaufman et al. 2018). Other RNA-binding proteins such as Rbm47 and Igf2bp1 are involved in head formation and embryonic patterning and retinal ganglion cell axon growth, respectively, during zebrafish embryogenesis (Guan et al. 2013, Gaynes et al. 2015). In addition, insulin-like growth factor 2 mRNA-binding proteins (Igf2bps) ensures the stability and translation of target mRNAs (Huang et al. 2018). Another RNA-binding protein, Rbm15, also has an important role in zebrafish embryonic liver development (Hu et al. 2020). These findings suggest the essential roles of RNA-binding proteins in developing zebrafish.

The factors of development of the body axis and the primordial germ cells in zebrafish are localized to the vegetal pole of the egg. After the activation of the egg, the axis induction factors shift off-centre asymmetrically, while the primordial germ cell factors witness a symmetric shift that is directed by the animal movement. Embryonic axis determination is one of the key steps for the proper development of zebrafish. Localization of various maternal RNA transcripts helps in the proper determination of dorsal and ventral regions of the embryo. mRNAs such as *deleted in azoospermia-like* (*dazl)* or *bruno-like* (*brul*) were showed localized to the vegetal pole. Specific localization has a distinct effect on axis specification and development of the embryo (Suzuki et al. 2000). Bone morphogenetic protein (Bmp) and nodal signalling help in axis specification (Fulton et al. 2020).

Majority of the studies have reported that Nodal signalling has a significant role in the mesoderm and endoderm positioning (Hagos & Dougan 2007, Zorn & Wells 2009). However, recent findings suggest that the Nodal-related genes and fibroblast growth factor (Fgf) signalling determine the endoderm and mesoderm formations (Hagos & Dougan 2007). The demarcation between the endoderm and mesoderm is mediated by the cell autonomous Fgf signalling inhibitor dual specificity phosphatase 4 (Dusp4). Determination of the dorsal region of the embryo is regulated by the canonical Wnt signalling proteins in zebrafish. Maternally-encoded protein Wnt-8A transcripts localize to the vegetal pole and help in establishing the axis specification (Hino et al. 2018). Many of the vegetal pole-localized transcripts have essential functions in dorsoventral axis determination. The *vasa* transcript is associated with vegetal spindle pole and is asymmetrically distributed before germplasm specification in early embryos (Knaut et al. 2000). Maternally encoded *vertnin* (*vrtn*) transcript acts as a repressor of *bmp2b* expression. The *vrtn* transcripts localize to the vegetal pole and control the essential expression of *bmp2b* (Shao et al. 2017). It should be noted that genes such as *vasa, nanos1, dazl, bucky ball (buc), forkhead box protein H1* (*foxh1*)*, syntabulin* (*sybu*)*, wnt8a* and proteins such as Actin and Buc are present in zebrafish germ plasm (Kosaka et al. 2007), and are involved in animal-vegetal polarity (Marlow & Mullins 2008, Bontems et al. 2009) and dorsal determination (Nojima et al. 2010). Germ granules may function differently in transcriptionally active meiotic cells and transcriptionally quiescent early embryo. Thus, the maternal RNA and yolk components both help in active cell division and the development of an embryo to larval stages.

Epiboly is a process by which coordinated vegetal movement occurs and the spreading of cells is vital for the development of zebrafish. The role of serine-threonine kinase Mitogen activated protein kinase activated protein kinase 2 (Mapkap2) in embryonic development has been suggested by Holloway et al. (2009). The study revealed that Mapkap2 and its regulator p38 MAPK function within the yolk and they are involved in the regulation of epiboly in the zebrafish embryo. The study proposed that the p38 Mapkap2 kinase acts by mediating the gradual closure of the blastopore during epiboly.

The effect is achieved by modulating the activity of F-actin at the yolk cell margin circumference.

Chrispijn et al. (2018) reported the role of the *polycomb group* (*pcg*) genes in zebrafish embryonic development. The *pcg* genes encode transcriptional repressors that have a significant role in the overall development and differentiation of the embryo. The expression of the *pcg* genes was reported to reach maximum in the germ line compared to the somatic cells. Additionally, this study revealed that during both oogenesis and spermatogenesis, the *pcg* gene transcripts were present. The expression of the *pcg* genes was also noted in the developing gonads at 4- and 5-week post-fertilization.

1.8 Transcriptome analysis during zebrafish embryogenesis

Several studies have been reported on elucidation of functional transcripts in early embryonic development of zebrafish by utilizing various technologies (Mathavan et al. 2005, Alli Shaik et al. 2014, Mehjabin et al. 2019). Transcriptome analysis is a valuable approach to identify global changes of gene expression, and it can deliver essential indications in order to help understanding the embryogenesis and developmental processes (Ko 2001, Lieschke & Currie 2007). In the review by Aanes et al. (2013), the transcriptome dynamics is described by different forms of mRNA degradation, activation of inactive transcripts and commencement of transcription during early embryonic stages of zebrafish. Others have characterized the zebrafish transcriptome using RNA-sequencing technology for the period of early embryogenesis (Pauli et al. 2012, Heyn et al. 2014).

The transcriptome analysis by Mathavan et al. (2005) performed for 12 embryonic stages across cleavage, blastula, gastrula, segmentation, and pharyngula using microarrays revealed the temporal action of developmentally controlled genes during the embryogenesis of zebrafish. White et al. (2017) conducted a time course experiment and the mRNA expression throughout the overall zebrafish development phase, that is, from one cell to 5 days post-fertilization. The study findings revealed temporal expression of 23,642 genes based on RNA-Seq. Yang et al. (2013) in their transcriptome

profiling identified 24,065 different gene transcripts from 9 different zebrafish developmental time points. Another transcriptome study revealed 2539 high confidence novel transcripts from zebrafish embryos during pre- (256-cell stage) and post-ZGA (6 hpf) by using single-molecule real-time sequencing (SMRT-Seq) technology (Nudelman et al. 2018). The single cell RNA-seq technology was applied to profile the transcriptome of early zebrafish PGCs (primordial germ cells) at 3 different embryonic stages such at 6, 11 and 24 hpf. This study revealed expression of about 5099 to 7376 genes (Zhang et al. 2019). Rauwerda et al. (2017) found 6734 transcribed genes through high-resolution time-course analysis from 5 to 8 hpf stages of embryos. Recently, the full-length transcriptome sequencing of unfertilized eggs was conducted by using PacBio RS II sequence technology (Mehjabin et al. 2019).

1.9 Some proteomics approaches in developmental biology

Proteomics help to understand mechanisms of development (Knoll-Gellida et al. 2006, Ziv et al. 2008, Kristoffersen et al. 2009, Samaee et al. 2009, Yang et al. 2019). Proteomics analysis provides a full overview of proteins (function, structure, post-translational modifications and interaction) in the cell, tissue, or organism at different developmental stages. There are four major steps in every proteomics method: i) sample quality check, ii) sample preparation, iii) protein separation, and iv) protein identification and quantification (Deracinois et al. 2013). Different types of proteomics approaches are available including gel-based and non-gel-based approaches such as label-free quantification and labelled quantification (Zhu et al. 2009, Abdallah et al. 2012, Pappireddi et al. 2019). Mass spectrometry is the key technology in the proteomics field. It is a robust investigative technique applied to identify and quantify known proteins within a given sample. It also reveals the structure and chemical nature of various molecules. The entire procedure involves the transition of the sample into gaseous ions, with or without fragmentation, and identifies their respective mass to charge ratios *m/z* and abundance (Pitt 2009).

1.9.1 Gel-based quantification

This is a classical proteomics approach. Separation of sample is carried out either by "in-gel" electrophoresis approach or "off gel" chromatography approach that pre-fractionates proteins/peptides into separate liquid fractions with an immobilized pH gradient gel strip for further proteomics analysis. Two-dimensional electrophoresis (2-DE) is the most common "in-gel" electrophoresis. In the first dimension, proteins are separated based on the net charge at different pH values through isoelectric focusing, and the second dimension of separation is carried out based on the molecular weight. Subsequently, proteins are quantified with mass spectroscopy (O'Farrell 1975). Today, this method can visualize over 10,000 spots corresponding to over 1000 proteins on a single 2-DE gel (Schulze & Usadel 2010). Two-dimensional difference gel electrophoresis (2D-DIGE) is an advanced version of 2-DE, making use of cyanine fluorescent dyes (Cy2, Cy3 and Cy5) to allow quantitative comparison of two to three samples in a single gel. However, 2-DE is not suitable for high throughput screening of the total proteins (Petrak et al. 2008). These techniques have some other limitations such as quantification within a specified molecular weight range (Zhu et al. 2009), poor identification of low abundant proteins (Gygi et al. 2000, Petrak et al. 2008), poor reproducibility (Lilley et al. 2002), and multiple proteins accumulation in a single spot that leads to inaccurate quantification (Abdallah et al. 2012).

1.9.2 Shotgun proteomics

The non-gel-based, "shotgun" proteomic methods such as multidimensional protein identification (MudPIT) overcomes some problems occurring in the gel-based methods. It is suitable for analysing large-scale protein expression and characterization of complex samples (Domon & Aebersold 2006, Motoyama & Yates III 2008, Pappireddi et al. 2019). Shotgun proteomics is an excellent approach for qualitative analysis. Proteins isolated from cells, tissues, embryos, or the whole organisms are digested into peptides by using proteases such as trypsin (Gundry et al. 2010). Trypsin cleaves the peptide bond at the C-termini of lysine and arginine residues to form multiple peptides based on the polarity, size and charge. These peptides are separated with reverse-phase high-performance

liquid chromatography (RP-HPLC) and subsequently identified and quantified (semi-quantitatively) using LC-MS/MS (Olsen et al. 2004, Lee et al. 2016). This technique is suitable for high-throughput screening of the total proteins. The limitation of this approach is that it is not suitable for accurate quantification and comparison of multiple samples at the same time.

For semi-quantitative analysis, MS spectra obtained after shotgun LC-MS/MS can be used to search proteins against the organism-specific non-redundant database using the Mascot search engine (Perkins et al. 1999). It calculates the Exponentially Modified Protein Abundance Index (emPAI) score of each identified protein based on protein coverage of the matched peptide in database search (Ishihama et al. 2005). Semiquantitative analysis can be used with labelled or label-free protein samples.

1.9.3 Label-free quantification

For the label-free quantitative methods, the sample preparation, separation, identification and quantification of each sample is performed individually. Quantification of proteins is based on two types of measurements: i) ion intensity changes such as peak heights or peptide peak areas in chromatography, ii) identified proteins spectral counting after MS/MS analysis (Bondarenko et al. 2002, Zhu et al. 2009, Pappireddi et al. 2019). This method is used for the relative quantification of proteins. The relative abundance can be determined as the number of detected peptides divided by the number of theoretically visible number of peptides for each protein, called a protein abundance index, PAI (Rappsilber et al. 2002). Besides, it is also possible to determine the absolute abundance of proteins, that is the absolute amount of protein in the mixture, using emPAI (Ishihama et al. 2005).

Sequential window acquisition of all theoretical mass spectra (SWATH). SWATH is a label-free quantification method, in which data-dependent acquisition (DDA) is used to generate peptide spectral library to match with the MS spectra obtained by the data-independent acquisition (DIA) (Stahl et al. 1996). The method has outstanding quantification accuracy and precision (Huang et al. 2015, Krasny et al. 2018). This is a stand-alone proteome profiling approach and can also be used to validate other

quantitative proteomics results. It is a cost-effective and less complicated protocol compared to labelled quantification methods (Figure 7). However, when the quantities between the sample differ greatly, the protein quantification may not be accurate (Li et al. 2012).
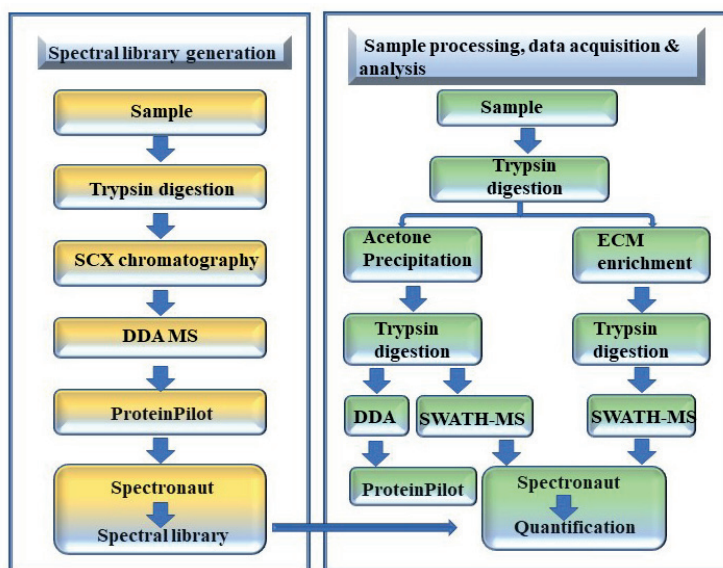
Figure 7. Schematic workflow for the identification and quantification of protein using Sequential Window Acquisition of all Theoretical mass spectra (SWATH). Preparation of spectral library (yellow), sample processing, data acquisition and analysis (green) are the vital steps in this method (Source: Krasny et al. 2018).

1.9.4 Labelled quantification: Chemical labelling

The labelling methods for relative quantification analysis are categorized into two main groups: metabolic and chemical isotope tags labelling (Abdallah et al. 2012). In chemical labelling, peptides or proteins are tagged through a chemical reaction (Schulze & Usadel 2010). In metabolic labelling, the label is introduced to the biological material through a medium (Ong et al. 2002).

Isotope-coded affinity tags (ICAT). ICAT is a gel-free MS-based proteomics method. In this technique, the isotopes are incorporated into two different samples that are to be compared. This approach uses a chemical reagent that consists of a biotin portion (as an affinity tag), a linker (incorporate the heavy or light isotopes) and a terminal group (to alkylate specifically thiol group) (Gygi et al. 1999, Chan et al. 2015). Preparation of the sample consists of steps including trypsin digestion, labelling with ICAT tag, purification by streptavidin containing beads, and analysis by LC-MS/MS (Blackstock & Mann 2000). Quantification of proteins is based on LC-MS peak areas of cysteine-containing peptides (Smolka et al. 2001). The disadvantage of this approach is that it is not suitable for multiple sample comparisons and also not applicable to cysteine-free proteins (Wiese et al. 2007, Chan et al. 2015).

Isobaric tags for relative and absolute quantification (iTRAQ). iTRAQ method is developed based on the MudPIT approach. Protein samples are fragmented using proteolytic enzymes and then chemically labelled by isobaric tags. These isobaric tags are composed of three moieties, a reporter group (based on N-methylpiperazine), a neutral balance group (carbonyl group) and a primary amine-reactive group (Ross et al. 2004). There are currently two types of iTRAQ kits available: 4-plex (4 samples labelled with 4 tags) and 8-plex (8 samples labelled with 8 tags). The reagent labels (tags) N-terminus and side chain amines of all peptides from different samples. The neutral balance group ensures that the iTRAQ labelled peptide shows the same mass to sustain an overall mass of 145 Da for 4-plex and 305 Da for 8-plex (Pierce et al. 2008, Pichler et al. 2010). In this method, equal amounts of total protein samples are digested with an enzyme, such as trypsin, to generate peptides. Different iTRAQ tags are added to peptides from different samples and covalently linked with lysine side chains and N-termini of peptides. All labelled peptides are pooled into one sample mixture. The pooled samples go through the desalting process and are subsequently fractioned by reversed-phase high-performance liquid chromatography (RP-HPLC) and examined by tandem mass spectrometry (LC-MS/MS) for both detection and quantification. The fragmented tags produce a low molecular mass reporter ions which can be utilized to relatively quantify the proteins and the corresponding peptides (Pierce et al. 2008,

Pichler et al. 2010). iTRAQ approach is used to achieve relative quantitation of proteins in complex mixtures by utilizing mass spectrometry (Ow et al. 2009). However, iTRAQ enables only a relative quantification of proteins. Another practical disadvantage is the relative quantification limited to the proteins present in all the tagged (4- or 8-plex) samples. If a given protein is present in high abundance in one of the tagged samples in a given iTRAQ set, the absence versus presence of that protein in low abundance in another sample cannot be distinguished (Figure 8).
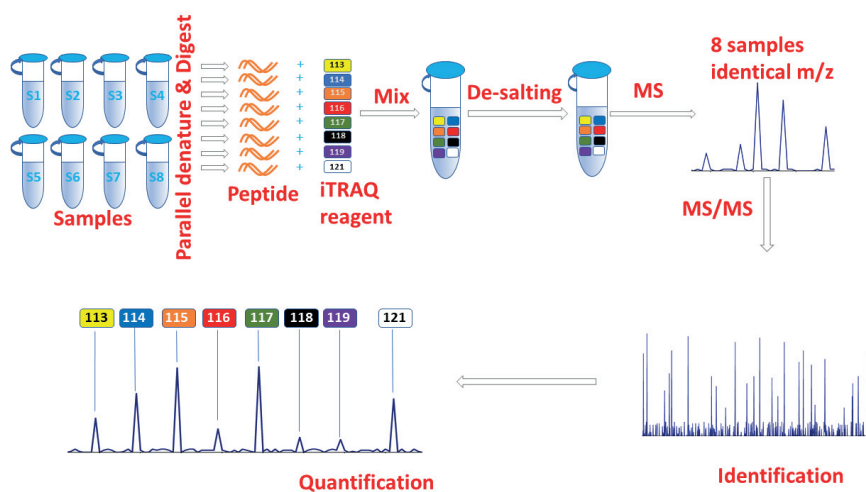
Figure 8. Schematic workflow for the identification and quantification of proteins in iTRAQ method. The process starts with a sample preparation step that consists of digestion of samples and labelling of peptides with iTRAQ reagent followed by desalting. The peptide identification is done by MS/MS. Quantification is performed by comparing the peak intensities of the iTRAQ reporter ions (Figure is prepared by Sheshanth Purushothaman; Source: modified from SCIEX).

Tandem Mas Tag (TMT). This is a chemical labelling and MS/MS-based quantitative approach (Thompson et al. 2003). It utilizes N-hydroxy succinimide (NHS) chemistry, and it has three functional groups: (i) amine-reactive group (ii) an isotopic reporter group and (iii) isotopic balancer group which can normalize the total mass of the tags (Parker et al. 2012). The amine-reactive group reacts with lysine which contains N-terminal amine groups and ε-amine groups to connect the tags to the peptides (Sturm et al. 2014).

The reagent reacts with multiple samples by chemical derivatization combined with various types of the same isobaric tag that appear as a single peak in whole MS scans. Subsequently, the daughter ions are released in the MS/MS study that can be applied for relative quantification. The advantages and disadvantages of the TMT approach are similar to those of the iTRAQ method.

1.9.5 Labelled quantification - Metabolic labelling

Stable Isotopic Labelling with Amino Acids in Cell Culture (SILAC). This is a metabolic labelling quantitative approach, via the substitution of only one or two amino acids of the growth medium with stable isotope (^{13}C and/or ^{15}N)-labelled amino acids (Mann 2006). Leucine, arginine or lysine are the predominantly used amino acids for the stable isotope labelling. Leucine and lysine are essential amino acids that cannot be synthesized by the cells (Ong et al. 2002). Although arginine is not an essential amino acid in the vertebrate animals, it is an essential amino acid in cell culture (Ong et al. 2003). Therefore, after several rounds of cell culture, stable-isotope-labelled amino acids in the culture media can be essentially incorporated into all proteins of the cells. In MS spectra, every single peptide occurs as a pair and the peak intensities yield ratio of the protein abundance in the sample (Geiger et al. 2010, Abdallah et al. 2012). This approach produces large amounts of labelled proteins, which facilitate pre-fractionation or enrichment processes that can improve the coverage and sensitivity of LC/MS analysis. However, the labelling process requires lengthy cell culture and the process should be performed under sterile conditions (Becker 2008). Also, similar to the ICAT approach, it is difficult to compare multiple samples using SILAC labelling strategy (Figure 9).
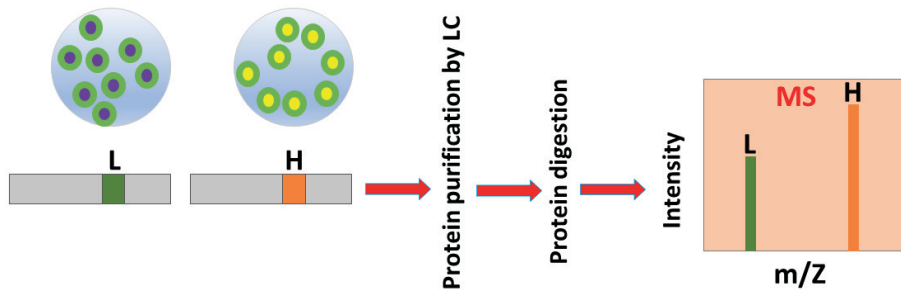
Figure 9. Schematic representation of Stable Isotopic Labelling with Amino Acids in Cell Culture (SILAC) method principle. Samples are incubated in a medium containing light (L) and heavy (H) arginine or lysine. The lysates from the two conditions are combined and purified with LC. The purified proteins are then digested and subsequently, the peptides are quantified by LC-MS/MS (Figure prepared by Sheshanth Purushothaman).

1.9.6 Immunohistochemistry (IHC)

Immunohistochemistry (IHC) is a technique that employs antibodies to determine the spatial distribution of a specific antigen based on antigen-antibody interaction. The immune reactive products are located by applying various markers including fluorescence dyes, enzymes, radioactive elements, colloidal gold and chromogenic substrate (Coons & Kaplan 1950, Mason & Sammons 1978, Duraiyan et al. 2012). The samples (both frozen and fresh) are fixed with fixative agents, embedded and sectioned. The sliced sections are treated with targeted antibodies. Fluorescent dyes allow separate detection of co-localized targets (Duraiyan et al. 2012), and it is easier to locate low and high abundant target proteins on the same slide. This method cannot be used for quantification. The major drawbacks of this technique are unavailability of many antibodies, high cost of reagents, and sensitivity to salt contamination. Also, high variability due to insufficient enzymatic digestion can reduce the accuracy of the results (Roche et al. 2006, Buchwalow & Böcker 2010, Duraiyan et al. 2012, Dabbs 2017).

1.10 Proteome studies in zebrafish and other polylecithal animals

Proteome studies have been carried out on adult zebrafish testis and ovary (Groh et al. 2011), gills (De Souza et al. 2009), brain (Singh et al. 2010) and heart (Zhang et al. 2010). However, knowledge of proteome in early stage zebrafish embryos is limited due to the vast abundance of yolk proteins, notably Vitellogenins, masking the presence of less abundant proteins (Link et al. 2006, Gündel et al. 2007). Fifty-one proteins have been detected in 8 hpf zebrafish embryos through mass spectrometry (MS) combined with two-dimensional gel electrophoresis (Link et al. 2006). In another analysis performed using liquid chromatography/ mass spectrometry (LC/MS), 509 and 210 proteins were found in zebrafish embryos at 72 and 120 hpf, respectively (Lin et al. 2009), whereas in a yet another study a total of 1384 proteins were identified in 72 and 120 hpf zebrafish embryos, utilizing two-dimensional liquid chromatography coupled to tandem mass spectrometry, 2DLC-MS/MS (Lucitt et al. 2008). Some proteins were characterized in ten developmental stages of zebrafish embryos (6 hpf to 1 week post-fertilization) (Tay et al. 2006). Another proteome study was carried out during 5 dpf of the zebrafish embryos by applying LC-MS/MS. In total, 159 proteins were identified (Rahlouni et al. 2015). The above studies detected not many proteins due to lack of proper deyolking methods.

Proteomic studies have also been performed on embryos of other polylecithal animals. Several proteomic approaches were utilized to *Xenopus laevis* embryos, including mass spectrometry (Smits et al. 2014), iTRAQ-based mass spectrometry (Sun et al. 2014), or tandem mass tag (TMT)-based LC/MS (Peshkin et al. 2015) to identify thousands of proteins during embryonic development. Interestingly, more than 11,000 proteins were identified in unfertilized *Xenopus laevis* eggs (Wühr et al. 2014). A recent study by Zhu et al. (2020) on chicken (*Gallus gallus*) egg yolk proteins employed a combined approach involving 2-dimensional gel electrophoresis (2-DE) and matrix-assisted laser desorption/ ionization time-of-flight tandem mass spectrometry (MALDI-TOF).

Until now, all proteome profile analyses of zebrafish embryos have been performed from the shield stage (6 hpf) onwards. There are no published studies yet focusing on

earlier developmental stages, in cleavage and blastula periods. Therefore, information regarding the dynamics of maternal and newly synthesized zygotic proteins would provide new insights into crucial events during early embryogenesis of zebrafish.

2. Objectives

The general objective of this PhD study was to **identify and characterize the proteome of zebrafish embryos during early developmental stages**.

The specific objectives were:

1) To develop an efficient procedure for reducing the amount of yolk in early zebrafish embryos to enable LC-MS/MS-based proteomics (**Paper I**).

2) To elucidate the proteome of vegetal part of embryos during the early development of zebrafish (**Paper II**).

3) To illuminate protein dynamics during early development of zebrafish embryos (**Paper III**).

3. General discussion

The aim of this study was to understand the identity and functions of proteins with critical roles during the early developmental stages of zebrafish. The approaches adopted in the study, divided into three reports (**Papers I-III**), are illustrated in Figure 10. The primary task was to identify the proteins from the early embryos. In this context, it should be noted that it is difficult to accurately identify most of the proteins due to that the polylecithal embryos, like those of zebrafish, contain a very high amount of yolk proteins. Yolk proteins are mainly comprised of Vitellogenins, and this overwhelming abundance interferes in detection of other proteins. To overcome this challenge, we employed dechorionation and deyolking treatment, which allowed us to remove the whole chorion and most of the yolk portion (**Paper I**). This improved procedure to remove the yolk was compared with the existing procedure by Link et al. (2006). Liquid chromatography-tandem mass spectrometry (LC-MS/MS)-based shotgun proteomics was employed to identify proteins associated with selected developmental stages of zebrafish. We adapted the deyolking procedure for the early stages of zebrafish embryonic development (1-, 16-, 32-cell, oblong and bud stages). This strategy enabled to obtain the first insight into early developmental stage-linked proteome of zebrafish. Proteomic analyses of such early stages have not previously been reported.

In **Paper II**, the proteome of vegetal part of zebrafish embryo was characterized based on the zygote and cleavage stages. Among others, the study demonstrated the presence of translational machinery and active translation in the vegetal cytoplasm at the onset of the development. Vegetal proteome at the early stages (1-, 16- and 32- cell stages) of development has not been previously reported in the literature.

To map protein dynamics during early development (unfertilized, fertilized, 1-, 4-, 16-, 32-, 128- cell, oblong, 50% epiboly and bud stages) of zebrafish embryos, relative quantification was performed utilizing isobaric tags for relative and absolute quantification (iTRAQ). The iTRAQ results were verified using independent two-dimensional liquid chromatography mass spectrometry (2 D-LC–MS) shotgun-based analysis and sequential window acquisition of all theoretical mass spectra (SWATH,

Paper III). SWATH was employed only for three developmental stages. The generated dataset provides the first zebrafish early embryonic proteome information.
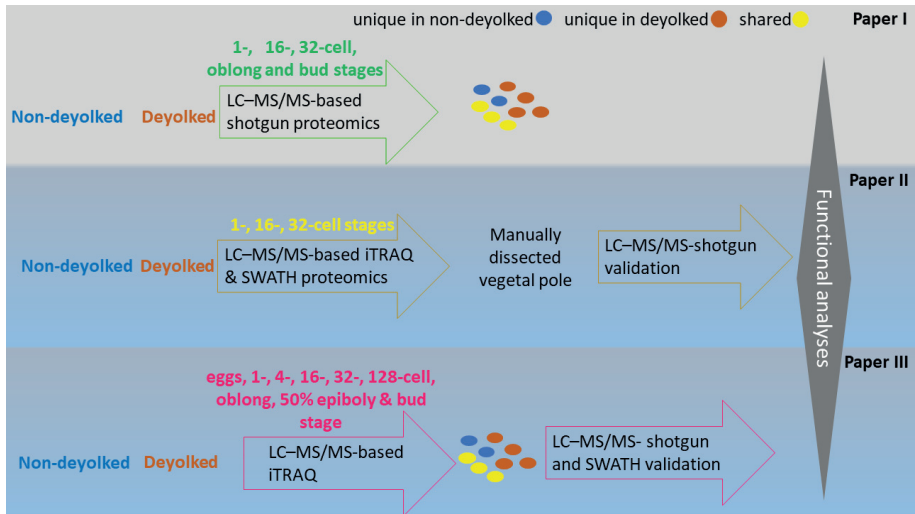
Figure 10. Schematic representation of methodological approaches. LC-MS/MS-based iTRAQ, LC-MS/MS-based shotgun and SWATH approaches were adopted to identity the proteins of different developmental stages of zebrafish. The GO term and KEGG pathway analyses gave insights into the roles of the identified proteins.

3.1. Importance of effective deyolking procedure

Non-eutherian vertebrates are characterized by the presence of variable amounts of yolk in their eggs. Vitellogenins (Vgs) are the most important yolk precursor proteins. These proteins are synthesized by the liver and the process is controlled by the estrogen signalling. Later, Vgs are secreted into the bloodstream to be incorporated into the oocytes, where they accumulate as necessary nutrients for future embryogenesis. Vitellogenesis refers to the period and process during which the vitellogenin-derived egg yolk builds up within the oocytes (Chen et al. 1997, Celius & Walther 1998, Prakash et al. 2007). Vitellogenins are conserved in insects, fishes, birds, reptiles and egg-laying mammals (Chen et al. 1997, Li & Zhang 2017). Eggs of lamprey, lung fish, frogs and toads contain moderate levels of yolk (mesolecithal eggs), whereas teleost fishes, gymnophiona (legless amphibians), birds, reptiles and monotremes (egg-laying

mammals) have substantial amount of yolk (macrolecithal or polylecithal eggs; (Finn et al. 2009). High level of yolk proteins is a methodological challenge in proteomics research because their overwhelming abundance can mask the less abundant proteins, thus limiting their identification. As demonstrated in **Papers I**, **II** and **III**, when sampled embryos were deyolked (yolk amount reduced through deyolking procedure), the number of identified proteins considerably increased as compared to non-deyolked counterparts: 2362 versus 764 (**Paper I**), and 5617 versus 2444 (**Paper III**). It is likely that the developed deyolking protocol could be employed in enhancing the detection of proteins in polylecithal eggs of other species than zebrafish (**Paper I**). It should be noted that compared to the existing protocol (Link et al. 2006), the lower temperature and shorter time of the dechorionation step in our method prevented further development of embryos, particularly in the cleavage stages, thereby allowing investigations at a specific embryonic stage. Our deyolking protocol (**Paper I**) produced almost 3.1 and 2.5-fold higher yields at the 1-cell and high stage embryos, respectively, compared to the reference protocol. Most importantly, our procedure was effective enough to be applied to the earliest developmental stages of zebrafish, enabling the first insight into maternally deposited proteins as well as proteins produced from maternal transcripts.

The deyolking procedure yielded numerous proteins related to various important processes such as RNA processing, cell adhesion, RNA metabolic process, mRNA splicing and spliceosome, cell cycle, nucleic acid binding, chromatin organization, chromosome organization, protein transport, metal binding, cell apoptosis, and cell signalling pathways. These mechanisms are connected to morphology, cellular growth and proliferation and gene expression (Mathavan et al. 2005, Aanes et al. 2013, Heyn et al. 2014). Only through the deyolking procedure we could identify significant number of proteins connected to these mechanisms.

The unique proteins (deyolked vs non-deyolked) from non-deyolked samples (**Paper I**) provided clues on the proteins that were lost after deyolking. These proteins were subjected to GO enrichment analysis. **Paper I** identified unique non-deyolked proteins of 5 stages such as 1-, 16- and 32- cell, oblong and bud stages).

Table 1. Summary of unique proteins (depleted during deyolking) in non-deyolked samples 1-, 16- and 32-cell, oblong and bud stages of zebrafish embryos and the associated GO terms (**Paper I**).

GO terms	Protein names
Proteolysis	Ubiquitin-specific peptidase 14 (Usp14) and Proteasome 26S subunit, non-ATPase 6 (Psmd6)
Translation	Ribosomal protein L17 (Rpl17) and Ribosomal protein S13 (Rps13)
Protein targeting to lysosome involved in chaperone-mediated autophagy	Lysosomal-associated membrane protein 2 (Lamp2)
Ribosome biogenesis	40S Ribosomal protein S7 (Rps7), and Ribosomal protein S10 (Rps10)
Microtubule cytoskeleton organization	Microtubule-associated protein, RP/EB family, member 1a (Mapre1a) and Tubulin beta chain (tubb6)
Organelle assembly	Ezrin (Ezrb) and Ubiquitin-like-conjugating enzyme ATG3 (Atg3)
Chaperone complex	Chaperonin-containing TCP1, subunit 5 (epsilon; Cct5), and T-complex protein 1 subunit gamma (Tcp1)

Maternal-to-zygotic transition co-ordinated by the degradation of maternal mRNAs and proteins is essential for embryogenesis (Ma et al. 2001, DeRenzo & Seydoux 2004, Shin et al. 2012). There are two major pathways for degradation of intracellular proteins; autophagy-mediated lysosomal degradation and ubiquitin-proteasome-mediated degradation (Shin et al. 2013). The ubiquitin-proteasome system is responsible for the degradation of damaged or unwanted proteins through proteolysis (Rock et al. 1994).

Before the degradation of proteins by the 26S proteasome, the proteins need to be polyubiquitinated by E1/E2/E3 set of enzymes (Hershko & Ciechanover 1998, Tanaka 2009). Our study also revealed unique non-deyolked proteins which were lost during the deyolking and that target lysosomes, indicating lysosome degradation of maternal proteins (Hershko & Ciechanover 1998, Tanaka 2009). Hence, the presence of proteasomal and lysosomal machinery in zebrafish vegetal portion that we examined suggests its active role in maternal proteins' degradation during early embryogenesis. These depleted proteins are also associated with some other pathways (summarized in Table 1). This study suggests that both non-deyolked and deyolked embryos can be employed to cover maximum proteins for the proteomics studies.

3.2. Vegetal embryonic proteome

Although the process of deyolking generally increased the number of identified proteins (**Paper I**), we found that some proteins were absent in the deyolked samples as compared to the non-deyolked counterparts. It was unclear whether this was due to the presence or absence of these proteins in the yolk portion, or to their random removal during the deyolking process. We were unsuccessful to collect clean yolk samples due to small size embryos and organization of the yolk in tiny yolk granules (Halbach et al. 2020). Hence, we performed a quantitative experiment to reveal the differential abundance of proteins in deyolked versus non-deyolked samples using iTRAQ in three early developmental stages (1-, 16- and 32- cell). An independent shotgun-based LC-MS/MS qualitative study gave an indication on protein distribution in the manually dissected vegetal parts (**Paper II**). Their functional terms suggested their localization to the vegetal cytoplasm rather than inside yolk granules; this was further supported by immunohistochemistry for the selected proteins (**Paper II**). These proteins were linked to active translational, post-translational, protein processing activity, protein turnover, fatty acid degradation, lysosomal degradation, axis specification, cytokinesis and epiboly formation.

Our study found both small (40S) and large (60S) ribosomal unit proteins such as S16, S5 and L24, L6, L4, respectively, in the vegetal pole of early zebrafish embryos (**Paper II**).

We also detected translation factors, including translation elongation factor 2b (eEF2b) and chaperones, including heat shock protein HSP 90-beta (HSP90β). These proteins that were present in the vegetal pole were highly enriched in translation and post-translational functional categories. This information that suggests protein translation in the vegetal pole has not yet been reported in earlier publications.

In addition, we discovered the presence of proteins linked to protein processing activities in endoplasmic reticulum (Protein disulfide-isomerase), proteasome (Proteasome 26S subunit, non-ATPase 2), and other proteins in the vegetal part of zebrafish embryos (**Paper II**). These data strongly indicate functions in fatty acid degradation and lysosomal degradation. Lipids have a vital role in cellular signalling, maintaining cellular structures and energy homeostasis (Belkhou et al. 1991, Spiegel & Merrill Jr 1996, Simons & Ikonen 1997). Nevertheless, there is a limited knowledge about the role of lipids in vertebrate embryogenesis and development. The maternally deposited lipids in the yolk are energy source for a developing organism (Heras et al. 2000, Rosa et al. 2005, Hölttä-Vuori et al. 2010). The essential fatty acids required for structural development are deposited inside yolk cells and mobilized when needed (Wiegand 1996). Zebrafish were studied for numerous aspects of lipid biology including the genes regulating lipid processing, lipid metabolism and the role of lipids in diseases (Schlegel & Stainier 2006, Flynn et al. 2009, Carten et al. 2011). We identified vegetal proteins involved in fatty acid degradation in the earliest developmental stages. Also, we found acyl-CoA dehydrogenase (Acadm) and enoyl-CoA hydratase / long-chain 3-hydroxyacyl-CoA dehydrogenase (HadhaA) in 1-cell and 16 -cell stages, and Hydroxyacyl-CoA dehydrogenase trifunctional multienzyme complex subunit beta (Hadhb) in 1-cell and 32-cell stages (**Paper II**); this supports the necessity of lipid metabolism in early embryonic nutrition.

Lysosomes are specialized organelle involved in catabolic degradation of biomacromolecules that are essential for the developing embryo, essential for the utilization of the yolk during embryogenesis (Braulke & Bonifacino 2009). We have limited knowledge about the lysosomal localizations and function during the early embryonic development. We found lysosomal-associated enzymes alpha-mannosidase

(Man2b1) and tripeptidyl-peptidase I (Tpp1) in yolk portion of early zebrafish embryos (**Paper II**). Alpha-mannosidase is a glycosidase enzyme from lysosome which is required to hydrolyse glycans from N-linked oligosaccharide glycans at different developmental stages in fishes (Seko et al. 1991, Fan et al. 2010). The presence of acid glycosidase in the yolk was previously found in *Xenopus laevis* eggs (Wall & Meleka 1985, Jorgensen et al. 2009). Selective deposition of glycosidase was also observed in the yolk of zebrafish (Fan et al. 2010). Sugars liberated from the catabolism of vitellogenin N-glycans might be used as a carbon source or N-glycan precursor in the embryo (Fan et al. 2010). Another lysosomal hydrolase, tripeptidyl-peptidase I (Tpp1) is a serine protease enzyme that functions in lysosome to cleave N-terminal exopeptidase from substrates with limited endopeptidase activity (Lin et al. 2001). Loss-of-function in *tpp1* gene causes late infantile neuronal ceroid lipofuscinosis type 2 disease (Sleat et al. 1997, Rawlings & Barrett 1999). Similarly to the proteasomal degradation process, presence of lysosome degradation process in the vegetal part of early embryos suggest an active role in the degradation of biomacromolecules contained in the yolk for the nutrition in early embryogenesis.

Embryonic axis determination is one of the key steps for the proper development of zebrafish (Gore et al. 2005). Ablation of the vegetal portion of embryos results in ventralized embryos, confirming the localization of the axis formation determinants in the vegetal embryo (Ober & Schulte-Merker 1999). Vegetal pole-ablated embryos also lack a proper formation of trunk region, mesoderm, and neuroectoderm; thus demonstrating that the signalling factors for these regions are being present in the vegetal part (Ober & Schulte-Merker 1999). Accurate localization of various maternal transcripts in the vegetal pole is mediated by an intricate network of cortical microtubules. The microtubules originating from the vegetal pole orient perpendicularly and are found to extend into the whole embryo. The microtubules help in accurate alignment of various maternal factors to the vegetal pole and help in establishing the embryonal axes (Lu et al. 2011, Tran et al. 2012). The gene *cofilin* 1 (*cfl1*) has a critical role in cytokinesis in zebrafish (Preziosi 2012). *cfl1* is important for the connection between deep cell layer (DEL), enveloping layer (EVL) and cell movements through the

zebrafish gastrulation (Lin et al. 2010). Cloutier (2011) reported that *cfl1* mutants have defective swim bladder development, and abnormal eye structure. Various proteins identified in the **Paper II** have non-nutritional functions and are involved in the development of the embryos of zebrafish. Cytoskeletal proteins such as Tubulin alpha chain (Tuba4l), Tubulin beta chain (Tubb4b), and Cofilin 1(Cfl1) were enriched in the vegetal embryos.

3.3. Early embryonic proteome

The genome in early developmental stages of zebrafish is transcriptionally inert; the first zygotic transcripts are produced at the 64-cell stage, but they become active (zygote genome activation, ZGA) only at around 10-11th stage of cell division (Heyn et al. 2014, Lee et al. 2014). Before maternal-to-zygotic transition (MZT), maternally deposited transcripts and proteins drive the development (Du et al. 2016, Winata et al. 2018, Schulz & Harrison 2019, Vastenhouw et al. 2019, Chen & Good 2020). Information about the early transcriptome appear comprehensive (Mathavan et al. 2005, Aanes et al. 2011, Vesterlund et al. 2011, Pauli et al. 2012, Aanes et al. 2013, Heyn et al. 2014, White et al. 2017, Nudelman et al. 2018, Mehjabin et al. 2019). However, data on a corresponding maternal proteome, as well as on translation products of maternal transcripts prior to ZGA, appear scarce. The current study (**Papers I**, **II**, and **III**) is one of the first major contributions to the field of early developmental proteomics in zebrafish.

3.3.1. Proteins of the unfertilized eggs

We found the presence of Palmitoyl-protein thioesterase 1 (Ppt1) in unfertilized eggs, besides the existence of Iduronate 2-sulfatase (Ids), Clathrin light chain A (Clta) and Beta-hexosaminidase (Hexa; **Paper III**). These enzymes have specific functions during lysosomal degradation of embryonic nutrients. Iduronate 2-sulfatase is essential for brain development, suggesting that the nutrients in the unfertilized eggs will be utilized also in the later stages also (Holmes 2017). Clathrin helps in the formation of coated vesicles and hexosaminidase helps in degradation of glycosphingolipids (Hepbildikler et al. 2002, Mousavi et al. 2004, Demydchuk et al. 2017). These proteins in the unfertilized

eggs were associated with the lysosome degradation process suggesting their critical role in the degradation of biomacromolecules for the nutrition in early embryogenesis.

3.3.2. Proteins of the pre-MZT to post-MZT stages

We found the presence of at least six proteins that are involved in biogenesis and regulation of miRNA: Dicer1, Argonaute-2 (Ago2), Argonaute-4 (Ago4), Piwi-like protein 1 (Piwil1), DiGeorge syndrome critical region 8 (Dgcr8) and Drosha (**Paper III**). These proteins were present in all the three phases, pre-MZT, MZT and post-MZT. Primary miRNA transcripts are processed by Microprocessor, formed by RNase III–type enzyme Drosha and the double-stranded RNA-binding protein Dgcr8, whereas further canonical processing of resulting precursor miRNAs is performed by another RNase III-type enzyme, Dicer 1 (Bartel 2004). Inactivation of *dicer-1* in zebrafish results in developmental disturbance and death of embryos by day 10 of development (Wienholds et al. 2003). miRNAs, notably miR-430 family, have important roles in regulation of early development and maternal transcript clearance (Giraldez et al. 2006). Ago proteins use miRNA as an antisense template to bind their targets, notably mRNAs, and hence have important roles in controlling the transcript stability across various stages of embryonal development and in formation of organs (Cheloufi et al. 2010). Whereas PIWI proteins, such as Piwil1, are another class of Argonaute proteins and have role in transposon silencing, notably in the germline development, using piRNAs as templates (Houwing et al. 2007). Our results indicate the involvement of miRNA and piRNA-mediated regulation in control of embryonic development of zebrafish from the earliest stages.

Pre-MZT stage proteins such as TATA-box-binding protein and TATA-box-binding protein-associated factors, as well as RNA polymerase II-related proteins were identified in the current study (**Paper III**). The transcriptome analysis of zebrafish pre-MZT stages of embryo by Ferg et al. (2007) reported that genes linked to the above-mentioned proteins belong to transcription machinery. TATA-box-binding protein-dependent transcription is required, among others, for controlling *miR-430*, a regulatory RNA essential for maternal RNA degradation (Ferg et al. 2007). TATA binding protein is required for zygotic transcription of RNA polymerase II (Pol II). During development of

mouse embryos, TBP-independent transcription of Pol II also occurs (Bártfai et al. 2004, Ferg et al. 2007). These findings suggest the involvement of TBP in the clearance of maternal RNA and zygotic transcription of certain genes during MZT.

Apolipoprotein eb (Apoeb), Keratin, type I cytoskeletal 18 (Krt18), Keratin 4 (Krt4), Histone H3.3 (H3f3a), Heat shock cognate 71 (Hspa8) and KH domain-containing, RNA-binding, signal transduction-associated 1a (Khdrbs1a) have been detected from 1-cell to bud stage (**Papers III**). Most of these proteins were also identified in **Paper I**. The present findings corroborate earlier observations of Vesterlund et al. (2011) where the corresponding set of genes had similar expression dynamics. In addition, as detected in our study, the maximum expression was noted at 50% epiboly (Vesterlund et al. 2011). The RNA binding protein Khdrbs1 recognizes the effector proteins involved in regulating mRNA stability and decay during the MZT stage of zebrafish (Vejnar et al. 2018). Wang et al. (2018) reported that *khdrbs* is involved in the vertebrate brain development. The gene *apoeb* is essential in zebrafish fin and scale morphogenesis (Wang et al. 2006). The keratin *krt4* is involved in the regulation of epidermal development in zebrafish (Eisenhoffer et al. 2017). *h3f3a* is one of the genes that encode histone H3.3, having functions in cell proliferation and formation of head skeleton mesoderm-like ectomesenchymal precursors in zebrafish (Cox et al. 2012). The *hspa8* gene has a critical role during normal lens development in the zebrafish eye (Krone et al. 2003). The constant presence of these proteins (**Paper III**) and transcripts (Vesterlund et al. 2011) throughout the early development suggests their constitutive role across maternal, maternal-to-zygotic, and zygotic phases of the developmental control.

The current study identified another protein, Polo-like kinase 1 (Plk1), that is constitutively present from 1- cell to 128-cell stage and the abundance this protein also increases drastically from oblong stage (**Paper III**). The *plk1* is known to be crucial for mitosis in the early embryonic development of zebrafish. *plk1* depletion results in mitotic arrest and finally death by 6 days post-fertilization in zebrafish (Jeong et al. 2010). The current observations aligned with the report of Jeong et al. (2010) and likely indicate that the proteins are involved in mitotic division during the embryonic development.

Of the multiple proteins identified and quantified (**Paper III**), several showed interesting features. Transcripts corresponding to the genes *bucky ball (buc)*, and microtubule actin crosslinking factor 1, *macf1* (Bontems et al. 2009, Escobar-Aguirre et al. 2017, Fuentes et al. 2018) have been reported to be highly enriched in early embryos of zebrafish. The *macf1* has a vital role in maintaining animal-vegetal coordinates and cytoskeleton establishment during early embryogenesis of zebrafish. This gene product works as a linker between actin filaments, microtubules and intermediate filaments, and regulate Balbiani body (Bp) disassembly and nucleus positioning, which are crucial events for cell polarity (Bontems et al. 2009, Gupta et al. 2010, Escobar-Aguirre et al. 2017). Buc is a germ plasm marker and has a critical role in the establishment of animal-vegetal axis in zygotes through Bp formation, besides its role in maternal transcript localisation in cytoplasm of early oocytes (Marlow & Mullins 2008, Bontems et al. 2009, Riemer et al. 2015). In our study, Buc was present only at the 32-cell stage, indicating either the synthesis of this protein from maternal transcript and the immediate degradation or, more likely, showing the inability to detect it in other stages due to the insufficient sensitivity of the methods used. Macf1, on the other hand, was present in all the stages and we observed a gradual increasing trend in its abundance from 1-cell to bud stage (**Paper III**), which suggests that it is first maternally deposited and then translated from both maternal and zygotic transcripts. The Macf1 has a crucial role in the regulation of animal-vegetal coordinates and cytoskeleton establishment throughout the embryonic development.

Maternal Insulin-like growth factor-2 mRNA binding proteins 3 (Igf2bp3) is crucial for early embryo development of zebrafish (Ren et al. (2020). The maternal *igf2bp3* mutants had various aberrations including defective cell division and cytoskeleton assembly during early embryonic stages of development. GO analysis showed *igf2bp3* enrichment in RNA regulation and metabolism, epigenetic modification processes, cell division and cytoskeleton organization (Ren et al. 2020). In the present study, Igf2bp3 was detected throughout all the stages (**Paper III**), indicating the crucial role of this protein in RNA regulation, cell division and cytoskeleton organization during pre-MZT, MZT and post-MZT stages of zebrafish embryonic development.

The transcript of *claudin* was accumulated during early zebrafish development and it was associated with cell regulation and cell adhesion (Mathavan et al. 2005). Claudin is necessary to maintain tight junction contacts between two cell layers during the formation of epiboly (Gupta & Ryan 2010). In our study, we identified the protein Claudin-like protein ZF-A89, Cldnd, in **Paper III**. This suggest that this protein have a vital role in epiboly formation.

The present data indicate that proteins identified from pre-MZT to post-MZT are involved in various early developmental functions such cell division, mitosis, miRNA biosynthesis, circadian rhythms, migrations, translation, nucleic acid binding, cell regulation and cell adhesion, maternal RNA degradation, regulating mRNA stability and decay, maintaining animal-vegetal coordinates, cytoskeleton establishment, epiboly formation, and lens development during zebrafish embryogenesis.

3.4. Advances of the current proteomics study

Proteomics studies give in-depth information of the biological processes in an organism. However, the approach to study zebrafish embryos is marred by technical challenges. These challenges can be attributed to lack of sensitive techniques and presence of yolk in early embryos (Winata et al. 2018). The correlation between levels of protein and mRNA in vertebrate development helps in understanding the exact functional dynamics between them. In a study on *Xenopus laevis* embryos, it was observed that most protein data can be accurately predicted from the mRNA levels. Thus, studying the proteome could help in understanding the turnover of many of the important transcripts (Peshkin et al. 2015). It should be noted that many studies found poor correlation between transcriptome and proteome (Lichtinghagen et al. 2002, Alli Shaik et al. 2014, Smits et al. 2014). This would justify importance of proteomics studies. Zebrafish egg proteome is highly indicative of the proper embryo development. Aberrant protein expression or mis-localization of proteins results in eggs of poor quality and hence understanding the proteome of early embryos and eggs have gained significance (Yilmaz et al. 2017).

A proteomics study offers distinct advantages when compared to genomic analysis alone. Identification of peptides by mass spectrometry-based methods helps in accurately understanding the expressed genes. Thus, such proteome studies in genome sequencing projects could help in the construction of reliable translation-based databases that could validate the genome data simultaneously (Tanner et al. 2007). A similar strategy, termed as proteogenomic mapping, has been considered as a better method than genome annotation alone. Genome annotation would result in identification of open reading frames (ORFs), which could be fragments of longer ORF with no evidence for translatability. However, mapping the proteome would help in enhanced accuracy for predicting the ORF utilisation in an organism (Jaffe et al. 2004).

Proteome of early embryos of zebrafish would help in understanding the molecular events occurring during the embryogenesis. Earlier studies on identification of proteins in deyolked zebrafish embryos met limited success in its magnitude as the deyolking methods were not optimized. Hence, development of better methods has been important (Lucitt et al. 2008, Lößner et al. 2012). There are no reports published previously on proteome of early zebrafish embryos in pre-MZT, and thus this study (**Paper I**) appears the first to elucidate such a significant observation. **Paper II** is the first quantitative proteomic study performed in order to understand the protein dynamics at the vegetal pole of early stages of zebrafish embryos. And **Paper III** is the first quantitative proteomic study that has been achieved on early stages of zebrafish embryos.

3.5. Strengths and limitations of the methodological approaches

Several labelled quantification methods such as Isotope-coded affinity tags (ICAT), Isobaric tags for relative and absolute quantitation (iTRAQ), Tandem mass tag (TMT), and Stable isotopic labelling with amino acids in cell culture (SILAC) have been developed for analyzing the proteins in various samples. iTRAQ and TMT utilize chemical labelling approach whereas SILAC uses a metabolic labelling method to tag specific amino acids. ICAT labelling cannot be used for cysteine-free proteins and for comparison of multiple samples (Chan et al. 2015) see also *Section 1.9*). iTRAQ and TMT label all the digested

peptides combined with extensive separation (such as 2-D LC) prior to MS, which allow for high coverage of the proteome. Both techniques, allow for multiplexing, that is simultaneous comparison of multiple samples within a single experiment. iTRAQ for relative quantification has not been utilized before for the studies of early zebrafish embryos (**Papers II and III**). Shotgun-based proteomics can be easily applied for high-throughput studies and for analysis of complex protein samples. Before the advent of labelling techniques, proteome analysis was performed by gel-based quantification such as 2-dimensional gel electrophoresis (2-DE) and matrix-assisted laser desorption/ ionization time-of-flight tandem mass spectrometry (Zhu et al. 2020). The utilisation of labelling techniques has helped in overcoming the limitations associated with gel-based quantification such as inaccurate quantification of proteins in spots due to presence of multiple proteins, lack of accurate identification of low abundant proteins and limited dynamics range (Petrak et al. 2008, Zhu et al. 2009, Abdallah et al. 2012). Although the iTRAQ analyses provide information regarding the abundance dynamics of individual proteins in different developmental stages, iTRAQ cannot generate data of proteins that are completely absent at least in one of the developmental stages. This is due to precursor ion selection (sometimes there are ions having close m/z values because the selected precursor that may enter the collision cell and contribute towards the background signals of the reporter ions) and the impurity of isotopes (the isotopes used to label each channel are not 100% pure). Thus, they also contribute to the signals of adjacent reporter channels.

Shotgun method helped to confirm the presence or absence of a particular protein in a particular developmental stage (**Paper III**). Shotgun method can also provide semiquantitative information of the identified proteins. We have also used this approach to compare the protein abundances (semi-quantitative data) of non-deyolked and deyolked samples and to evaluate the efficiency of the deyolking method (**Paper I**). The shotgun LC-MS/MS method is very useful for semiquantitative calculation of the proteins. The shotgun LC-MS/MS technique is applicable for screening of proteins and can identify a greater number of proteins from limited protein samples compared to a gel-based- LC-MS (Link et al. 2006, Tay et al. 2006, Lucitt et al. 2008).

To validate the presence of proteins in different developmental stages, it is essential to use targeted methods like single reaction monitoring/multiple reaction monitoring (SRM/MRM) or SWATH MS. In our study, we opted for more advanced targeted method, SWATH MS, which is a data-independent acquisition (DIA) approach that allows accurate and reproducible label-free quantification of proteins (Krasny et al. 2018). This validation method has better sensitivity and accuracy than the traditional ELISA-based methods for detection to quantify proteins from many samples. The acquired data from SWATH MS method aligned with iTRAQ results and helped to validate the differentially abundant proteins from both deyolked and non-deyolked samples (**Paper II**), as well as the presence of proteins in a particular stage (**Paper III**). In this study, 1D-LCMS was performed with SWATH analysis (**Paper II**); here, the coverage of the proteome is not as good as the iTRAQ with 2D-LCMS. SWATH with 2D-LCMS would be difficult to achieve due to technical issues, and impractical due to long analysis time and high cost involved.

Immunohistochemistry (IHC) helps to localize the interesting proteins in the tissues by using appropriate fluorophore tagged antibodies. In this study, IHC was initially performed with fluorescence secondary antibody and images were captured with fluorescence microscope. To reconfirm the fluorescence imaging results, we used bright field immunohistochemistry by using normal secondary antibody and bright field microscopy to complement the immunofluorescent study (**Paper II**).

4. Conclusions

In conclusions (Figure 11), in this PhD project we:

- Developed an improved deyolking procedure, which enabled for the proteome analysis in early zebrafish embryos for the first time (**Paper I**).

- Identified the vegetal part proteins that are associated with active translational, post-translational, protein processing activity, protein turnover, fatty acid degradation, lysosomal degradation, axis specification, cytokinesis and epiboly formation (**Paper II**).

- Identified proteome of unfertilized eggs (**Paper III**).

- Identified proteins that are supplied maternally as well as those translated from maternal and zygotic transcripts (**Paper III).**

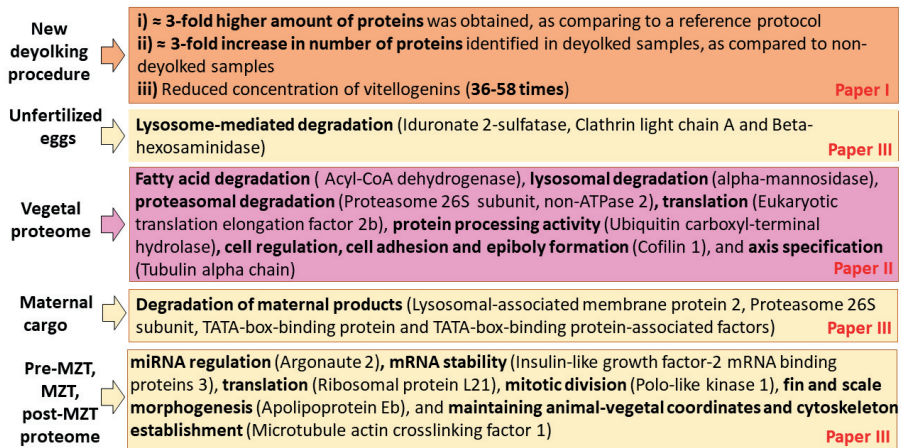|	
New deyolking procedure	**i) ≈ 3-fold higher amount of proteins** was obtained, as comparing to a reference protocol **ii) ≈ 3-fold increase in number of proteins** identified in deyolked samples, as compared to non-deyolked samples **iii)** Reduced concentration of vitellogenins (**36-58 times**) **Paper I**
Unfertilized eggs	**Lysosome-mediated degradation** (Iduronate 2-sulfatase, Clathrin light chain A and Beta-hexosaminidase) **Paper III**
Vegetal proteome	**Fatty acid degradation** (Acyl-CoA dehydrogenase), **lysosomal degradation** (alpha-mannosidase), **proteasomal degradation** (Proteasome 26S subunit, non-ATPase 2)**, translation** (Eukaryotic translation elongation factor 2b), **protein processing activity** (Ubiquitin carboxyl-terminal hydrolase)**, cell regulation, cell adhesion and epiboly formation** (Cofilin 1), and **axis specification** (Tubulin alpha chain) **Paper II**
Maternal cargo	**Degradation of maternal products** (Lysosomal-associated membrane protein 2, Proteasome 26S subunit, TATA-box-binding protein and TATA-box-binding protein-associated factors) **Paper III**
Pre-MZT, MZT, post-MZT proteome	**miRNA regulation** (Argonaute 2)**, mRNA stability** (Insulin-like growth factor-2 mRNA binding proteins 3), **translation** (Ribosomal protein L21), **mitotic division** (Polo-like kinase 1), **fin and scale morphogenesis** (Apolipoprotein Eb), and **maintaining animal-vegetal coordinates and cytoskeleton establishment** (Microtubule actin crosslinking factor 1) **Paper III**

Figure 11. Schematic representation of main conclusions made in this thesis work.

5. Future perspectives

The developed effective deyolking procedure (**Paper I**) can be applied in order to understand the yolk proteins of other polylecithal animals such as teleost fishes, gymnophiona (legless amphibians), reptiles and birds. Additional studies have to be performed to understand the detailed mechanisms involved in the events of early embryogenesis. For example, mRNA and small RNA analysis of manually dissected embryos from 3 cleavage stages (**Paper II**) and all described developmental stages in **Paper III** could be employed to infer the mechanisms underlying early embryonic development. This additional information will provide a molecular picture of zebrafish early embryogenesis and advance our understanding of the temporal and spatial knowledge of early embryogenesis. Proteins such as Eukaryotic translation elongation factor 2b (eEf2b), Elongation factor 1-alpha (eEf1α), Ribosomal protein S16 (Rps16) and chaperones, such as Heat shock protein HSP 90-beta (Hsp90β) have been found in vegetal part of cleavage stage embryos (**Paper II**). However, detailed mechanisms of their function remain unclear. Characterization of these proteins with CRISPR-mediated knockout assay can be done to unveil their functions during cleavage stage of zebrafish embryogenesis (Idigo et al. 2020). The transcription factor Nanog was identified at all the developmental stages (1-cell to bud stage). Previous work has shown that Nanog has a critical role in MZT. However, the function of Nanog in early embryogenesis is poorly understood. Characterization of Nanog by CRISPR-mediated knockout assay will help to understand its functions in the early embryogenesis i.e. prior to MZT stage (**Paper III**).

The deyolking protocol can be further refined to recover more proteins from the animal pole, to generate information that is not included in this PhD project. Since the abovementioned mutants such as that of Nanog is available for proteome and transcriptomic analyses on the cleavage stages, they can be used to provide insights into specific functions of the proteins of interest (Gagnon et al. 2018, Idigo et al. 2020). In addition, microscopic analysis of the cleavage stages of early embryos will throw light on defects caused by the lack of the above-mentioned proteins on vegetal or animal poles. To our knowledge, protein mutants (eEf2b, Rps16 and Hsp90β) are not yet available. Hence, future studies can look into the possibility of producing mutants to

reveal their actual functions. Overall, a combination of molecular, morphological and microscopic approaches can be employed to functionally dissect the mechanisms and functions of genes/proteins of interest. Taken together, the strategy will help in our understanding of the mechanisms governing early embryogenesis.

6. References

Aanes H, Winata CL, Lin CH, Chen JP, Srinivasan KG, Lee SG, Lim AY, Hajan HS, Collas P, Bourque G, Gong Z, Korzh V, Aleström P, Mathavan S (2011) Zebrafish mRNA sequencing deciphers novelties in transcriptome dynamics during maternal to zygotic transition. Genome Research 21:1328-1338

Aanes H, Collas P, Aleström P (2013) Transcriptome dynamics and diversity in the early zebrafish embryo. Briefings in Functional Genomics 13:95-105

Abdallah C, Dumas-Gaudot E, Renaut J, Sergeant K (2012) Gel-based and gel-free quantitative proteomics approaches at a glance. International Journal of Plant Genomics 2012:1- 17

Alli Shaik A, Wee S, Li RHX, Li Z, Carney TJ, Mathavan S, Gunaratne J (2014) Functional mapping of the zebrafish early embryo proteome and transcriptome. Journal of Proteome Research 13:5536-5550

Amsterdam A, Burgess S, Golling G, Chen W, Sun Z, Townsend K, Farrington S, Haldi M, Hopkins N (1999) A large-scale insertional mutagenesis screen in zebrafish. Genes and Development 13:2713-2724

Arab S, Gramolini AO, Ping P, Kislinger T, Stanley B, van Eyk J, Ouzounian M, MacLennan DH, Emili A, Liu PP (2006) Cardiovascular proteomics: tools to develop novel biomarkers and potential applications. Journal of the American College of Cardiology 48:1733-1741

Avilés-Pagán EE, Orr-Weaver TL (2018) Activating embryonic development in *Drosophila* Seminars in Cell and Developmental Biology. Elsevier, p 100-110

Baltzer F (1964) Theodor Boveri. Science 144:809-815

Barckmann B, Simonelig M (2013) Control of maternal mRNA stability in germ cells and early embryos. Biochimica et Biophysica Acta (BBA)-Gene Regulatory Mechanisms 1829:714-724

Baroux C, Autran D, Gillmor C, Grimanelli D, Grossniklaus U (2008) The maternal to zygotic transition in animals and plants Cold Spring Harbor Symposia on Quantitative Biology. Cold Spring Harbor Laboratory Press, p 89-100

Bartel DP (2004) MicroRNAs: genomics, biogenesis, mechanism, and function. Cell 116:281-297

Bártfai R, Balduf C, Hilton T, Rathmann Y, Hadzhiev Y, Tora L, Orbán L, Müller F (2004) TBP2, a vertebrate-specific member of the TBP family, is required in embryonic development of zebrafish. Current Biology 14:593-598

Baxendale S, Whitfield TT (2014) Zebrafish inner ear development and function. In: Romand R, Varela-Nieto I (eds) Development of Auditory and Vestibular Systems. Elsevier, Amesterdam, The Netherlands, p 63-105

Bazzini AA, Lee MT, Giraldez AJ (2012) Ribosome profiling shows that miR-430 reduces translation before causing mRNA decay in zebrafish. Science 336:233-237

Beams HW, Kessel RG, Shih CY, Tung HN (1985) Scanning electron microscope studies on blastodisc formation in the zebrafish, *Brachydanio rerio*. Journal of Morphology 184:41-49

Becker GW (2008) Stable isotopic labeling of proteins for quantitative proteomic applications. Briefings in Functional Genomics and Proteomics 7:371-382

Behrndt M, Salbreux G, Campinho P, Hauschild R, Oswald F, Roensch J, Grill SW, Heisenberg C-P (2012) Forces driving epithelial spreading in zebrafish gastrulation. Science 338:257-260

Belkhou R, Cherel Y, Heitz A, Robin J-P, Le Maho Y (1991) Energy contribution of proteins and lipids during prolonged fasting in the rat. Nutrition Research 11:365-374

Bensch R, Song S, Ronneberger O, Driever W (2013) Non-directional radial intercalation dominates deep cell behavior during zebrafish epiboly. Biology Open 2:845-854

Bettegowda A, Lee K-B, Smith GW (2007) Cytoplasmic and nuclear determinants of the maternal-to-embryonic transition. Reproduction, Fertility and Development 20:45-53

Blackstock W, Mann M (2000) Proteomics: A Trends Guide. Elsevier, Amesterdam, The Netherlands

Blythe SA, Wieschaus EF (2015) Coordinating cell cycle remodeling with transcriptional activation at the *Drosophila* MBT. Current Topics in Developmental Biology 113:113-148

Bondarenko PV, Chelius D, Shaler TA (2002) Identification and relative quantitation of protein mixtures by enzymatic digestion followed by capillary reversed-phase liquid chromatography– tandem mass spectrometry. Analytical Chemistry 74:4741-4749

Bontems F, Stein A, Marlow F, Lyautey J, Gupta T, Mullins MC, Dosch R (2009) Bucky ball organizes germ plasm assembly in zebrafish. Current Biology 19:414-422

Bourc'his D, Xu GL, Lin CS, Bollman B, Bestor TH (2001) Dnmt3L and the establishment of maternal genomic imprints. Science 294:2536-2539

Braulke T, Bonifacino JS (2009) Sorting of lysosomal proteins. Biochimica et Biophysica Acta 1793:605-614

Briggs E, Wessel GM (2006) In the beginning… animal fertilization and sea urchin development. Developmental Biology 300:15-26

Bruce AEE (2016) Zebrafish epiboly: Spreading thin over the yolk. Developmental Dynamics 245:244-258

Buchwalow IB, Böcker W (2010) Immunohistochemistry. Basics and Methods 1:1-149

Burns KH, Viveiros MM, Ren Y, Wang P, DeMayo FJ, Frail DE, Eppig JJ, Matzuk MM (2003) Roles of NPM2 in chromatin and nucleolar organization in oocytes and embryos. Science 300:633-636

Burton GJ, Hempstock J, Jauniaux E (2001) Nutrition of the human fetus during the first trimester—a review. Placenta 22:S70-S77

Burton GJ, Watson AL, Hempstock J, Skepper JN, Jauniaux E (2002) Uterine glands provide histiotrophic nutrition for the human fetus during the first trimester of pregnancy. The Journal of Clinical Endocrinology & Metabolism 87:2954-2959

Callard GV, Tarrant AM, Novillo A, Yacci P, Ciaccia L, Vajda S, Chuang G-Y, Kozakov D, Greytak S, Sawyer S (2011) Evolutionary origins of the estrogen signaling system: insights from amphioxus. The Journal of Steroid Biochemistry and Molecular Biology 127:176-188

Carroll DJ, Albay DT, Hoang KM, O'Neill FJ, Kumano M, Foltz KR (2000) The relationship between calcium, MAP kinase, and DNA synthesis in the sea urchin egg at fertilization. Developmental Biology 217:179-191

Carten JD, Bradford MK, Farber SA (2011) Visualizing digestive organ morphology and function using differential fatty acid metabolism in live zebrafish. Developmental Biology 360:276-285

Celius T, Walther BT (1998) Oogenesis in Atlantic salmon (*Salmo salar L.*) occurs by zonagenesis preceding vitellogenesis in vivo and in vitro. Journal of Endocrinology 158:259-266

Chan JCY, Zhou L, Chan ECY (2015) The isotope‐coded affinity tag method for quantitative protein profile comparison and relative quantitation of cysteine redox modifications. Current Protocols in Protein Science 82:23.22. 21-23.22. 19

Cheloufi S, Dos Santos CO, Chong MM, Hannon GJ (2010) A dicer-independent miRNA biogenesis pathway that requires Ago catalysis. Nature 465:584-589

Chen H, Good MC (2020) Imaging nascent transcription in wholemount vertebrate embryos to characterize zygotic genome activation. Methods in Enzymology 638:139-165

Chen J-S, Sappington TW, Raikhel AS (1997) Extensive sequence conservation among insect, nematode, and vertebrate vitellogenins reveals ancient common ancestry. Journal of Molecular Evolution 44:440-451

Chen J, Streit A (2013) Induction of the inner ear: stepwise specification of otic fate from multipotent progenitors. Hearing Research 297:3-12

Chisholm RL, Firtel RA (2004) Insights into morphogenesis from a simple developmental system. Nature Reviews Molecular Cell Biology 5:531-541

Chrispijn ND, Andralojc KM, Castenmiller C, Kamminga LM (2018) Gene expression profile of a selection of Polycomb Group genes during zebrafish embryonic and germ line development. PloS One 13:e0200316

Cloutier H (2011) The role of actin-binding protein Cofilin 1 in *Danio rerio* embryonic development. Electronic Theses and Dissertations:1605

Coons AH, Kaplan MH (1950) Localization of antigen in tissue cells: II. Improvements in a method for the detection of antigen by means of fluorescent antibody. The Journal of Experimental Medicine 91:1

Coticchio G, Dal Canto M, Mignini Renzini M, Guglielmo MC, Brambillasca F, Turchi D, Novara PV, Fadini R (2015) Oocyte maturation: gamete-somatic cells interactions, meiotic resumption, cytoskeletal dynamics and cytoplasmic reorganization. Human Reproduction Update 21:427-454

Cox SG, Kim H, Garnett AT, Medeiros DM, An W, Crump JG (2012) An essential role of variant histone H3.3 for ectomesenchyme potential of the cranial neural crest. PLoS Genetics 8:e1002938

Dabbs DJ (2017) Diagnostic Immunohistochemistry E-Book: Theranostic and Genomic Applications. Elsevier Health Sciences, Amsterdam, The Netherlands

Davidson EH (1990) How embryos work: a comparative view of diverse modes of cell fate specification. Development 108:365-389

De Robertis EM, Larrain J, Oelgeschläger M, Wessely O (2000) The establishment of Spemann's organizer and patterning of the vertebrate embryo. Nature Reviews Genetics 1:171-181

De Souza AG, MacCormack TJ, Wang N, Li L, Goss GG (2009) Large-scale proteome profile of the zebrafish (*Danio rerio*) gill for physiological and biomarker discovery studies. Zebrafish 6:229-238

Demydchuk M, Hill CH, Zhou A, Bunkóczi G, Stein PE, Marchesan D, Deane JE, Read RJ (2017) Insights into hunter syndrome from the structure of iduronate-2-sulfatase. Nature Communications 8:15786

Deracinois B, Flahaut C, Duban-Deweer S, Karamanos Y (2013) Comparative and quantitative global proteomics approaches: an overview. Proteomes 1:180-218

DeRenzo C, Seydoux G (2004) A clean start: degradation of maternal proteins at the oocyte-to-embryo transition. Trends in Cell Biology 14:420-426

Deshpande G, Calhoun G, Schedl P (2004) Overlapping mechanisms function to establish transcriptional quiescence in the embryonic *Drosophila* germline. Development 131:1247-1257

Despic V, Dejung M, Gu M, Krishnan J, Zhang J, Herzel L, Straube K, Gerstein MB, Butter F, Neugebauer KM (2017) Dynamic RNA–protein interactions underlie the zebrafish maternal-to-zygotic transition. Genome Research 27:1184-1194

Dhillon SS, Torell F, Donten M, Lundstedt-Enkel K, Bennett K, Rännar S, Trygg J, Lundstedt T (2019) Metabolic profiling of zebrafish embryo development from blastula period to early larval stages. PloS One 14:e0213661

Domon B, Aebersold R (2006) Mass spectrometry and protein analysis. Science 312:212-217

Dooley K, Zon LI (2000) Zebrafish: a model system for the study of human disease. Current Opinion in Genetics and Development 10:252-256

Dosch R, Wagner DS, Mintzer KA, Runke G, Wiemelt AP, Mullins MC (2004) Maternal control of vertebrate development before the midblastula transition: mutants from the zebrafish i. Developmental Cell 6:771-780

Du Z, Chen X, Li X, He K, Ji S, Shi W, Hao A (2016) Protein palmitoylation activate zygotic gene expression during the maternal-to-zygotic transition. Biochemical and Biophysical Research Communications 475:194-201

Duraiyan J, Govindarajan R, Kaliyappan K, Palanisamy M (2012) Applications of immunohistochemistry. Journal of Pharmacy & Bioallied Sciences 4:S307

Dutta A, Sinha DK (2017) Zebrafish lipid droplets regulate embryonic ATP homeostasis to power early development. Open Biology 7:170063

Edson MA, Nagaraja AK, Matzuk MM (2009) The mammalian ovary from genesis to revelation. Endocrine Reviews 30:624-712

Eisenhoffer GT, Slattum G, Ruiz OE, Otsuna H, Bryan CD, Lopez J, Wagner DS, Bonkowsky JL, Chien CB, Dorsky RI, Rosenblatt J (2017) A toolbox to study epidermal cell types in zebrafish. Journal of Cell Science 130:269-277

Ernst SG (1997) A century of sea urchin development. American Zoologist 37:250-259

Escobar-Aguirre M, Zhang H, Jamieson-Lucy A, Mullins MC (2017) Microtubule-actin crosslinking factor 1 (Macf1) domain function in Balbiani body dissociation and nuclear positioning. PLoS Genetics 13:e1006983

Essner JJ, Vogan KJ, Wagner MK, Tabin CJ, Yost HJ, Brueckner M (2002) Conserved function for embryonic nodal cilia. Nature 418:37-38

Essner JJ, Amack JD, Nyholm MK, Harris EB, Yost HJ (2005) Kupffer's vesicle is a ciliated organ of asymmetry in the zebrafish embryo that initiates left-right development of the brain, heart and gut. Development 132:1247-1260

Ettensohn CA (2017) Sea urchins as a model system for studying embryonic development. Reference Module in Biomedical Sciences Amsterdam: Elsevier

Fan X, Klein M, Flanagan-Steet HR, Steet R (2010) Selective yolk deposition and mannose phosphorylation of lysosomal glycosidases in zebrafish. The Journal of Biological Chemistry 285:32946-32953

Ferg M, Sanges R, Gehrig J, Kiss J, Bauer M, Lovas A, Szabo M, Yang L, Straehle U, Pankratz MJ, Olasz F, Stupka E, Müller F (2007) The TATA-binding protein regulates maternal mRNA degradation and differential zygotic transcription in zebrafish. The EMBO Journal 26:3945-3956

Finn RN, Kolarevic J, Kongshaug H, Nilsen F (2009) Evolution and differential expression of a vertebrate vitellogenin gene cluster. BMC Evolutionary Biology 9:1-12

Flynn EJ, Trent CM, Rawls JF (2009) Ontogeny and nutritional control of adipogenesis in zebrafish (*Danio rerio*). Journal of Lipid Research 50:1641-1652

Foe VE, Alberts BM (1983) Studies of nuclear and cytoplasmic behaviour during the five mitotic cycles that precede gastrulation in *Drosophila* embryogenesis. Journal of Cell Science 61:31-70

Fraher D, Sanigorski A, Mellett NA, Meikle PJ, Sinclair AJ, Gibert Y (2016) Zebrafish embryonic lipidomic analysis reveals that the yolk cell is metabolically active in processing lipid. Cell Reports 14:1317-1329

Fuentes R, Mullins MC, Fernández J (2018) Formation and dynamics of cytoplasmic domains and their genetic regulation during the zebrafish oocyte-to-embryo transition. Mechanisms of Development 154:259-269

Fulton T, Trivedi V, Attardi A, Anlas K, Dingare C, Arias AM, Steventon B (2020) Axis specification in zebrafish is robust to cell mixing and reveals a regulation of pattern formation by morphogenesis. Current Biology 30:2984-2994. e2983

Gagnon JA, Obbad K, Schier AF (2018) The primary role of zebrafish nanog is in extra-embryonic tissue. Development 145

Gaynes JA, Otsuna H, Campbell DS, Manfredi JP, Levine EM, Chien CB (2015) The rna binding protein Igf2bp1 is required for zebrafish rgc axon outgrowth in vivo. PloS One 10:e0134751

Ge C, Lu W, Chen A (2017) Quantitative proteomic reveals the dynamic of protein profile during final oocyte maturation in zebrafish. Biochemical and Biophysical Research Communications 490:657-663

Geiger T, Cox J, Ostasiewicz P, Wisniewski JR, Mann M (2010) Super-SILAC mix for quantitative proteomics of human tumor tissue. Nature Methods 7:383-385

Gerhard GS, Cheng KC (2002) A call to fins! Zebrafish as a gerontological model. Aging Cell 1:104-111

Giraldez AJ, Mishima Y, Rihel J, Grocock RJ, Van Dongen S, Inoue K, Enright AJ, Schier AF (2006) Zebrafish MiR-430 promotes deadenylation and clearance of maternal mRNAs. Science 312:75-79

Gore AV, Maegawa S, Cheong A, Gilligan PC, Weinberg ES, Sampath K (2005) The zebrafish dorsal axis is apparent at the four-cell stage. Nature 438:1030-1035

Gouw JW, Pinkse MW, Vos HR, Moshkin Y, Verrijzer CP, Heck AJ, Krijgsveld J (2009) In vivo stable isotope labeling of fruit flies reveals post-transcriptional regulation in the maternal-to-zygotic transition. Molecular & Cellular Proteomics 8:1566-1578

Groh KJ, Nesatyy VJ, Segner H, Eggen RI, Suter MJ-F (2011) Global proteomics analysis of testis and ovary in adult zebrafish (*Danio rerio*). Fish Physiology and Biochemistry 37:619-647

Groisman I, Jung M-Y, Sarkissian M, Cao Q, Richter JD (2002) Translational control of the embryonic cell cycle. Cell 109:473-483

Guan R, El-Rass S, Spillane D, Lam S, Wang Y, Wu J, Chen Z, Wang A, Jia Z, Keating A, Hu J, Wen XY (2013) rbm47, a novel RNA binding protein, regulates zebrafish head development. Developmental Dynamics 242:1395-1404

Gündel U, Benndorf D, von Bergen M, Altenburger R, Küster E (2007) Vitellogenin cleavage products as indicators for toxic stress in zebra fish embryos: a proteomic approach. Proteomics 7:4541-4554

Gundry RL, White MY, Murray CI, Kane LA, Fu Q, Stanley BA, Van Eyk JE (2010) Preparation of proteins and peptides for mass spectrometry analysis in a bottom‐up proteomics workflow. Current Protocols in Molecular Biology 90:10.25. 11-10.25. 23

Gupta IR, Ryan AK (2010) Claudins: unlocking the code to tight junction function during embryogenesis and in disease. Clinical Genetics 77:314-325

Gupta T, Marlow FL, Ferriola D, Mackiewicz K, Dapprich J, Monos D, Mullins MC (2010) Microtubule actin crosslinking factor 1 regulates the Balbiani body and animal-vegetal polarity of the zebrafish oocyte. PLoS Genetics 6:e1001073-e1001073

Guzel Y, Oktem O (2017) Understanding follicle growth in vitro: Are we getting closer to obtaining mature oocytes from in vitro‐grown follicles in human? Molecular Reproduction and Development 84:544-559

Gygi SP, Rist B, Gerber SA, Turecek F, Gelb MH, Aebersold R (1999) Quantitative analysis of complex protein mixtures using isotope-coded affinity tags. Nature Biotechnology 17:994-999

Gygi SP, Corthals GL, Zhang Y, Rochon Y, Aebersold R (2000) Evaluation of two-dimensional gel electrophoresis-based proteome analysis technology. Proceedings of the National Academy of Sciences 97:9390-9395

Haffter P, Granato M, Brand M, Mullins MC, Hammerschmidt M, Kane DA, Odenthal J, Van Eeden F, Jiang Y-J, Heisenberg C-P (1996) The identification of genes with unique and essential functions in the development of the zebrafish, *Danio rerio*. Development 123:1-36

Hagos EG, Dougan ST (2007) Time-dependent patterning of the mesoderm and endoderm by Nodal signals in zebrafish. BMC Developmental Biology 7:22

Halbach K, Ulrich N, Goss K-U, Seiwert B, Wagner S, Scholz S, Luckenbach T, Bauer C, Schweiger N, Reemtsma T (2020) Yolk sac of zebrafish embryos as backpack for chemicals? Environmental Science & Technology 54:10159-10169

Hao R, Bondesson M, Singh AV, Riu A, McCollum CW, Knudsen TB, Gorelick DA, Gustafsson J-Å (2013) Identification of estrogen target genes during zebrafish embryonic development through transcriptomic analysis. PloS One 8:e79020

Harrison MM, Eisen MB (2015) Transcriptional activation of the zygotic genome in *Drosophila*. Current Topics in Developmental Biology 113:85-112

Hart NH (1990) Fertilization in teleost fishes: mechanisms of sperm-egg interactions. International Review of Cytology 121:1-66

Harvey SA, Sealy I, Kettleborough R, Fenyes F, White R, Stemple D, Smith JC (2013) Identification of the zebrafish maternal and paternal transcriptomes. Development 140:2703-2710

Hepbildikler ST, Sandhoff R, Kolzer M, Proia RL, Sandhoff K (2002) Physiological substrates for human lysosomal beta -hexosaminidase S. Journal of Biological Chemistry 277:2562-2572

Heras H, Gonzalez-Baró M, Pollero RJ (2000) Lipid and fatty acid composition and energy partitioning during embryo development in the shrimp *Macrobrachium borellii*. Lipids 35:645-651

Hershko A, Ciechanover A (1998) The ubiquitin system. Annual Review of Biochemistry 67:425-479

Hertwig O (1875) Contribution to the knowledge of the formation, fertilization and division of the animal egg [*in German*]. W. Engelmann, University of Chicago, USA

Heyn P, Kircher M, Dahl A, Kelso J, Tomancak P, Kalinka AT, Neugebauer KM (2014) The earliest transcribed zygotic genes are short, newly evolved, and different across species. Cell Reports 6:285-292

Hino H, Nakanishi A, Seki R, Aoki T, Yamaha E, Kawahara A, Shimizu T, Hibi M (2018) Roles of maternal *wnt8a* transcripts in axis formation in zebrafish. Developmental Biology 434:96-107

Holley SA (2006) Anterior–posterior differences in vertebrate segments: specification of trunk and tail somites in the zebrafish blastula. Genes and Development 20:1831-1837

Holloway BA, de la Torre Canny SG, Ye Y, Slusarski DC, Freisinger CM, Dosch R, Chou MM, Wagner DS, Mullins MC (2009) A novel role for MAPKAPK2 in morphogenesis during zebrafish development. PLoS Genetics 5:e1000413

Holmes RS (2017) Comparative studies of vertebrate iduronate 2-sulfatase (IDS) genes and proteins: evolution of a mammalian X-linked gene. 3 Biotech 7:22

Hölttä-Vuori M, Salo VT, Nyberg L, Brackmann C, Enejder A, Panula P, Ikonen E (2010) Zebrafish: gaining popularity in lipid research. Biochemical Journal 429:235-242

Houwing S, Kamminga LM, Berezikov E, Cronembold D, Girard A, van den Elst H, Filippov DV, Blaser H, Raz E, Moens CB, Plasterk RH, Hannon GJ, Draper BW, Ketting RF (2007) A role for Piwi and piRNAs in germ cell maintenance and transposon silencing in Zebrafish. Cell 129:69-82

Howe K, Clark MD, Torroja CF, Torrance J, Berthelot C, Muffato M, Collins JE, Humphray S, McLaren K, Matthews L (2013) The zebrafish reference genome sequence and its relationship to the human genome. Nature 496:498-503

Howley C, Ho RK (2000) mRNA localization patterns in zebrafish oocytes. Mechanisms of Development 92:305-309

Hu L, Li H, Chi Z, He J (2020) Loss of the RNA-binding protein Rbm15 disrupts liver maturation in zebrafish. The Journal of Biological Chemistry 295:11466-11472

Huang H-F, Sheng J-Z (2014) Gamete and embryo-fetal origins of adult diseases. Springer, New York, USA

Huang H, Weng H, Sun W, Qin X, Shi H, Wu H, Zhao BS, Mesquita A, Liu C, Yuan CL, Hu Y-C, Hüttelmaier S, Skibbe JR, Su R, Deng X*et al.* (2018) Recognition of RNA N6-methyladenosine by IGF2BP proteins enhances mRNA stability and translation. Nature Cell Biology 20:285-295

Huang Q, Yang L, Luo J, Guo L, Wang Z, Yang X, Jin W, Fang Y, Ye J, Shan B (2015) SWATH enables precise label‑free quantification on proteome scale. Proteomics 15:1215-1223

Idigo NJ, Soares DC, Abbott CM (2020) Translation elongation factor 1A2 is encoded by one of four closely related eef1a genes and is dispensable for survival in zebrafish. Bioscience Reports 40:BSR20194191

Ikegami R, Hunter P, Yager TD (1999) Developmental activation of the capability to undergo checkpoint-induced apoptosis in the early zebrafish embryo. Developmental Biology 209:409-433

Ishihama Y, Oda Y, Tabata T, Sato T, Nagasu T, Rappsilber J, Mann M (2005) Exponentially modified protein abundance index (emPAI) for estimation of absolute protein amount in proteomics by the number of sequenced peptides per protein. Molecular & Cellular Proteomics 4:1265-1272

Jaffe JD, Berg HC, Church GM (2004) Proteogenomic mapping as a complementary method to perform genome annotation. Proteomics 4:59-77

Jeong K, Jeong JY, Lee HO, Choi E, Lee H (2010) Inhibition of Plk1 induces mitotic infidelity and embryonic growth defects in developing zebrafish embryos. Developmental Biology 345:34-48

Jorgensen P, Steen JA, Steen H, Kirschner MW (2009) The mechanism and pattern of yolk consumption provide insight into embryonic nutrition in *Xenopus*. Development 136:1539-1548

Jukam D, Shariati SAM, Skotheim JM (2017) Zygotic genome activation in vertebrates. Developmental Cell 42:316-332

Kane DA, Warga RM, Kimmel CB (1992) Mitotic domains in the early embryo of the zebrafish. Nature 360:735-737

Kane DA, Kimmel CB (1993) The zebrafish midblastula transition. Development 119:447-456

Kane DA, Hammerschmidt M, Mullins MC, Maischein H-M, Brand M, van Eeden F, Furutani-Seiki M, Granato M, Haffter P, Heisenberg C-P (1996) The zebrafish epiboly mutants. Development 123:47-55

Kaufman OH, Lee K, Martin M, Rothhämel S, Marlow FL (2018) rbpms2 functions in Balbiani body architecture and ovary fate. PLoS Genetics 14:e1007489

Kaushik S, Georga I, Koumoundouros G (2011) Growth and body composition of zebrafish (*Danio rerio*) larvae fed a compound feed from first feeding onward: toward implications on nutrient requirements. Zebrafish 8:87-95

Keller JM, Keller ET (2018) The use of mature zebrafish (*Danio rerio*) as a model for human aging and disease. In: Ram JL, Conn PM (eds) Conn's Handbook of Models for Human Aging. Elsevier, Amsterdam, The Netherlands, p 351-359

Kettleborough RN, Busch-Nentwich EM, Harvey SA, Dooley CM, de Bruijn E, van Eeden F, Sealy I, White RJ, Herd C, Nijman IJ (2013) A systematic genome-wide analysis of zebrafish protein-coding gene function. Nature 496:494-497

Khan FR, Alhewairini SS (2018) Zebrafish (*Danio rerio*) as a model organism. IntechOpen, London, UK

Kimelman D, Martin BL (2012) Anterior–posterior patterning in early development: three strategies. Wiley Interdisciplinary Reviews: Developmental Biology 1:253-266

Kimmel CB, Ballard WW, Kimmel SR, Ullmann B, Schilling TF (1995) Stages of embryonic development of the zebrafish. Developmental Dynamics 203:253-310

Knaut H, Pelegri F, Bohmann K, Schwarz H, Nüsslein-Volhard C (2000) Zebrafish vasa RNA but not its protein is a component of the germ plasm and segregates asymmetrically before germline specification. The Journal of Cell Biology 149:875-888

Knoll-Gellida A, André M, Gattegno T, Forgue J, Admon A, Babin PJ (2006) Molecular phenotype of zebrafish ovarian follicle by serial analysis of gene expression and proteomic profiling, and comparison with the transcriptomes of other animals. BMC Genomics 7:1-28

Ko MS (2001) Embryogenomics: developmental biology meets genomics. Trends in Biotechnology 19:511-518

Kobayashi W (1985) Communications of oocyte-granulosa cells in the chum salmon ovary detected by transmission electron microscopy: (oocyte/granulosa cell/intercellular junction/salmonid ovary/teleost). Development, Growth & Differentiation 27:553-561

Kocer A, Reichmann J, Best D, Adams IR (2009) Germ cell sex determination in mammals. MHR: Basic Science of Reproductive Medicine 15:205-213

Kosaka K, Kawakami K, Sakamoto H, Inoue K (2007) Spatiotemporal localization of germ plasm RNAs during zebrafish oogenesis. Mechanisms of Development 124:279-289

Krasny L, Bland P, Kogata N, Wai P, Howard BA, Natrajan RC, Huang PH (2018) SWATH mass spectrometry as a tool for quantitative profiling of the matrisome. Journal of Proteomics 189:11-22

Kristoffersen BA, Nerland A, Nilsen F, Kolarevic J, Finn RN (2009) Genomic and proteomic analyses reveal non–neofunctionalized vitellogenins in a basal clupeocephalan, the atlantic herring, and point to the origin of maturational yolk proteolysis in marine teleosts. Molecular Biology and Evolution 26:1029-1044

Krone PH, Evans TG, Blechinger SR (2003) Heat shock gene expression and function during zebrafish embryogenesis Seminars in Cell and Developmental Biology. Elsevier, p 267-274

Langley AR, Smith JC, Stemple DL, Harvey SA (2014) New insights into the maternal to zygotic transition. Development 141:3834-3841

Laubichler MD, Davidson EH (2008) Boveri's long experiment: sea urchin merogones and the establishment of the role of nuclear chromosomes in development. Developmental Biology 314:1-11

Lee H-J, Kim H-J, Liebler DC (2016) Efficient microscale basic reverse phase peptide fractionation for global and targeted proteomics. Journal of Proteome Research 15:2346-2354

Lee MT, Bonneau AR, Takacs CM, Bazzini AA, DiVito KR, Fleming ES, Giraldez AJ (2013) Nanog, Pou5f1 and SoxB1 activate zygotic gene expression during the maternal-to-zygotic transition. Nature 503:360-364

Lee MT, Bonneau AR, Giraldez AJ (2014) Zygotic genome activation during the maternal-to-zygotic transition. Annual Review of Cell and Developmental Biology 30:581-613

Lesch BJ, Page DC (2012) Genetics of germ cell development. Nature Reviews Genetics 13:781-794

Li-Villarreal N, Forbes MM, Loza AJ, Chen J, Ma T, Helde K, Moens CB, Shin J, Sawada A, Hindes AE, Dubrulle J, Schier AF, Longmore GD, Marlow FL, Solnica-Krezel L (2015) Dachsous1b cadherin regulates actin and microtubule cytoskeleton during early zebrafish embryogenesis. Development 142:2704-2718

Li H, Zhang S (2017) Functions of vitellogenin in eggs. In: Kloc M (ed) Oocytes. Springer, New York, USA, p 389-401

Li L, Zheng P, Dean J (2010) Maternal control of early mouse development. Development 137:859-870

Li Z, Adams RM, Chourey K, Hurst GB, Hettich RL, Pan C (2012) Systematic comparison of label-free, metabolic labeling, and isobaric chemical labeling for quantitative proteomics on LTQ Orbitrap Velos. Journal of Proteome Research 11:1582-1590

Lichtinghagen R, Musholt PB, Lein M, Römer A, Rudolph B, Kristiansen G, Hauptmann S, Schnorr D, Loening SA, Jung K (2002) Different mRNA and protein expression of matrix metalloproteinases 2 and 9 and tissue inhibitor of metalloproteinases 1 in benign and malignant prostate tissue. European Urology 42:398-406

Lieschke GJ, Currie PD (2007) Animal models of human disease: zebrafish swim into view. Nature Reviews Genetics 8:353

Lilley KS, Razzaq A, Dupree P (2002) Two-dimensional gel electrophoresis: recent advances in sample preparation, detection and quantitation. Current Opinion in Chemical Biology 6:46-50

Lin CW, Yen ST, Chang HT, Chen SJ, Lai SL, Liu YC, Chan TH, Liao WL, Lee SJ (2010) Loss of cofilin 1 disturbs actin dynamics, adhesion between enveloping and deep cell layers and cell movements during gastrulation in zebrafish. PloS One 5:e15331

Lin L, Sohar I, Lackland H, Lobel P (2001) The human CLN2 protein/tripeptidyl-peptidase I is a serine protease that autoactivates at acidic pH. Journal of Biological Chemistry 276:2249-2255

Lin Y, Chen Y, Yang X, Xu D, Liang S (2009) Proteome analysis of a single zebrafish embryo using three different digestion strategies coupled with liquid chromatography–tandem mass spectrometry. Analytical Biochemistry 394:177-185

Lindeman RE, Pelegri F (2012) Localized products of futile cycle/lrmp promote centrosome-nucleus attachment in the zebrafish zygote. Current Biology 22:843-851

Link V, Shevchenko A, Heisenberg C-P (2006) Proteomics of early zebrafish embryos. BMC Developmental Biology 6:1-9

Lößner C, Wee S, Ler SG, Li RH, Carney T, Blackstock W, Gunaratne J (2012) Expanding the zebrafish embryo proteome using multiple fractionation approaches and tandem mass spectrometry. Proteomics 12:1879-1882

Lu F-I, Thisse C, Thisse B (2011) Identification and mechanism of regulation of the zebrafish dorsal determinant. Proceedings of the National Academy of Sciences 108:15876-15880

Lubzens E, Young G, Bobe J, Cerdà J (2010) Oogenesis in teleosts: how fish eggs are formed. General and Comparative Endocrinology 165:367-389

Lucitt MB, Price TS, Pizarro A, Wu W, Yocum AK, Seiler C, Pack MA, Blair IA, FitzGerald GA, Grosser T (2008) Analysis of the zebrafish proteome during embryonic development. Molecular & Cellular Proteomics 7:981-994

Ma J, Svoboda P, Schultz RM, Stein P (2001) Regulation of zygotic gene activation in the preimplantation mouse embryo: global activation and repression of gene expression1. Biology of Reproduction 64:1713-1721

Machaty Z, Miller AR, Zhang L (2017) Egg activation at fertilization. In: Pelegri F, Danilchik M, Sutherland A (eds) Vertebrate Development. Springer, New York, USA, p 1-47

Mann M (2006) Functional and quantitative proteomics using SILAC. Nature reviews Molecular Cell Biology 7:952-958

Marlow FL, Mullins MC (2008) Bucky ball functions in Balbiani body assembly and animal-vegetal polarity in the oocyte and follicle cell layer in zebrafish. Developmental Biology 321:40-50

Marlow FL (2010) Maternal control of development in vertebrates Colloquium Series on Developmental Biology. Morgan & Claypool Life Sciences, p 1-196

Marsal M, Martin-Blanco E (2017) Contractility, differential tension and membrane removal direct zebrafish epiboly biomechanics. bioRxiv:113282

Mason D, Sammons R (1978) Alkaline phosphatase and peroxidase for double immunoenzymatic labelling of cellular constituents. Journal of Clinical Pathology 31:454-460

Mathavan S, Lee SG, Mak A, Miller LD, Murthy KRK, Govindarajan KR, Tong Y, Wu YL, Lam SH, Yang H (2005) Transcriptome analysis of zebrafish embryogenesis using microarrays. PLoS Genetics 1:e29

Mehjabin R, Xiong L, Huang R, Yang C, Chen G, He L, Liao L, Zhu Z, Wang Y (2019) Full-length transcriptome sequencing and the discovery of new transcripts in the unfertilized eggs of zebrafish (*Danio rerio*). G3: Genes, Genomes, Genetics:g3. 200997.202019

Mei W, Lee KW, Marlow FL, Miller AL, Mullins MC (2009) hnRNP I is required to generate the Ca2+ signal that causes egg activation in zebrafish. Development (Cambridge, England) 136:3007-3017

Mendez R, Richter JD (2001) Translational control by CPEB: a means to the end. Nature Reviews Molecular Cell Biology 2:521-529

Meyers JR (2018) Zebrafish: development of a vertebrate model organism. Current Protocols Essential Laboratory Techniques 16:e19

Miyares RL, de Rezende VB, Farber SA (2014) Zebrafish yolk lipid processing: a tractable tool for the study of vertebrate lipid transport and metabolism. Disease Models & Mechanisms 7:915-927

Mizuno T, Yamaha E, Kuroiwa A, Takeda H (1999) Removal of vegetal yolk causes dorsal deficencies and impairs dorsal-inducing ability of the yolk cell in zebrafish. Mechanisms of Development 81:51-63

Moens CB, Donn TM, Wolf-Saxon ER, Ma TP (2008) Reverse genetics in zebrafish by TILLING. Briefings in Functional Genomics and Proteomics 7:454-459

Motoyama A, Yates III JR (2008) Multidimensional LC separations in shotgun proteomics. Analytical Chemistry 80:7187-7193

Mousavi SA, Malerød L, Berg T, Kjeken R (2004) Clathrin-dependent endocytosis. Biochemical Journal 377:1-16

Müller UK, van Leeuwen JL (2004) Swimming of larval zebrafish: ontogeny of body waves and implications for locomotory development. Journal of Experimental Biology 207:853-868

Murphey RD, Stern HM, Straub CT, Zon LI (2006) A chemical genetic screen for cell cycle inhibitors in zebrafish embryos. Chemical Biology & Drug Design 68:213-219

Myers DC, Sepich DS, Solnica-Krezel L (2002) Convergence and extension in vertebrate gastrulae: cell movements according to or in search of identity? Trends in Genetics 18:447-455

Nelson JS, Grande TC, Wilson MV (2016) Fishes of the World. John Wiley & Sons, Hoboken, New Jersey

Newport J, Kirschner M (1982) A major developmental transition in early *Xenopus* embryos: I. characterization and timing of cellular changes at the midblastula stage. Cell 30:675-686

Nguyen-Chi ME, Bryson-Richardson R, Sonntag C, Hall TE, Gibson A, Sztal T, Chua W, Schilling TF, Currie PD (2012) Morphogenesis and cell fate determination within the adaxial cell equivalence group of the zebrafish myotome. PLoS Genetics 8:e1003014

Nicolas J-M (1999) Vitellogenesis in fish and the effects of polycyclic aromatic hydrocarbon contaminants. Aquatic Toxicology 45:77-90

Nojima H, Rothhämel S, Shimizu T, Kim CH, Yonemura S, Marlow FL, Hibi M (2010) Syntabulin, a motor protein linker, controls dorsal determination. Development 137:923-933

North TE, Goessling W, Walkley CR, Lengerke C, Kopani KR, Lord AM, Weber GJ, Bowman TV, Jang I-H, Grosser T (2007) Prostaglandin E2 regulates vertebrate haematopoietic stem cell homeostasis. Nature 447:1007

Nosek J, Krajhanzl A, Kocourek J (1984) Binding of the cortical granule lectin to the jelly envelope in mature perch ova. The Histochemical Journal 16:429-431

Nudelman G, Frasca A, Kent B, Sadler KC, Sealfon SC, Walsh MJ, Zaslavsky E (2018) High resolution annotation of zebrafish transcriptome using long-read sequencing. Genome Research 28:1415-1425

O'Farrell PH (1975) High resolution two-dimensional electrophoresis of proteins. Journal of Biological Chemistry 250:4007-4021

Ober EA, Schulte-Merker S (1999) Signals from the yolk cell induce mesoderm, neuroectoderm, the trunk organizer, and the notochord in zebrafish. Developmental Biology 215:167-181

Ohta T, Iwamatsu T, Tanaka M, Yoshimoto Y (1990) Cortical alveolus breakdown in the eggs of the freshwater teleost *Rhodeus ocellatus ocellatus*. The Anatomical Record 227:486-496

Okabe N, Xu B, Burdine RD (2008) Fluid dynamics in zebrafish Kupffer's vesicle. Developmental dynamics: an official publication of the American Association of Anatomists 237:3602-3612

Olsen JV, Ong S-E, Mann M (2004) Trypsin cleaves exclusively C-terminal to arginine and lysine residues. Molecular & Cellular Proteomics 3:608-614

Ong S-E, Blagoev B, Kratchmarova I, Kristensen DB, Steen H, Pandey A, Mann M (2002) Stable isotope labeling by amino acids in cell culture, SILAC, as a simple and accurate approach to expression proteomics. Molecular & Cellular Proteomics 1:376-386

Ong SE, Kratchmarova I, Mann M (2003) Properties of 13C-substituted arginine in stable isotope labeling by amino acids in cell culture (SILAC). Journal Proteome Research 2:173-181

Ow SY, Salim M, Noirel J, Evans C, Rehman I, Wright PC (2009) iTRAQ underestimation in simple and complex mixtures:"the good, the bad and the ugly". Journal of Proteome Research 8:5347-5355

Pappireddi N, Martin L, Wühr M (2019) A review on quantitative multiplexed proteomics. ChemBioChem 20:1210-1224

Parichy DM, Elizondo MR, Mills MG, Gordon TN, Engeszer RE (2009) Normal table of postembryonic zebrafish development: staging by externally visible anatomy of the living fish. Developmental Dynamics 238:2975-3015

Parker J, Zhu N, Zhu M, Chen S (2012) Profiling thiol redox proteome using isotope tagging mass spectrometry. Journal of Visualized Experiments 61:e3766

Pauli A, Valen E, Lin MF, Garber M, Vastenhouw NL, Levin JZ, Fan L, Sandelin A, Rinn JL, Regev A, Schier AF (2012) Systematic identification of long noncoding RNAs expressed during zebrafish embryogenesis. Genome Research 22:577-591

Payer B, Saitou M, Barton SC, Thresher R, Dixon JP, Zahn D, Colledge WH, Carlton MB, Nakano T, Surani MA (2003) Stella is a maternal effect gene required for normal early development in mice. Current Biology 13:2110-2117

Perkins DN, Pappin DJC, Creasy DM, Cottrell JS (1999) Probability-based protein identification by searching sequence databases using mass spectrometry data. Electrophoresis 20:3551-3567

Peshkin L, Wühr M, Pearl E, Haas W, Freeman Jr RM, Gerhart JC, Klein AM, Horb M, Gygi SP, Kirschner MW (2015) On the relationship of protein and mRNA dynamics in vertebrate embryonic development. Developmental Cell 35:383-394

Peterson RT, Shaw SY, Peterson TA, Milan DJ, Zhong TP, Schreiber SL, MacRae CA, Fishman MC (2004) Chemical suppression of a genetic mutation in a zebrafish model of aortic coarctation. Nature Biotechnology 22:595

Petrak J, Ivanek R, Toman O, Cmejla R, Cmejlova J, Vyoral D, Zivny J, Vulpe CD (2008) Deja vu in proteomics. A hit parade of repeatedly identified differentially expressed proteins. Proteomics 8:1744-1749

Pichler P, Köcher T, Holzmann J, Mazanek M, Taus T, Ammerer G, Mechtler K (2010) Peptide labeling with isobaric tags yields higher identification rates using iTRAQ 4-plex compared to TMT 6-plex and iTRAQ 8-plex on LTQ Orbitrap. Analytical Chemistry 82:6549-6558

Pierce A, Unwin RD, Evans CA, Griffiths S, Carney L, Zhang L, Jaworska E, Lee C-F, Blinco D, Okoniewski MJ (2008) Eight-channel iTRAQ enables comparison of the activity of six leukemogenic tyrosine kinases. Molecular & Cellular Proteomics 7:853-863

Pitt JJ (2009) Principles and applications of liquid chromatography-mass spectrometry in clinical biochemistry. The Clinical Biochemist Reviews 30:19

Postlethwait JH, Woods IG, Ngo-Hazelett P, Yan Y-L, Kelly PD, Chu F, Huang H, Hill-Force A, Talbot WS (2000) Zebrafish comparative genomics and the origins of vertebrate chromosomes. Genome Research 10:1890-1902

Prakash O, Goswami SV, Sehgal N (2007) Establishment of ELISA for murrel vitellogenin and choriogenin, as biomarkers of potential endocrine disruption. Comparative Biochemistry and Physiology Part C: Toxicology & Pharmacology 146:540-551

Preziosi CA (2012) Expression and regulation of cofilin isoforms in *Danio rerio*. Electronic Theses and Dissertations:1815

Rahlouni F, Szarka S, Shulaev V, Prokai L (2015) A survey of the impact of deyolking on biological processes covered by shotgun proteomic analyses of zebrafish embryos. Zebrafish 12:398-407

Rappsilber J, Ryder U, Lamond AI, Mann M (2002) Large-scale proteomic analysis of the human spliceosome. Genome Research 12:1231-1245

Rauwerda H, Pagano JF, de Leeuw WC, Ensink W, Nehrdich U, de Jong M, Jonker M, Spaink HP, Breit TM (2017) Transcriptome dynamics in early zebrafish embryogenesis determined by high-resolution time course analysis of 180 successive, individual zebrafish embryos. BMC Genomics 18:287

Rawlings ND, Barrett AJ (1999) Tripeptidyl-peptidase I is apparently the CLN2 protein absent in classical late-infantile neuronal ceroid lipofuscinosis. Biochimica et Biophysica Acta (BBA)-Protein Structure and Molecular Enzymology 1429:496-500

Raz E (2003) Primordial germ-cell development: the zebrafish perspective. Nature Reviews Genetics 4:690-700

Rees BB, Patton C, Grainger JL, Epel D (1995) Protein synthesis increases after fertilization of sea urchin eggs in the absence of an increase in intracellular pH. Developmental Biology 169:683-698

Ren F, Lin Q, Gong G, Du X, Dan H, Qin W, Miao R, Xiong Y, Xiao R, Li X (2020) Igf2bp3 maintains maternal RNA stability and ensures early embryo development in zebrafish. Communications Biology 3:1-10

Riemer S, Bontems F, Krishnakumar P, Gömann J, Dosch R (2015) A functional Bucky ball-GFP transgene visualizes germ plasm in living zebrafish. Gene Expression Patterns 18:44-52

Roche PC, Hsi ED, Firfer BL (2006) Immunohistochemistry: principles and advances. In: Detrick B (ed) Manual of Molecular and Clinical Laboratory Immunology, 7th Edition. American Society of Microbiology, Washington, USA, p 396-402

Rock KL, Gramm C, Rothstein L, Clark K, Stein R, Dick L, Hwang D, Goldberg AL (1994) Inhibitors of the proteasome block the degradation of most cell proteins and the generation of peptides presented on MHC class I molecules. Cell 78:761-771

Rosa R, Calado R, Andrade A, Narciso L, Nunes M (2005) Changes in amino acids and lipids during embryogenesis of European lobster, *Homarus gammarus* (Crustacea: Decapoda). Comparative Biochemistry and Physiology Part B: Biochemistry and Molecular Biology 140:241-249

Ross PL, Huang YN, Marchese JN, Williamson B, Parker K, Hattan S, Khainovski N, Pillai S, Dey S, Daniels S (2004) Multiplexed protein quantitation in Saccharomyces cerevisiae using amine-reactive isobaric tagging reagents. Molecular & Cellular Proteomics 3:1154-1169

Roustaian P, Litvak MK (2007) Effect of yolk redistribution at different developmental stages on survivorship of zebrafish embryos. Journal of Fish Biology 70:1642-1646

Roxo-Rosa M, Lopes SS (2019) The zebrafish kupffer's vesicle: a special organ in a model organism to study human diseases. IntechOpen, London, UK

Sagerström CG, Gammill LS, Veale R, Sive H (2005) Specification of the enveloping layer and lack of autoneuralization in zebrafish embryonic explants. Developmental dynamics: an official publication of the American Association of Anatomists 232:85-97

Saito T, Pšenička M, Goto R, Adachi S, Inoue K, Arai K, Yamaha E (2014) The origin and migration of primordial germ cells in sturgeons. PloS One 9:e86861

Sakaguchi T, Mizuno T, Takeda H (2002) Formation and patterning roles of the yolk syncytial layer. In: Solnica-Krezel L (ed) Pattern Formation in Zebrafish. Springer, New York, USA, p 1-14

Samaee SM, Lahnsteiner F, Giménez G, Estévez A, Sarg B, Lindner H (2009) Quantitative composition of vitellogenin‒derived yolk proteins and their effects on viability of embryos and larvae of common dentex (*Dentex dentex*), a marine pelagophil teleost. Journal of Experimental Zoology Part A: Ecological Genetics and Physiology 311:504-520

Sant KE, Timme-Laragy AR (2018) Zebrafish as a model for toxicological perturbation of yolk and nutrition in the early embryo. Current Environmental Health Reports 5:125-133

Schier AF (2001) Axis formation and patterning in zebrafish. Current Opinion in Genetics and Development 11:393-404

Schlegel A, Stainier DY (2006) Microsomal triglyceride transfer protein is required for yolk lipid utilization and absorption of dietary lipids in zebrafish larvae. Biochemistry 45:15179-15187

Schmitz B, Campos-Ortega JA (1994) Dorso-ventral polarity of the zebrafish embryo is distinguishable prior to the onset of gastrulation. Roux's Archives of Developmental Biology 203:374-380

Schulz KN, Harrison MM (2019) Mechanisms regulating zygotic genome activation. Nature Reviews Genetics 20:221-234

Schulze WX, Usadel B (2010) Quantitation in mass-spectrometry-based proteomics. Annual Review of Plant Biology 61:491-516

Seko A, Kitajima K, Inoue Y, Inoue S (1991) Peptide:N-glycosidase activity found in the early embryos of *Oryzias latipes* (Medaka fish). The first demonstration of the occurrence of peptide:N-glycosidase in animal cells and its implication for the presence of a de-N-glycosylation system in living organisms. Journal of Biological Chemistry 266:22110-22114

Selman K, Wallace RA (1986) Gametogenesis in *Fundulus heteroclitus*. American Zoologist 26:173-192

Selman K, Wallace RA (1989) Cellular aspects of oocyte growth in teleosts. Zoological Science 6:211-231

Selman K, Wallace RA, Sarka A, Qi X (1993) Stages of oocyte development in the zebrafish, *Brachydanio rerio*. Journal of Morphology 218:203-224

Shao M, Wang M, Liu Y-Y, Ge Y-W, Zhang Y-J, Shi D-L (2017) Vegetally localised Vrtn functions as a novel repressor to modulate *bmp2b* transcription during dorsoventral patterning in zebrafish. Development 144:3361-3374

Shermoen AW, McCleland ML, O'Farrell PH (2010) Developmental control of late replication and S phase length. Current Biology 20:2067-2077

Shin S-W, Shimizu N, Tokoro M, Nishikawa S, Hatanaka Y, Anzai M, Hamazaki J, Kishigami S, Saeki K, Hosoi Y, Iritani A, Murata S, Matsumoto K (2012) Mouse zygote-specific proteasome assembly chaperone important for maternal-to-zygotic transition. Biology Open 2:170-182

Shin S-W, Murata S, Matsumoto K (2013) The Ubiquitin-proteasome system in the maternal-to-zygotic transition. Journal of Mammalian Ova Research 30:79-85

Simons K, Ikonen E (1997) Functional rafts in cell membranes. Nature 387:569-572

Singh SK, Sundaram CS, Shanbhag S, Idris MM (2010) Proteomic profile of zebrafish brain based on two-dimensional gel electrophoresis matrix-assisted laser desorption/ionization MS/MS analysis. Zebrafish 7:169-177

Sleat DE, Donnelly RJ, Lackland H, Liu CG, Sohar I, Pullarkat RK, Lobel P (1997) Association of mutations in a lysosomal protein with classical late-infantile neuronal ceroid lipofuscinosis. Science 277:1802-1805

Smits AH, Lindeboom RG, Perino M, van Heeringen SJ, Veenstra GJ, Vermeulen M (2014) Global absolute quantification reveals tight regulation of protein expression in single *Xenopus* eggs. Nucleic Acids Research 42:9880-9891

Smolka MB, Zhou H, Purkayastha S, Aebersold R (2001) Optimization of the isotope-coded affinity tag-labeling procedure for quantitative proteome analysis. Analytical Biochemistry 297:25-31

Solomon KS, Kudoh T, Dawid IB, Fritz A (2003) Zebrafish foxi1 mediates otic placode formation and jaw development. Development 130:929-940

Spiegel S, Merrill Jr AH (1996) Sphingolipid metabolism and cell growth regulation. The FASEB Journal 10:1388-1397

Stahl DC, Swiderek KM, Davis MT, Lee TD (1996) Data-controlled automation of liquid chromatography/tandem mass spectrometry analysis of peptide mixtures. Journal of the American Society for Mass Spectrometry 7:532-540

Stainier DY, Fishman MC (1994) The zebrafish as a model system to study cardiovascular development. Trends in Cardiovascular Medicine 4:207-212

Stickney HL, Barresi MJ, Devoto SH (2000) Somite development in zebrafish. Developmental dynamics: an official publication of the American Association of Anatomists 219:287-303

Sturm RM, Lietz CB, Li L (2014) Improved isobaric tandem mass tag quantification by ion mobility mass spectrometry. Rapid Communications in Mass Spectrometry 28:1051-1060

Sullivan C, Kim CH (2008) Zebrafish as a model for infectious disease and immune function. Fish & Shellfish Immunology 25:341-350

Sun L, Bertke MM, Champion MM, Zhu G, Huber PW, Dovichi NJ (2014) Quantitative proteomics of *Xenopus laevis* embryos: expression kinetics of nearly 4000 proteins during early development. Scientific Reports 4:4365

Sun Q, Liu X, Gong B, Wu D, Meng A, Jia S (2017) Alkbh4 and Atrn act maternally to regulate zebrafish epiboly. International Journal of Biological Sciences 13:1051

Suzuki H, Maegawa S, Nishibu T, Sugiyama T, Yasuda K, Inoue K (2000) Vegetal localization of the maternal mRNA encoding an EDEN-BP/Bruno-like protein in zebrafish. Mechanisms of Development 93:205-209

Szeto DP, Kimelman D (2006) The regulation of mesodermal progenitor cell commitment to somitogenesis subdivides the zebrafish body musculature into distinct domains. Genes and Development 20:1923-1932

Tadros W, Lipshitz HD (2009) The maternal-to-zygotic transition: a play in two acts. Development 136:3033-3042

Talwar PK (1991) Inland fishes of India and adjacent countries. CRC Press, Boca Raton, Florida

Tanaka K (2009) The proteasome: overview of structure and functions. Proceedings of the Japan Academy Series B, Physical and Biological Sciences 85:12-36

Tanner S, Shen Z, Ng J, Florea L, Guigó R, Briggs SP, Bafna V (2007) Improving gene annotation using peptide mass spectrometry. Genome Research 17:231-239

Tay TL, Lin Q, Seow TK, Tan KH, Hew CL, Gong Z (2006) Proteomic analysis of protein profiles during early development of the zebrafish, *Danio rerio*. Proteomics 6:3176-3188

Thompson A, Schäfer J, Kuhn K, Kienle S, Schwarz J, Schmidt G, Neumann T, Hamon C (2003) Tandem mass tags: a novel quantification strategy for comparative analysis of complex protein mixtures by MS/MS. Analytical Chemistry 75:1895-1904

Tintori SC, Nishimura EO, Golden P, Lieb JD, Goldstein B (2016) A transcriptional lineage of the early *C. elegans* embryo. Developmental Cell 38:430-444

Tlili S, Yin J, Rupprecht J-F, Mendieta-Serrano M, Weissbart G, Verma N, Teng X, Toyama Y, Prost J, Saunders T (2019) Shaping the zebrafish myotome by intertissue friction and active stress. Proceedings of the National Academy of Sciences 116:25430-25439

Tong ZB, Gold L, Pfeifer KE, Dorward H, Lee E, Bondy CA, Dean J, Nelson LM (2000) Mater, a maternal effect gene required for early embryonic development in mice. Nature Genetics 26:267-268

Tran LD, Hino H, Quach H, Lim S, Shindo A, Mimori-Kiyosue Y, Mione M, Ueno N, Winkler C, Hibi M (2012) Dynamic microtubules at the vegetal cortex predict the embryonic axis in zebrafish. Development 139:3644-3652

Trinkaus J (1992) The midblastula transition, the YSL transition and the onset of gastrulation in Fundulus. Development 116:75-80

Unhavaithaya Y, Park EA, Royzman I, Orr-Weaver TL (2013) Drosophila embryonic cell-cycle mutants. G3: Genes, Genomes, Genetics 3:1875-1880

Varshney GK, Pei W, LaFave MC, Idol J, Xu L, Gallardo V, Carrington B, Bishop K, Jones M, Li M (2015) High-throughput gene targeting and phenotyping in zebrafish using CRISPR/Cas9. Genome Research 25:1030-1042

Vastenhouw NL, Cao WX, Lipshitz HD (2019) The maternal-to-zygotic transition revisited. Development 146

Vejnar CE, Messih MA, Takacs CM, Yartseva V, Oikonomou P, Christiano R, Stoeckius M, Lau S, Lee MT, Beaudoin J-D, Darwich-Codore H, Walther TC, Tavazoie S, fuentes DC-, Giraldez AJ (2018) A post-

transcriptional regulatory code for mRNA stability during the zebrafish maternal-to-zygotic transition. bioRxiv:292441

Vesterlund L, Jiao H, Unneberg P, Hovatta O, Kere J (2011) The zebrafish transcriptome during early development. BMC Developmental Biology 11:30

Vicente-Manzanares M, Webb DJ, Horwitz AR (2005) Cell migration at a glance. Journal of Cell Science 118:4917-4919

Wall DA, Meleka I (1985) An unusual lysosome compartment involved in vitellogenin endocytosis by *Xenopus* oocytes. The Journal of Cell Biology 101:1651 - 1664

Wang H, Tan JT, Emelyanov A, Korzh V, Gong Z (2005) Hepatic and extrahepatic expression of vitellogenin genes in the zebrafish, *Danio rerio*. Gene 356:91-100

Wang S, Yang Q, Wang Z, Feng S, Li H, Ji D, Zhang S (2018) Evolutionary and expression analyses show co-option of *khdrbs* genes for origin of vertebrate brain. Frontiers in Genetics 8:225

Wang YH, Chen YH, Lin YJ, Tsai HJ (2006) Spatiotemporal expression of zebrafish keratin 18 during early embryogenesis and the establishment of a keratin 18:RFP transgenic line. Gene Expression Patterns 6:335-339

Warga RM, Kimmel CB (1990) Cell movements during epiboly and gastrulation in zebrafish. Development 108:569-580

Whitaker M (2006) Calcium at fertilization and in early development. Physiological Reviews 86:25-88

White RJ, Collins JE, Sealy IM, Wali N, Dooley CM, Digby Z, Stemple DL, Murphy DN, Billis K, Hourlier T (2017) A high-resolution mRNA expression time course of embryonic development in zebrafish. Elife 6:e30860

Wiegand MD (1996) Composition, accumulation and utilization of yolk lipids in teleost fish. Reviews in Fish Biology and Fisheries 6:259-286

Wienholds E, Koudijs MJ, van Eeden FJ, Cuppen E, Plasterk RH (2003) The microRNA-producing enzyme Dicer1 is essential for zebrafish development. Nature Genetics 35:217-218

Wiese S, Reidegeld KA, Meyer HE, Warscheid B (2007) Protein labeling by iTRAQ: a new tool for quantitative mass spectrometry in proteome research. Proteomics 7:340-350

Winata CL, Łapiński M, Pryszcz L, Vaz C, bin Ismail MH, Nama S, Hajan HS, Lee SGP, Korzh V, Sampath P (2018) Cytoplasmic polyadenylation-mediated translational control of maternal mRNAs directs maternal-to-zygotic transition. Development 145

Woolley K, Martin P, Driever W, Stemple D (2000) Axis-inducing activities and cell fates of the zebrafish organizer. Development 127:3407-3417

Wragg J, Müller F (2016) Transcriptional regulation during zygotic genome activation in zebrafish and other anamniote embryos. Advances in Genetics 95:161-194

Wu X, Viveiros MM, Eppig JJ, Bai Y, Fitzpatrick SL, Matzuk MM (2003) Zygote arrest 1 (Zar1) is a novel maternal-effect gene critical for the oocyte-to-embryo transition. Nature Genetics 33:187-191

Wühr M, Freeman Jr RM, Presler M, Horb ME, Peshkin L, Gygi SP, Kirschner MW (2014) Deep proteomics of the *Xenopus laevis* egg using an mRNA-derived reference database. Current Biology 24:1467-1475

Yang H, Zhou Y, Gu J, Xie S, Xu Y, Zhu G, Wang L, Huang J, Ma H, Yao J (2013) Deep mRNA sequencing analysis to capture the transcriptome landscape of zebrafish embryos and larvae. PloS One 8:e64058

Yang P, Humphrey SJ, Cinghu S, Pathania R, Oldfield AJ, Kumar D, Perera D, Yang JY, James DE, Mann M (2019) Multi-omic profiling reveals dynamics of the phased progression of pluripotency. Cell Systems 8:427-445. e410

Yilmaz O, Patinote A, Nguyen TV, Com E, Lavigne R, Pineau C, Sullivan CV, Bobe J (2017) Scrambled eggs: Proteomic portraits and novel biomarkers of egg quality in zebrafish (*Danio rerio*). PloS One 12:e0188084

Yilmaz O, Patinote A, Nguyen T, Bobe J (2018) Multiple vitellogenins in zebrafish (*Danio rerio*): quantitative inventory of genes, transcripts and proteins, and relation to egg quality. Fish Physiology and Biochemistry 44:1509-1525

Yin J, Lee R, Ono Y, Ingham PW, Saunders TE (2018) Spatiotemporal coordination of FGF and Shh signaling underlies the specification of myoblasts in the zebrafish embryo. Developmental Cell 46:735-750. e734

Zalik SE, Lewandowski E, Kam Z, Geiger B (1999) Cell adhesion and the actin cytoskeleton of the enveloping layer in the zebrafish embryo during epiboly. Biochemistry and Cell Biology 77:527-542

Zhang J, Lanham KA, Peterson RE, Heideman W, Li L (2010) Characterization of the adult zebrafish cardiac proteome using online pH gradient strong cation exchange‐RP 2D LC coupled with ESI MS/MS. Journal of Separation Science 33:1462-1471

Zhang K, Smith GW (2015) Maternal control of early embryogenesis in mammals. Reproduction, Fertility and Development 27:880-896

Zhang M, Zhai Y, Zhang S, Dai X, Li Z (2020) Roles of N6-Methyladenosine (m6A) in stem cell fate decisions and early embryonic development in mammals. Frontiers in Cell and Developmental Biology 8:782

Zhang X, Li X, Li R, Zhang Y, Li Y, Li S (2019) Transcriptomic profile of early zebrafish PGCs by single cell sequencing. PloS One 14:e0220364

Zhong L, Yuan L, Rao Y, Li Z, Zhang X, Liao T, Xu Y, Dai H (2014) Distribution of vitellogenin in zebrafish (*Danio rerio*) tissues for biomarker analysis. Aquatic Toxicology 149:1-7

Zhu W, Smith JW, Huang C-M (2009) Mass spectrometry-based label-free quantitative proteomics. Journal of Biomedicine and Biotechnology 2010

Zhu W, Zhang J, He K, Geng Z, Chen X (2020) Proteomic analysis of fertilized egg yolk proteins during embryonic development. Poultry Science

Ziv T, Gattegno T, Chapovetsky V, Wolf H, Barnea E, Lubzens E, Admon A (2008) Comparative proteomics of the developing fish (zebrafish and gilthead seabream) oocytes. Comparative Biochemistry and Physiology Part D: Genomics and Proteomics 3:12-35

Zorn AM, Wells JM (2009) Vertebrate endoderm development and organ formation. Annual Review of
    Cell and Developmental 25:221-251

Paper I

Article

Proteomics Analysis of Early Developmental Stages of Zebrafish Embryos

Kathiresan Purushothaman [1], Prem Prakash Das [2], Christopher Presslauer [1], Teck Kwang Lim [2], Steinar D. Johansen [1], Qingsong Lin [2],* and Igor Babiak [1],*

[1] Genomics Group, Faculty of Biosciences and Aquaculture, Nord University, 8049 Bodø, Norway;
    kathiresan.purushothaman@nord.no (K.P.); cpressla@hotmail.com (C.P.); steinar.d.johansen@nord.no (S.D.J.)
[2] Department of Biological Sciences, National University of Singapore, 14 Science Drive 4, Singapore 117543,
    Singapore; dbsppd@nus.edu.sg (P.P.D.); dbslimtk@nus.edu.sg (T.K.L.)
* Correspondence: dbslinqs@nus.edu.sg (Q.L.); igor.s.babiak@nord.no (I.B.)

check for
updates

Abstract: Zebrafish is a well-recognized organism for investigating vertebrate development and human diseases. However, the data on zebrafish proteome are scarce, particularly during embryogenesis. This is mostly due to the overwhelming abundance of egg yolk proteins, which tend to mask the detectable presence of less abundant proteins. We developed an efficient procedure to reduce the amount of yolk in zebrafish early embryos to improve the Liquid chromatography–tandem mass spectrometry (LC–MS)-based shotgun proteomics analysis. We demonstrated that the deyolking procedure resulted in a greater number of proteins being identified. This protocol resulted in approximately 2-fold increase in the number of proteins identified in deyolked samples at cleavage stages, and the number of identified proteins increased greatly by 3–4 times compared to non-deyolked samples in both oblong and bud stages. Gene Ontology and Kyoto Encyclopedia of Genes and Genomes (KEGG) analysis revealed a high number of functional proteins differentially accumulated in the deyolked versus non-deyolked samples. The most prominent enrichments after the deyolking procedure included processes, functions, and components related to cellular organization, cell cycle, control of replication and translation, and mitochondrial functions. This deyolking procedure improves both qualitative and quantitative proteome analyses and provides an innovative tool in molecular embryogenesis of polylecithal animals, such as fish, amphibians, reptiles, or birds.

Keywords: egg yolk; embryonic development; LC–MS/MS shotgun proteomics; proteome; zebrafish

1. Introduction

Zebrafish have become a prominent and broadly used model system to study developmental biology, neurogenetic disorders, genetics, toxicology, reproduction, pathology, and pharmacology [1–5]. The genome annotation is relatively well developed [6], and the embryonic transcriptome of zebrafish has been characterized in several studies [7–11]. However, knowledge about the comprehensive proteome dynamics during embryogenesis in zebrafish remains elusive.

Proteome in zebrafish is usually investigated in adult organs or tissues [12–15]. The overwhelming occurrence of vitellogenin yolk proteins is a limiting factor in a polylecithal embryo, such as in zebrafish, as it hinders global identification of less abundant proteins using mass spectrometry-based techniques [4,16]. Proteolytic peptides of yolk proteins can potentially subdue the ionization of the less abundant proteolytic peptides of non-yolk proteins [17,18]. Consequently, abundant yolk proteins can potentially interfere with the identification of cellular proteins, although the degree of such interference is unknown. To reduce the abundance of yolk proteins, deyolking protocols are employed; they have been used in a number of studies on zebrafish embryos and larvae from 3.3 h post-fertilization (hpf) to

7 days post-fertilization (dpf) [16,19–21]. In most extensive studies to date, 5267 and 8363 proteins were identified in zebrafish deyolked embryos at 24 hpf [22,23].

So far, all the studies on zebrafish embryonic proteome were conducted on embryos being at a certain developmental advancement, and the information on the early stages, particularly before the maternal-to-zygotic transition (MZT), is missing. Pre-MZT stages of development are characterized by rapid, synchronous cell cycles (cleavages), and the development is driven by maternally-provided factors, including transcriptome and proteome [24]. Therefore, a knowledge of maternal proteome dynamics seems to be essential for understanding the regulation of early embryonic development in zebrafish. We improved the deyolking procedure, allowing the efficient capture and identification of proteins from the onset of development (1-cell stage). The protocol yielded 2 times more identified proteins compared to the non-deyolked counterparts in cleavage stages, and 3–4 times at oblong and bud stages. Also, the protocol caused minimal loss of proteins. Our improved protocol was effective for the subsequent systematic proteomics studies of zebrafish early embryonic development, and it is applicable to studies on other polylecithal animals.

2. Results

2.1. Efficiency of the New Extraction Protocol

Application of the existing deyolking protocol [16] to zebrafish early embryos requires a considerable amount of embryos to be sampled, yet the representation of low-abundance proteins is reduced (unpublished observation). Therefore, we developed an improved protocol. The major differences are related to the timing and temperature of the dechorionation step, separation of the protein pellet from a liquid fraction, and the wash step (Figure 1).

Reference protocol:
1-step deyolking + 2-step washing

Current protocol:
3-step deyolking + 1-step washing

Dechorionation: proteolysis (15-30 min) at 37°C

Dechorionation: proteolysis (4-5 min) at room temperature

Disrupt the yolk membranes by repeated pipetting (200 µl tip)

Disrupt the yolk membranes by repeated pipetting (100 µl tip)

Centrifuge at 300 g for 30 s; discard the supernatant

Centrifuge at 15,400 g for 1 min, 3 times; discard the supernatant

Wash the pellet (wash buffer) and centrifuge at 300 g for 30 s, 2 times; discard the supernatant

Wash the pellet (10 mM Tris-HCl) and centrifuge at 15,400 g for 1 min; discard the supernatant

Protein extraction
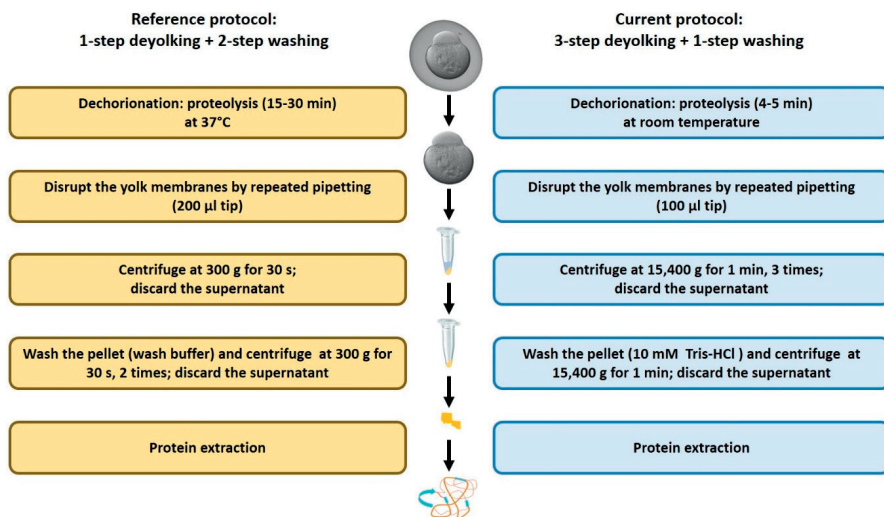
Protein extraction

Figure 1. Schematic representation of major differences between the reference [16] and the current deyolking protocols. The detailed information is given in the text.

We compared our protocol to the protocols by Link et al. [16], which were based on 1-step deyolking with or without subsequent washing steps. For a fair comparison, we compared the reference 1-step deyolking procedure without washing [16] to our 1-step deyolking procedure without washing, and the reference 1-step deyolking plus double wash procedure [16] to our 3-step deyolking plus single wash procedure.

Both methods resulted in a reduction of yolk proteins, and the washing steps further depleted the protein content. Nevertheless, our new protocol yielded a larger number of unique proteins from a smaller number of embryos. We obtained approximately 1.7-fold increase in protein concentration per embryo sample when applying the 1-step deyolking process. When using our 3-step deyolking + single wash protocol, the protein yields per embryo sample were 3.1- and 2.5-fold higher (1-cell and high stage embryos, respectively) than those obtained with the reference protocols [16] with 1-step deyolking + double wash (Figure 2A). The effective number of 1-cell stage embryos needed to collect a workable amount of protein (30 µg) was approximately 2 or 3 times lower when using our 1-step deyolking or 3-step deyolking + single wash protocols, respectively; for the high stage embryos, this number of embryos was approximately 2 times lower than that of the respective reference protocols (Figure 2B). Also, compared to our new protocol, less amount of proteins was harvested with the reference protocol (Figure 2B).
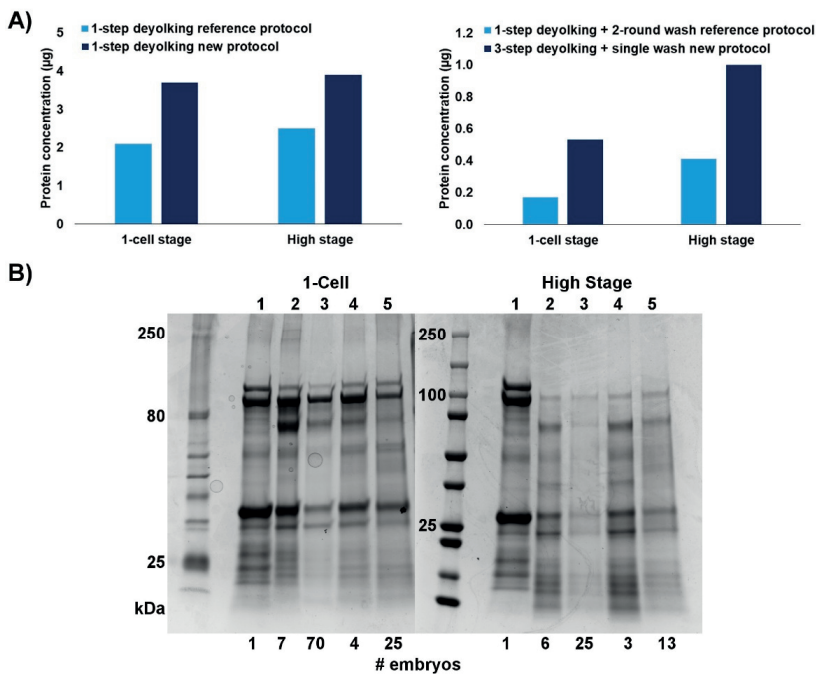

Figure 2. Comparison of the efficiencies of deyolking protocols: reference [16] versus the new one. (**A**) Protein concentration obtained using protocols in 1-step versions (left chart) and in full versions (right chart). (**B**) SDS-PAGE of proteins extracted from zebrafish embryos at 1-cell stage (left panel) and high stage (right panel) using the reference protocols versus new protocols. Lane 1—non-deyolked embryo (control); Lane 2—1-step deyolking reference protocol [16]; Lane 3—1-step deyolking + double wash reference protocol [16]; Lane 4—1-step deyolking (new method); and Lane 5—3-step deyolking + single wash (new method). At the bottom line, number of embryos is given for each sample, from which the proteins were extracted.

2.2. Proteome in Deyolked Versus Non-Deyolked Samples

Generally, the amount of extracted total protein per embryo increased with the developmental advancement of the embryo, and the deyolking procedure greatly reduced the protein concentration. However, this reduction was decreasing from over 25-fold in cleavage stages (1-cell, 16-cell, and 32-cell stages) to approximately 15-fold in the bud stage (Table 1).

Table 1. The amount of protein extracted from deyolked versus non-deyolked embryos.

Developmental Stage	Number of Embryos	Total Sample Volume (μL)	Amount of Extracted Protein (μg)		
			Total	Per μL	Per Embryo
Non-deyolked					
1-cell	28	119	395.08	3.32	14.11
16-cell	20	88	327.36	3.72	16.37
32-cell	40	170	697.00	4.10	17.42
Oblong	20	120	478.80	3.99	23.94
Bud	20	92	524.40	5.70	26.22
Deyolked					
1-cell	575	94	304.56	3.24	0.53
16-cell	300	58	191.41	3.30	0.63
32-cell	400	99	277.22	2.81	0.69
Oblong	225	42	246.54	5.87	1.09
Bud	250	70	413.70	5.91	1.65

Analysis of the digested protein samples using the one-dimensional (1D) mass spectrometry (MS)/MS shotgun proteomics approach (1D shotgun) consistently demonstrated that the deyolking procedure resulted in a greater number of proteins being identified (Supplementary File 1). In the non-deyolked samples, the total numbers of proteins identified throughout the developmental stages were relatively consistent, ranging from 338 to 434 proteins identified in the 1-cell and bud stages, respectively. By comparison, the numbers of proteins identified in deyolked samples in all the developmental stages were considerably higher than in the non-deyolked counterparts. In the cleavage stages, these differences were approximately 2-fold, and increased to over 3-fold in the later developmental stages, ranging from 696 to 1687 proteins identified in the 1-cell and bud stages, respectively (Figure 3A, Supplementary File 1). In contrast to the non-deyolked samples, where there was no apparent correlation between the developmental progression and the total number of proteins identified, deyolked samples resulted in a consistent number of proteins identified throughout cleavage stages (1-cell, 16-cell, and 32-cell), which considerably increased in the later developmental stages (Figure 3A). Most of the proteins identified in the non-deyolked samples were also found in the deyolked counterparts (Figure 3A, Supplementary File 1). The number of proteins unique to the non-deyolked samples (that is, not found in the deyolked counterparts) was relatively stable throughout the developmental stages. In contrast, most of the proteins identified in the deyolked samples were unique, meaning that they were not found in the non-deyolked counterparts, and the number of unique proteins apparently increased throughout the embryonic development from the cleavage stages to the bud stage (Figure 3A, Supplementary File 1).

When looking only to the proteins shared between the non-deyolked and deyolked samples, representation of vitellogenin in the deyolked samples was substantially reduced (36–58 times, depending on developmental stage; Supplementary File 2). At the same time, the representation of non-vitellogenin proteins in the deyolked samples was considerably elevated (2–6 times, depending on developmental stage; Supplementary File 3).
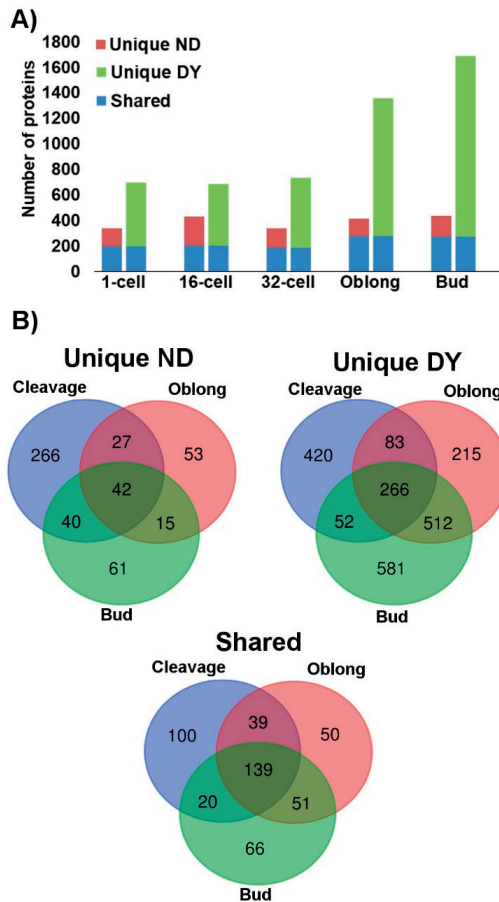
Figure 3. Numbers of proteins identified in samples from intact (non-deyolked, ND) versus deyolked (DY) zebrafish embryos. Unique proteins were found in either ND or DY embryos, whereas shared proteins were found in both ND and DY embryos. (**A**) Total number of unique and shared proteins in ND (left column) and DE embryos (right column) at 1-cell, 16-cell, 32-cell, oblong, and bud developmental stages. (**B**) Specificity and overlap of the identified proteins across the critical stages of early embryonic development: Cleavage stages (1-, 16-, and 32-cell stages combined), maternal–zygotic transition (oblong), and post-maternal–zygotic transition (bud).

Among the 504 proteins unique to non-deyolked samples, most of them were specific to the cleavage stages, and 42 proteins were found in all the developmental stages. By comparison, out of 2129 proteins unique to the deyolked samples, 420 proteins were found in the cleavage stages only, and 266 proteins were found commonly in all the deyolked samples. In contrast to the non-deyolked sample counterparts, a substantial proportion of unique proteins was found in either or both oblong and bud stages. In total, 465 proteins were present in both non-deyolked and deyolked samples across all the developmental stages (Figure 3B, Supplementary File 1).

2.3. Functional Annotations of the Proteome

In both non-deyolked and deyolked samples, the identified proteins were substantially involved in metabolic, ribosome, and biosynthesis of secondary metabolite and proteasome pathways,

while enrichments specific to sampling protocol and/or developmental stage were found in certain pathways, such as in proteasome, RNA transport, or thermogenesis pathways (Table 2).

Table 2. Significant ($p < 0.05$) pathways identified by Kyoto Encyclopedia of Genes and Genomes (KEGG) analysis of proteins from non-deyolked (ND) cleavage, oblong, and bud stage zebrafish embryos, and their deyolked (DY) counterparts. Numbers of proteins mapped to annotated pathways are given.

Pathway Name	ND-Cleavage Stage-Unique	ND- Oblong & Bud Stages Unique	ND-Common in All Stages	DY-Cleavage Stage Unique	DY-Oblong & Bud Stages Unique	DY-Common in All Stages	Shared Proteins
map01100 Metabolic pathways	22	23	6	66	62	87	69
map03010 Ribosome	27	11	2	21	19	11	52
map01110 Biosynthesis of secondary metabolites	12	11	3	21	25	27	32
map04714 Thermogenesis	2	6	1	28	6	37	20
map01200 Carbon metabolism	6	6	1	10	12	21	23
map04141 Protein processing in endoplasmic reticulum	4	0	0	5	14	11	20
map03050 Proteasome	14	4	1	1	15	0	14
map00010 Glycolysis / Gluconeogenesis	6	3	0	2	6	6	12
map00071 Fatty acid degradation	3	1	0	9	1	11	9
map01212 Fatty acid metabolism	8	3	0	7	0	10	8
map04530 Tight junction	5	5	2	6	13	2	7
map03013 RNA transport	7	0	0	3	22	1	6
map04110 Cell cycle	9	2	0	3	12	1	5
map04810 Regulation of actin cytoskeleton	5	1	1	6	12	1	4
map04144 Endocytosis	3	0	0	3	10	6	4
map00230 Purine metabolism	5	5	1	2	11	1	4
map03018 RNA degradation	3	0	0	0	8	1	4
map04210 Apoptosis	0	4	1	4	5	1	4
map00970 Aminoacyl-tRNA biosynthesis	2	1	1	8	12	1	3
map03030 DNA replication	4	3	0	0	14	0	3

Analysis of representation of the identified proteins annotated to functional Gene Ontology (GO) terms revealed multiple processes, functions, and components overrepresented and underrepresented in both non-deyolked and deyolked samples, with some of them specific to the developmental stage (Figure 4, Supplementary File 4).

To distinguish the effect of the extraction protocol (non-deyolked versus deyolked samples) from the biological features (natural representation of proteins at given developmental stage), we used functional annotations of proteins represented in both non-deyolked and deyolked samples from all the developmental stages as a filtering criterion. In this way, shared GO terms were established by: The same proteins identified in samples from both extraction methods ("Shared" dataset); different proteins in both datasets ("unique ND" and "unique DY" datasets) enriching the same terms; or partially the same and partially different proteins ("Shared" and "unique ND", "Shared" and "unique DY", and all the three datasets). Whereas, unique GO terms were established exclusively by proteins from either "unique ND" or "unique DY" datasets.
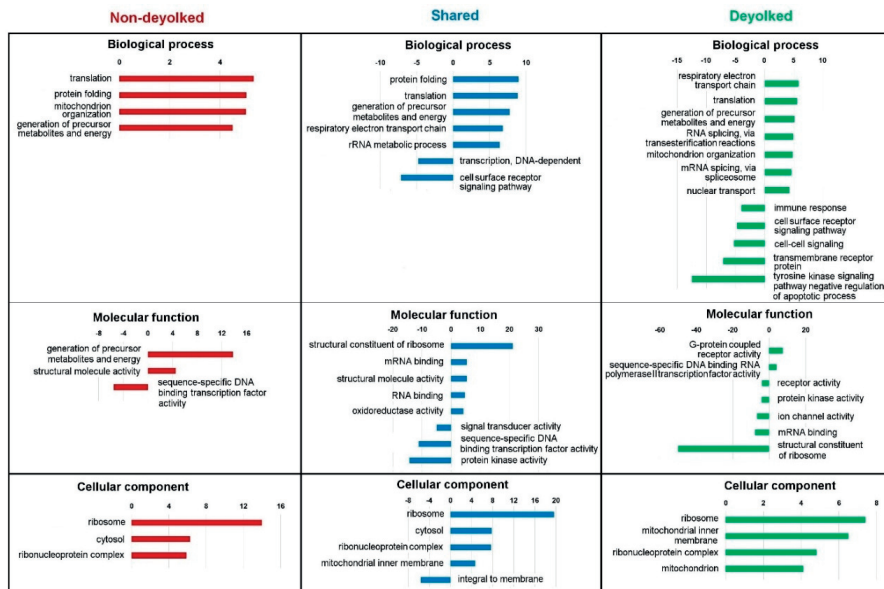
Figure 4. Significantly (false discovery rate (FDR) <0.05) enriched Gene Ontology (GO) terms from SLIM analysis for unique deyolked, unique non-deyolked, and shared proteins grouped by biological process, molecular function, and cellular component. Representation of GO terms containing a minimum 100 reference genes and a fold change ≥4 or ≤4 is given.

Clearly, the deyolking procedure yielded a considerable number of unique GO terms, which were not annotated with the proteins identified in the non-deyolked samples (Supplementary File 5). The most prominent, developmentally relevant examples included enrichment in: Cellular component organization, RNA splicing, DNA replication, intracellular transport, cell cycle, translational initiation, and mitochondrial organization, transport, and gene expression (biological process); ATP binding, GTP binding, NADH dehydrogenase activity, ribonucleoprotein complex binding, translation initiation factor activity, ribosome binding, and ligase activity (molecular function); chromosome, endoplasmic reticulum, Golgi-associated vesicle, polysome, spliceosomal complex, cytochrome, and mitochondrial ribosome, matrix, and respiratory chains I and II (cellular component). Similarly, underrepresentation in unique GO terms was developmentally relevant, and it included: Cell–cell signaling, chemical synaptic transmission, intracellular signal transduction, and immune response (biological process); DNA-binding transcription factor activity, transcription regulator activity, channel activity, G protein-coupled receptor activity, and kinase activity (molecular function); cell surface, extracellular region, and plasma membrane-bounded cell projection (cellular component). In contrast to the abundance of unique GO terms annotated with the "unique DY" dataset, there were very few unique GO terms associated with "unique ND" dataset, with the most notably enriched terms in molecular function: Carbohydrate binding and endopeptidase regulator activity (Supplementary Files 4 and 5).

A certain number of proteins was unique for a given developmental stage (that is, identified only in a single developmental stage), in both non-deyolked and deyolked samples. Interestingly, significantly enriched GO terms for these proteins were different for non-deyolked and deyolked samples, in all five developmental stages investigated (Supplementary File 6).

3. Discussion

The improved deyolking procedure resulted in a considerably high quantity of the extracted total protein (Figure 2A) We identified 2575 proteins in total. In the study by Link et al. [16], 57 proteins were found, but six of them were not identified, and two proteins had a duplicated ID. We manually retrieved these 50 IDs, and found that 47 (94%) proteins were present in our dataset. Two of the three proteins not found in our dataset were actually *Cyprinus carpio* and *Drosophila melanogaster* proteins, but their possible homologues in zebrafish were missing in our dataset as well. We used 3 times less embryos in our procedure (Figure 2B) than in the reference procedure [16]. Consequently, we were able to conduct the proteomics analysis of zygotic and cleavage stages of zebrafish for the first time. Most of the proteins identified in the cleavage stages were unique to these stages of development (786 out of 1494; Figure 2B). This indicates a massive dynamics of zebrafish developmental proteome. It needs to be noted that the protein sequence database, which we did not use for annotating MS data, does not include the sequences of micro-peptides. Therefore, we cannot determine whether the method is suitable for harvesting very small proteins and micro-peptides.

KEGG analysis showed that ribosome, biosynthesis of secondary metabolites, carbon metabolism, and proteasome pathways were detectable in all the samples (Table 2). Also, a number of GO terms were detected in both deyolked and non-deyolked datasets (Supplementary File 5). Nevertheless, we observed a substantial increase in the number of identified unique proteins in the deyolked samples as compared to the non-deyolked counterparts. Consequently, they enriched a number of developmentally relevant GO terms, such as the cell cycle, mitochondrial organization, and functions or translation initiation, which were not enriched in the non-deyolked samples (Supplementary File 5). These functional terms are essential for the proper growth and development of the early stage of embryos [25–28] Knowledge of developmentally relevant proteome will aid understanding the regulation of early embryonic development. The underrepresented GO terms in the deyolked samples were mainly related to cellular signaling, transcription, G protein-coupled receptor activity, and cell surface (Supplementary File 5). These terms were not found underrepresented in the non-deyolked samples. In contrast to the significant GO terms found uniquely in the deyolked samples, there were very few unique GO terms associated with "unique ND" dataset (Supplementary File 5); this indicates that the presence of many embryonic proteins is masked due to the high abundance of yolk.

The functional annotation of cleavage stage proteome is concordant with the canonical knowledge of the catabolism, cell cycle, subcellular organization, and the transcriptional quiescence of pre-MZT embryos [24,29]. Moreover, our data suggest active translation-related processes in the very early embryos. Since zygotic transcripts are not produced yet [8], maternally-provided mRNAs [30] were used to produce the translational machinery and perform the translation. Quantitative proteome analysis throughout the development would be needed to determine the extent of this process, though.

Although the dechorionation/deyolking procedure generally resulted in a substantial increase in the number of identified proteins, it also resulted in a loss of certain proteins as compared to the non-deyolked counterparts (Figure 3A), similarly to a study on 5 dpf zebrafish larvae [21]. Most of the previous proteomic studies did not address the problem of protein depletion due to the deyolking process, and they only used deyolked embryos for the analyses [16,21,22]. In the present study, approximately 30% of the proteins at cleavage stages and 12% at oblong and bud stages were not identified after the deyolking (Figure 3, Supplementary File 1). The GO analysis revealed that these lost proteins are involved in a number of biological processes (translation, protein folding, and mitochondrial organization), molecular functions (generation of precursor metabolites and energy), and cellular component (ribosome and cytosol; Supplementary File 4). Moreover, developmental stage-unique proteins enrich GO terms different for non-deyolked and deyolked samples, in all investigated developmental stages (Supplementary File 6). Altogether, our results suggest that deyolked and non-deyolked samples should be analyzed in parallel to extract a reliable information on the proteome in embryonic development.

4. Materials and Methods

4.1. Fish

The samples were collected at the zebrafish facility of the Nord University, Bodo, Norway. The experimental process and husbandry were performed in agreement with the Norwegian Regulation on Animal Experimentation (The Norwegian Animal Protection Act, No. 73 of 20 December 1974). This was certified by the National Animal Research Authority, Norway, General License for Fish Maintenance and Breeding no. 17.

The maintenance of zebrafish was done using an Aquatic Habitats recirculating system (Pentair, Apopka, FL, USA) and following established protocols [31]. The fish were fed newly hatched *Artemia sp.* nauplii (Pentair) and SDS zebrafish-specific diet (Special Diet Services, Essex, UK) according to the manufacturers' instruction. The zebrafish used in the experiment were from the AB line.

4.2. Sample Collection

Embryos originated from natural spawning and were collected at five developmental stages (Figure 5). Embryo development was monitored and staged according to Kimmel et al. [32]. For each developmental stage, embryo batches were divided into two variants: Non-deyolked and deyolked. The non-deyolked (intact) embryos were promptly snap-frozen in liquid nitrogen and subsequently stored at −80 °C. The deyolked embryo variants went through the process of dechorionation (removal of chorion) and deyolking. Additionally, the 1-cell (0.5 hpf) and high-stage (3.3 hpf) embryos were collected to compare our deyolking protocol with that by [16].
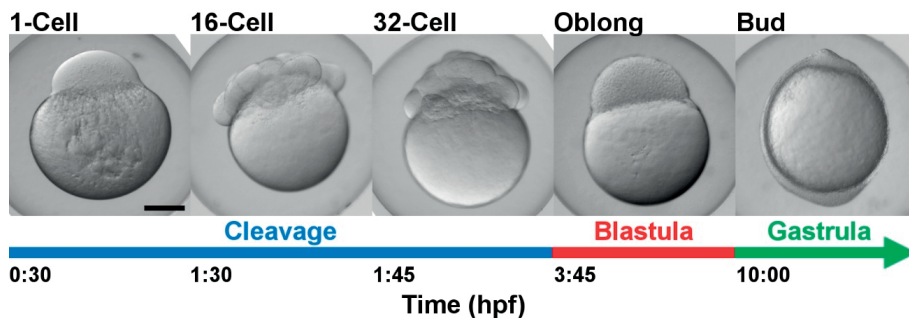

Figure 5. Developmental stages of zebrafish embryos sampled in the present study. hpf = hours post-fertilization at 28.5 °C.

4.3. Dechorionation and Deyolking

Embryos were placed in a Petri dish in phosphate-buffered saline (PBS) supplemented with 1.0 mg/mL Pronase (Sigma Aldrich, St. Louis, MO, USA) [31]. The enzymatic digestion of chorion was performed for 5 min at 37 °C with gentle shaking. Embryos were washed a minimum of 5 times with PBS or until all visible chorion fragments were removed.

The dechorionated embryos were processed using our modified protocol with 3-step deyolking and a single wash. The embryos were transferred to 1.5 mL Eppendorf tubes containing 1.0 mL of deyolking buffer (55 mM NaCl, 3.6 mM KCl, and 1.25 mM $NaHCO_3$) and were mechanically disrupted by pipetting repeatedly through a 100 µL tip. The content was gently mixed by inverting the tube several times before centrifugation at 13,000 RPM for 1 min at 4 °C. The supernatant containing the yolk was discarded, and the pellet was re-suspended with the deyolking buffer, vortexed, and centrifuged as above. The procedure was repeated two times. After this, the pellet was re-suspended with 10 mM Tris-HCl (pH 7.4), vortexed, and centrifuged as above. The supernatant was discarded and

the pellet (deyolked embryos) was snap-frozen in liquid nitrogen and stored at −80 °C. Additionally, for comparison of our protocol with that of [16], the dechorionated embryos at 1-cell and high stage were subjected to two types of deyolking protocols reported by Link et al. [16]: (1) 1-step deyolking, and (2) 1-step deyolking with two additional wash steps.

4.4. Protein Extraction

Both intact (non-deyolked) and deyolked embryo samples were lysed by adding 100 µL of sodium dodecyl sulphate (SDS) lysis buffer (1% SDS; Sigma-Aldrich, St. Louis, MO, USA), 0.5 M triethylammonium bicarbonate buffer pH 8.5 (TEAB; Sigma Aldrich), and 1 × Protease Inhibitor cocktail (Thermo Scientific, Rockford, IL, USA)). The tubes were vortexed and incubated at 90 °C for 30 min, then cooled on crushed ice for 5 min. The lysed material was centrifuged at 13,000 RPM for 20 min at 4 °C. The supernatant, containing the proteins, was collected and transferred to a new Eppendorf tube. The total protein concentration was quantified using a Qubit® 3.0 Fluorometer (Invitrogen, Eugene, OR, USA) and the Qubit™ Protein Assay Kit (Invitrogen) according to the manufacturer's instructions. After the quantification, the samples were freeze-dried (VirTis BenchTop™ K, Warminster, USA) at −80 °C for 18 h before being shipped to the Department of Biological Sciences, National University of Singapore for proteomics analysis.

4.5. Polyacrylamide Gel Electrophoresis

One-dimensional gel electrophoresis was performed to check the efficiency of deyolking protocol, as well as to compare the efficiency of our protocol with the previous ones. Approximately equal concentrations of proteins from each sample were supplemented with 2× SDS loading dye. The samples were denatured by incubation at 95 °C for 10 min and then the proteins were separated by SDS gel electrophoresis (4%–20% Mini-PROTEAN® TGX™ Precast Protein Gels, Bio-Rad, Hercules, California, USA) in SDS running buffer for 1 h. Afterwards, the gel was washed with deionized water for 10 min. The gel was stained with Coomassie Blue (Coomassie Brilliant Blue R-250, Bio-Rad) for 20 min, and de-stained with de-staining solution (40% methanol + 10% acetic acid) overnight at room temperature.

4.6. Tube-Gel Digestion and Sample Clean up

For each sample, 30 µg of proteins were used for downstream proteomics analyses. The samples were polymerized in a 10% polyacrylamide gel containing 4% SDS and subsequently fixed with a fixing reagent (50% methanol, 12% acetic acid) for 30 min at room temperature. The gel was cut into small pieces (1 mm^3) before being washed three times with 50 mM TEAB/50 % acetonitrile (*v/v*) and dehydrated with 100% acetonitrile. Next, samples were reduced using 5 mM Tris(2-carboxyethyl) phosphine (TCEP) at 57 °C for 60 min, followed by alkylation with 10 mM methyl methanethiosulfonate (MMTS) for 60 min at room temperature with occasional vortexing. The gel pieces were washed in 500 µL of 50 mM TEAB, dehydrated in 500 µL acetonitrile, and re-hydrated with 500 µL of 50 mM TEAB. The final dehydration step was performed using 100 µL acetonitrile. Trypsinization (1.5 µg trypsin) was performed at 37 °C for 16 h. The digested peptides were centrifuged at 6000× *g* for 10 min to collect the supernatant and stored at −20 °C (protocol modified from [17]. The samples were lyophilized and 30 µL of the dissolution buffer (0.5 M TEAB, pH 8.5) was added to each sample.

4.7. 1D LC–MS/MS Analysis

The separation of peptides was performed with an Eksigent nanoLC Ultra and ChiPLC-nanoflex (Eksigent, Dublin, CA, USA) in Trap-Elute configuration. The samples were desalted with a Sep-Pak tC 18 µL Elution Plate (Waters, Miltford, MA, USA), and reconstituted using 20 µL of 2% acetonitrile and 0.05% formic acid. Five microliters (µL) of each sample was loaded on a 200 µm × 0.5 mm trap column and eluted on a 75 µm × 15 cm analytical column (ChromXP C18-CL, 3 µm). A gradient formed by mobile phase A (2% acetonitrile, 0.1% formic acid) and mobile phase B (98% acetonitrile, 0.1% formic acid) was used to separate the sample content at a 0.3 µL/min flow rate. The following gradient elution

was used for peptide separation: 0–5% of mobile phase B in 1 min, 5–12% of mobile phase B in 15 min, 12–30% of mobile phase B in 104 min, 30–90% of mobile phase B in 2 min, 90–90% in 7 min, 90–5% in 3 min and held at 5% of mobile phase B for 13 min (protocol modified from [33]).

4.8. Protein Identification and Quantification

Peptide identification was carried out with the ProteinPilot 5.0 software Revision 4769 (AB SCIEX) using the Paragon database search algorithm (5.0.0.0.4767) and the integrated false discovery rate (FDR) analysis function. The data were searched against protein sequence databases downloaded from UniProt on May 2018 (total 119,356 entries). The MS/MS spectra obtained were searched using the following user-defined search parameters: Sample Type: Identification; Cysteine Alkylation: MMTS; Digestion: Trypsin; Instrument: TripleTOF5600; Special Factors: None; Species: *None*; ID Focus: Biological Modification; Database for 2018_May_uniprot-zebrafish.fasta; Search Effort: Thorough; FDR Analysis: Yes. The MS/MS spectra were searched against a decoy database to estimate FDR for peptide identification. The decoy database consisted of reversed protein sequences from the UniProt zebrafish database. FDR analysis was performed on the dataset and peptides identified with a confidence interval ≥95% were taken into account.

4.9. KEGG and Gene Ontology (GO) Functional Pathways Analysis

To analyse functional pathways associated with protein identified from deyolked and non-deyolked samples, KEGG analysis was performed. The FASTA files were submitted to online server "KAAS - KEGG Automatic Annotation Server" (https://www.genome.jp/kegg/kaas/) in order to get KEGG Orthology (KO) assignments [34]. To map KEGG pathways, the obtained KO numbers were submitted to KEGG mapper web server (http://www.genome.jp/kegg/tool/map_pathway2.html) [35].

GO annotation results and pathway of differentially expressed proteins in pairwise comparisons were obtained using Panther (Panther14.0, 2018_04) [36]. The web conversion tool (https://biodbnet-abcc.ncifcrf.gov) was used to convert unmapped UniProt Accession IDs to ZFIN ID. The web tool Biomart was used to convert unmapped ZFIN IDs to Gene stable ID and to manually identify the unmapped IDs by gene names [37]. UniProt was used to identify protein IDs discontinued (deleted) in the 2018_11 release [38].

5. Conclusions

We established an effective deyolking procedure for the proteome analysis of the early stages of zebrafish embryos. Elimination of most of the yolk from early stages of embryos significantly enhanced the identification of cellular proteins with LC–MS-based shotgun proteomics analysis. The improved protocol is applicable to low-input material, enabling investigation of the earliest stages of development. Also, we demonstrated that the deyolking procedure results in the depletion of certain parts of the proteome that can be important in embryonic development. Thus, we suggest that both deyolked and non-deyolked samples should be processed in parallel to ensure a reliable coverage of the proteome during the embryogenesis. Our deyolking procedure will improve both qualitative and quantitative proteome analyses throughout embryonic development of polylecithal animals, such as fish, amphibians, reptiles, and birds.

Abbreviations

ND	Non-deyolked
DY	Deyolked
SH	Shared
iTRAQ	Isobaric tag for relative and absolute quantitation
LC–MS/MS	Liquid chromatography–tandem mass spectrometry
1D LC–MS/MS	One-dimension liquid chromatography–tandem mass spectrometry
MZT	Maternal-to-zygotic transition
PBS	Phosphate-buffered saline
SDS	Sodium dodecyl sulfate
TCEP	Tris-(2-carboxyethyl) phosphine
MMTS	Methyl methane-thiosulfonate
TEAB	Triethylammonium bicarbonate
ACN	Acetonitrile
FDR	False discovery rate
COG	Clusters of orthologous groups
GO	Gene Ontology
KEGG	Kyoto Encyclopedia of Genes and Genomes

References

1. Amsterdam, A.; Hopkins, N. Mutagenesis strategies in zebrafish for identifying genes involved in development and disease. *Trends Genet.* **2006**, *22*, 473–478. [CrossRef] [PubMed]

2. Brownlie, A.; Donovan, A.; Pratt, S.J.; Paw, B.H.; Oates, A.C.; Brugnara, C.; Witkowska, H.E.; Sassa, S.; Zon, L.I. Positional cloning of the zebrafish sauternes gene: A model for congenital sideroblastic anaemia. *Nat. Genet.* **1998**, *20*, 244. [CrossRef] [PubMed]

3. Grosser, T.; Yusuff, S.; Cheskis, E.; Pack, M.A.; FitzGerald, G.A. Developmental expression of functional cyclooxygenases in zebrafish. *Proc. Natl. Acad. Sci. USA.* **2002**, *99*, 8418–8423. [CrossRef] [PubMed]

4. Gündel, U.; Benndorf, D.; von Bergen, M.; Altenburger, R.; Küster, E. Vitellogenin cleavage products as indicators for toxic stress in zebra fish embryos: A proteomic approach. *Proteom.* **2007**, *7*, 4541–4554. [CrossRef] [PubMed]

5. Hanisch, K.; Küster, E.; Altenburger, R.; Gündel, U. Proteomic signatures of the zebrafish (Danio rerio) embryo: Sensitivity and specificity in toxicity assessment of chemicals. *Int. J. Proteom.* 2010. [CrossRef] [PubMed]

6. Howe, K.; Clark, M.D.; Torroja, C.F.; Torrance, J.; Berthelot, C.; Muffato, M.; Collins, J.E.; Humphray, S.; McLaren, K.; Matthews, L. The zebrafish reference genome sequence and its relationship to the human genome. *Nature* **2013**, *496*, 498–503. [CrossRef]

7. Aanes, H.; Winata, C.L.; Lin, C.H.; Chen, J.P.; Srinivasan, K.G.; Lee, S.G.; Lim, A.Y.; Hajan, H.S.; Collas, P.; Bourque, G. Zebrafish mRNA sequencing deciphers novelties in transcriptome dynamics during maternal to zygotic transition. *Genome. Res.* **2011**, *21*, 1328–1338. [CrossRef]

8. Heyn, P.; Kircher, M.; Dahl, A.; Kelso, J.; Tomancak, P.; Kalinka, A.T.; Neugebauer, K.M. The earliest transcribed zygotic genes are short, newly evolved, and different across species. *Cell Rep.* **2014**, *6*, 285–292. [CrossRef]

9. Mehjabin, R.; Xiong, L.; Huang, R.; Yang, C.; Chen, G.; He, L.; Liao, L.; Zhu, Z.; Wang, Y. Full-Length Transcriptome Sequencing and the Discovery of New Transcripts in the Unfertilized Eggs of Zebrafish (Danio rerio). *G3* **2019**. [CrossRef]

10. Nudelman, G.; Frasca, A.; Kent, B.; Sadler, K.C.; Sealfon, S.C.; Walsh, M.J.; Zaslavsky, E. High resolution annotation of zebrafish transcriptome using long-read sequencing. *Genome. Res.* **2018**, *28*, 1415–1425. [CrossRef]

11. White, R.J.; Collins, J.E.; Sealy, I.M.; Wali, N.; Dooley, C.M.; Digby, Z.; Stemple, D.L.; Murphy, D.N.; Billis, K.; Hourlier, T. A high-resolution mRNA expression time course of embryonic development in zebrafish. *Elife* **2017**. [CrossRef] [PubMed]

12. De Souza, A.G.; Mac Cormack, T.J.; Wang, N.; Li, L.; Goss, G.G. Large-scale proteome profile of the zebrafish (Danio rerio) gill for physiological and biomarker discovery studies. *Zebrafish* **2009**, *6*, 229–238. [CrossRef] [PubMed]

13. Groh, K.J.; Nesatyy, V.J.; Segner, H.; Eggen, R.I.; Suter, M.J.-F. Global proteomics analysis of testis and ovary in adult zebrafish (Danio rerio). *Fish Physiol. Biochem.* **2011**, *37*, 619–647. [CrossRef]

14. Singh, S.K.; Sundaram, C.S.; Shanbhag, S.; Idris, M.M. Proteomic profile of zebrafish brain based on two-dimensional gel electrophoresis matrix-assisted laser desorption/ionization MS/MS analysis. *Zebrafish* **2010**, *7*, 169–177. [CrossRef] [PubMed]

15. Zhang, J.; Lanham, K.A.; Peterson, R.E.; Heideman, W.; Li, L. Characterization of the adult zebrafish cardiac proteome using online pH gradient strong cation exchange-RP 2D LC coupled with ESI MS/MS. *J. Sep. Sci.* **2010**, *33*, 1462–1471. [CrossRef] [PubMed]

16. Link, V.; Shevchenko, A.; Heisenberg, C.-P. Proteomics of early zebrafish embryos. *Bmc. Dev. Biol.* **2006**. [CrossRef] [PubMed]

17. Lu, W.; Yin, X.; Liu, X.; Yan, G.; Yang, P. Response of peptide intensity to concentration in ESI-MS-based proteome. *Sci. China Chem.* **2014**, *57*, 686–694. [CrossRef]

18. Vaidyanathan, S.; Kell, D.B.; Goodacre, R. Selective detection of proteins in mixtures using electrospray ionization mass spectrometry: Influence of instrumental settings and implications for proteomics. *Anal. Chem.* **2004**, *76*, 5024–5032. [CrossRef]

19. Lucitt, M.B.; Price, T.S.; Pizarro, A.; Wu, W.; Yocum, A.K.; Seiler, C.; Pack, M.A.; Blair, I.A.; FitzGerald, G.A.; Grosser, T. Analysis of the zebrafish proteome during embryonic development. *Mol. Cell Proteom.* **2008**, *7*, 981–994. [CrossRef]

20. Rahlouni, F.; Szarka, S.; Shulaev, V.; Prokai, L. A Survey of the Impact of Deyolking on Biological Processes Covered by Shotgun Proteomic Analyses of Zebrafish Embryos. *Zebrafish* **2015**, *12*, 398–407. [CrossRef]

21. Tay, T.L.; Lin, Q.; Seow, T.K.; Tan, K.H.; Hew, C.L.; Gong, Z. Proteomic analysis of protein profiles during early development of the zebrafish, Danio rerio. *Proteomics* **2006**, *6*, 3176–3188. [CrossRef] [PubMed]

22. Shaik, A.A.; Wee, S.; Li, R.H.X.; Li, Z.; Carney, T.J.; Mathavan, S.; Gunaratne, J. Functional mapping of the zebrafish early embryo proteome and transcriptome. *J. Proteome Res.* **2014**, *13*, 5536–5550. [CrossRef] [PubMed]

23. Lößner, C.; Wee, S.; Ler, S.G.; Li, R.H.; Carney, T.; Blackstock, W.; Gunaratne, J. Expanding the zebrafish embryo proteome using multiple fractionation approaches and tandem mass spectrometry. *Proteomics* **2012**, *12*, 1879–1882. [CrossRef] [PubMed]

24. Tadros, W.; Lipshitz, H.D. The maternal-to-zygotic transition: A play in two acts. *Development* **2009**, *136*, 3033–3042. [CrossRef]

25. Gong, Y.; Mo, C.; Fraser, S.E. Planar cell polarity signalling controls cell division orientation during zebrafish gastrulation. *Nature* **2004**, *430*, 689. [CrossRef]

26. Sugiyama, M.; Sakaue-Sawano, A.; Iimura, T.; Fukami, K.; Kitaguchi, T.; Kawakami, K.; Okamoto, H.; Higashijima, S.-i.; Miyawaki, A. Illuminating cell-cycle progression in the developing zebrafish embryo. *Proc. Natl. Acad. Sci. USA* **2009**, *106*, 20812–20817. [CrossRef]

27. Artuso, L.; Romano, A.; Verri, T.; Domenichini, A.; Argenton, F.; Santorelli, F.M.; Petruzzella, V. Mitochondrial DNA metabolism in early development of zebrafish (Danio rerio). *Biochim. Biophys. Acta.* **2012**, *1817*, 1002–1011. [CrossRef]

28. Sun, J.; Yan, L.; Shen, W.; Meng, A. Maternal Ybx1 safeguards zebrafish oocyte maturation and maternal-to-zygotic transition by repressing global translation. *Development* **2018**. [CrossRef]

29. Lee, M.T.; Bonneau, A.R.; Giraldez, A.J. Zygotic genome activation during the maternal-to-zygotic transition. *Annu. Rev. Cell Dev. Biol.* **2014**, *30*, 581–613. [CrossRef]

30. Lubzens, E.; Bobe, J.; Young, G.; Sullivan, C.V. Maternal investment in fish oocytes and eggs: The molecular cargo and its contributions to fertility and early development. *Aquaculture* **2017**, *472*, 107–143. [CrossRef]

31. Westerfield, M. A guide for the laboratory use of zebrafish (Danio rerio). *The Zebrafish Book* **2000**, *4*.

32. Kimmel, C.B.; Ballard, W.W.; Kimmel, S.R.; Ullmann, B.; Schilling, T.F. Stages of embryonic development of the zebrafish. *Dev. Dyn.* **1995**, *203*, 253–310. [CrossRef] [PubMed]

33. Suriyanarayanan, T.; Qingsong, L.; Kwang, L.T.; Mun, L.Y.; Seneviratne, C.J. Quantitative proteomics of strong and weak biofilm formers of Enterococcus faecalis reveals novel regulators of biofilm formation. *Mol. Cell Proteom.* **2018**, *17*, 643–654. [CrossRef] [PubMed]

34. Moriya, Y.; Itoh, M.; Okuda, S.; Yoshizawa, A.C.; Kanehisa, M. KAAS: An automatic genome annotation and pathway reconstruction server. *Nucleic. Acids Res.* **2007**, *35*, W182–W185. [CrossRef] [PubMed]

35. Kanehisa, M.; Sato, Y.; Kawashima, M.; Furumichi, M.; Tanabe, M. KEGG as a reference resource for gene and protein annotation. *Nucleic. Acids Res.* **2015**, *44*, D457–D462. [CrossRef] [PubMed]

36. Mi, H.; Huang, X.; Muruganujan, A.; Tang, H.; Mills, C.; Kang, D.; Thomas, P.D. PANTHER version 11: Expanded annotation data from Gene Ontology and Reactome pathways, and data analysis tool enhancements. *Nucleic. Acids Res.* **2016**, *45*, D183–D189. [CrossRef]

37. Zerbino, D.R.; Achuthan, P.; Akanni, W.; Amode, M.R.; Barrell, D.; Bhai, J.; Billis, K.; Cummins, C.; Gall, A.; Girón, C.G.; et al. Ensembl 2018. *Nucleic. Acids Res.* **2017**, *46*, D754–D761. [CrossRef]

38. Apweiler, R.; Bairoch, A.; Wu, C.H.; Barker, W.C.; Boeckmann, B.; Ferro, S.; Gasteiger, E.; Huang, H.; Lopez, R.; Magrane, M. UniProt: The universal protein knowledgebase. *Nucleic. Acids Res.* **2004**, *32*, D115–D119. [CrossRef]

Paper II

Vegetal proteome of early embryo of zebrafish

Purushothaman Kathiresan[1+], Prem Prakash Das[2+], Tao Shijie[2], Lim Teck Kwang[2], Steinar D. Johansen[1], Lin Qingsong[2*], and Igor Babiak[1*]

[1]Faculty of Biosciences and Aquaculture, Nord University, 8049 Bodø, Norway

[2]Department of Biological Sciences, National University of Singapore, 14 Science Drive 4, 117543 Singapore

+These authors share first co-authorship

*Corresponding authors

E-mail addresses:

Purushothaman Kathiresan: kathiresan.purushothaman@nord.no
Prem Prakash Das: dbsppd@nus.edu.sg
Tao Shijie: dbstaos@nus.edu.sg
Lim Teck Kwang: dbslimtk@nus.edu.sg
Steinar D. Johansen: steinar.d.johansen@nord.no
Lin Qingsong: dbslinqs@nus.edu.sg
Igor Babiak: igor.s.babiak@nord.no

Abstract

The embryonic proteome in polylecithal animals is poorly characterized due to the overwhelming presence of the yolk. Particularly, the information is scarce in the earliest stages of development. Here, we focused on the zygote and cleavage stages of the zebrafish embryos (1-, 16- and 32-cell stages) before maternal-to-zygotic transition. We have utilized the isobaric tags for relative and absolute quantification (iTRAQ[TM])-based quantitative proteomics to determine the differential proteome of intact (non-deyolked) embryos versus the deyolked ones. The iTRAQ results were validated using sequential window acquisition of all theoretical fragment ion spectra mass-spectrometry (SWATH MS) based quantitative proteomics. Further, we manually dissected and collected vegetal parts of embryos and performed shotgun LC-MS/MS-based qualitative analysis. We identified 133, 67 and 76 proteins common in both iTRAQ and shotgun-based proteomics datasets for 1-, 16- and 32-cell stage embryos, respectively. These proteins were highly enriched in processes related to translation, post-translational modifications, protein processing and carbon metabolism. Most of these vegetal proteins were of cytoplasmic origin. Also, we demonstrated the presence of ribosomal RNA in the vegetal pole providing additional evidence for the presence of translational machinery in this part of embryo. Immunohistochemical localization of ribosomal protein small subunit 16 (RPS16), eukaryotic translation elongation factor 2 (eEF2), and a chaperone heat shock protein 90-beta (HSP90β) demonstrated their ubiquitous expression in the vegetal cytoplasm, as well as on the membranes of yolk granules. The dynamics of quantitative vegetal proteome indicated *de novo* protein synthesis along with active modification and degradation. Together, these results demonstrate translational, post-translational, and protein processing activity in the vegetal part of the zygote and cleavage stage zebrafish embryos and give the first insight into the vegetal proteome.

Introduction

Zebrafish (*Danio rerio*) is widely used as a model organism to study the developmental biology of vertebrates (Dawid 2004). It is a lecithotrophic animal, and its embryonic and early larval developmental stages are dependent exclusively on yolk as a primary source of proteins, carbohydrates and lipids until the start of exogenous feeding, at ~5 days post-fertilization (dpf) (Allen & Pernet 2007). The yolk of zebrafish embryo is organized in yolk granules, separated with membranes (Thomas 1968, Beams et al. 1985). It is metabolically active in processing *N*-linked glycans and lipids already prior to the blastodisc formation (Fan et al. 2010, Fraher et al. 2016). As in most other oviparous animals, vitellogenins are the most abundant yolk protein precursors. They are synthesized in the mother´s liver upon signaling of estrogens produced in ovarian follicles, and further loaded into the oocytes (Lubzens et al. 2017). During the vitellogenesis, vitellogenins are cleaved into major yolk components: lipovitellin, phosvitin, and β'-c, which are stored in the cell as essential nutrients for future embryogenesis, as well as having immune-related functions (Li & Zhang 2017, Carducci et al. 2019). Apart from vitellogenins, mostly proteinases (Carnevali et al. 1999) and glycosidases (Fan et al. 2010) were studied in aspects of yolk nutritional activity. To our knowledge, no other non-vitellogenin proteins have been reported in the fish yolk. In the chicken yolk, besides vitellogenin cleavage products, other abundant yolk proteins include serum albumin, apovitellenins, IgY, ovalbumin, macroglobulin-like proteins, proteases, protease inhibitors, and antioxidative enzymes (Mann & Mann 2008, Farinazzo et al. 2009).

Upon the fish egg activation, the reorganization of ooplasm is intensive during the cleavage stages. The ooplasm separates from yolk granules and it streams towards the animal pole in the process of blastodisc formation (Beams et al. 1985). This process is driven by bulk actin dynamics in a cell cycle-dependent manner (Shamipour et al. 2019). During the first cell cleavages, axial streamers of ooplasm, in posterior-anterior orientation, are still observed within the yolk cell area (Beams et al. 1985) along with the peripherally located exoplasm (Fernández et al. 2006). So far, no direct evidence of ribosomal functions in the vegetal part of an embryo has been reported. Although early developmental transcriptome and its dynamics are fairly well characterized in zebrafish (Vesterlund et al. 2011, Rauwerda et al. 2017, White et al. 2017), and these maternally-provided transcripts serve as templates for the early translation (Krigsgaber & Neyfakh 1972), the vegetal proteome has not been investigated.

In this study, we characterized quantitative proteome of zebrafish zygote and cleavage stage embryos (1-, 16- and 32-cell stages) differentially for non-deyolking and deyolking extraction methods, using isobaric tags for relative and absolute quantitation

3

(iTRAQ) technique coupled with exponentially modified protein abundance index (emPAI)-MW deconvolution (EMMOL) method (Kim et al. 2012). Sequential window acquisition of all theoretical fragment ion spectra mass-spectrometry (SWATH-MS) has been used to validate iTRAQ results. We also performed Shotgun LC-MS/MS analysis of manually dissected vegetal portions of the embryos and localized chosen proteins using immunohistochemistry (IHC). Our study reveals that most of the vegetal proteome has cytoplasmic location, and that translation and post-translational and degradation processes are active during the early stages of development. We also identified the proteins involved in the carbon metabolism in the vegetal pole.

Material and Methods

Fish

We used AB line of zebrafish for collecting the embryos. For iTRAQ and SWATH experiments, and for RNA extraction from dissected vegetal portions, fish were maintained at the zebrafish facility of the Nord University, Bodø, Norway, at Aquatic Habitats Recirculating System (Pentair, Apopka, FL, USA). SDS zebrafish-specific diet (Special Diet Services, Essex, UK) were used to feed the zebrafish according to the manufacturer's guidelines. The experimental procedures and husbandry were performed in agreement with the Norwegian Regulation on Animal Experimentation (The Norwegian Animal Protection Act, No. 73 of 20 December 1974) and certified by the National Animal Research Authority (Utvalg for forsøk med dyr, forsøksdyrutvalget, Norway) General License for Fish Maintenance and Breeding (Godkjenning av avdeling for forsøksdyr) no. 17.

For the Shotgun LC-MS/MS analysis and IHC study, embryos were collected from fish kept at zebrafish facility, Occupational & Diving Medicine Centre, National University of Singapore (NUS), Singapore, and the experiments were conducted under the protocol number R17-1522. Fish were maintained under the routine procedures and conditions.

Sample collection

Embryos were obtained from the natural spawning of single parents. Newly fertilized eggs were transferred to a Petri dish (100 mm x 15 mm) placed at 28.5°C in a cell incubator. Embryos were collected at three different cleavage embryonic stages: 1-, 16- and 32-cells at 0.30, 1.30 and 1.45 h post-fertilization, respectively (Kimmel et al. 1995). For iTRAQ experiment, three replicates of 1-cell stage embryos, and two replicates of each 16- and 32-cell stage embryos were created. From each replicate, samples for both non-deyolking and deyolking extraction protocols were taken. Per replicate, there were

123   7, 6 and 6 embryos in non-deyolked samples, and 189, 151, and 145 embryos in deyolked
124   samples, for 1-, 16- and 32-cell stages, respectively. The non-deyolked embryos were
125   immediately snap-frozen in liquid nitrogen and further stored at -80˚C. The deyolked
126   embryos were prepared according to our published procedure (Purushothaman et al.
127   2019). For shotgun LC-MS/MS experiment, we used 5, 9 and 14 embryos at 1-, 16- and
128   32-cell stages, respectively. Embryos were placed on a Petri dish coated with 1% agarose
129   in E3 medium under a stereomicroscope. Their chorions were mechanically removed
130   using fine forceps. Approximately half of the yolk cell towards the lower, vegetal pole
131   was collected using a sharp needle tip. A special attention was paid to avoid
132   contamination with the blastodisc part. The dissected yolk portions were immediately
133   plunged into sodium dodecyl sulphate (SDS) lysis buffer followed by the total protein
134   extraction procedure.

Total protein extraction

136   Samples were treated with 100 µl of SDS lysis buffer composed of 1% SDS (Sigma-
137   Aldrich, St. Louis, MO, USA), 0.5 M triethylammonium bicarbonate pH 8.5 (TEAB; Sigma
138   Aldrich), and 1×Protease Inhibitor cocktail (Thermo Scientific, Rockford, IL, USA). The
139   samples were thoroughly mixed and incubated at 90˚C for 30 min, followed by
140   incubation on ice for 5 min. The lysed samples were centrifuged at 15,400 x g for 20 min
141   at 4˚C and the supernatant was collected into a new microcentrifuge tube. For
142   quantification of proteins, the Qubit® 3.0 Fluorometer (Invitrogen, Eugene, OR, USA)
143   and the Qubit™ Protein Assay Kit (Invitrogen) were used according to the
144   manufacturer's protocol. The samples of embryos collected for iTRAQ experiment were
145   lyophilized using (VirTis BenchTop™ K, Warminster, USA) at -80°C for 18 h and shipped
146   to the Department of Biological Sciences, NUS, Singapore, for further analysis. The
147   samples of dissected yolk portions were further processed without the lyophilization
148   step.

Tube-gel digestion and iTRAQ labelling

150   Total protein sample of 100 µg from each replicate (Supplementary Table S1) was
151   used for tube gel preparation according to Lu and Zhu (2005), with modifications. A 100
152   µl polyacrylamide gel was prepared as following: 25 µl of acrylamide (40%, 29:1)
153   solution, 3.5 µl of 1% ammonium persulfate, and 1.5 µl of TEMED, 100 µg protein sample
154   and water up to 100 µl. Polymerized gels were fixed for 30 min at room temperature
155   with a fixing solution (50% methanol, 12% acetic acid). Subsequently, gels were cut into
156   small pieces (~1 mm^3) and cleaned with 500 µl of washing solution I containing 50 mM
157   TEAB/50% (v/v) acetonitrile (ACN) and followed by dehydration with absolute ACN; this
158   step was repeated three times. The dehydrated gel pieces were reduced with 5 mM

159 TCEP at 57°C for 60 min and alkylated with 10 mM methyl methanethiosulfonate
160 (MMTS) for 60 min at room temperature with occasional vortexing. Afterwards, they
161 were washed with 500 µl of 50 mM TEAB and dehydrated with 500 µl of 100% ACN.
162 Then, the gel pieces were treated again with 500 µl of 50 mM TEAB and followed by
163 dehydration with 100 µl of absolute ACN. For trypsinization, the processed gel samples
164 were incubated with trypsin (1 µg of trypsin per 20 µg of proteins) at 37°C for 16 h. The
165 digested peptides were collected after centrifugation at 6000 × g for 10 min and the gel
166 pieces were mixed again with 200 µl each of 50 mM TEAB and absolute ACN for
167 subsequent collection of peptides in the supernatant. The collected supernatants were
168 combined and vacuum dried.

169   The dried peptide samples were re-dissolved with 30 µl of the dissolution buffer (0.5
170 M TEAB at pH 8.5). We used 2 sets of iTRAQ Reagents 8-plex kit (SCIEX, Foster City, CA)
171 to label the digested peptides according to manufacturer's protocol and each set was
172 pooled together (Supplementary Table S1). The pooled samples were desalted using
173 Sep-Pak C18 cartridge (Waters, Milford, MA), and subsequently lyophilized before
174 proceeding to 2D LC-MS/MS.

1D LC-MS/MS analysis (Shotgun-MS analysis)

176   Peptides were desalted with a Sep-Pak tC 18 µl Elution Plate (Waters, Miltford, MA,
177 USA) and vacuum dried, subsequently reconstituted using 30 µl of 2% ACN and 0.05%
178 formic acid. Five µl of each sample were loaded on a 200 µm × 0.5 mm trap column and
179 eluted on a 75 µm × 15 cm analytical column (ChromXP C18-CL, 3 µm). The separation
180 of sample content was performed with a gradient formed by mobile phase A (2% ACN,
181 0.1% formic acid) and mobile phase B (98% ACN, 0.1% formic acid) at a 0.3 µl/min flow
182 rate. The separation of peptides was performed by the following gradient elution: 0 to
183 5% of mobile phase B in 1 min, 5 to 12% of mobile phase B in 15 min, 12 to 30% of mobile
184 phase B in 104 min, 30 to 90% of mobile phase B in 2 min, 90 to 90% in 7 min, 90 to 5%
185 in 3 min and held at 5% of mobile phase B for 13 min.

2D LC-MS/MS analysis (iTRAQ)

187   After lyophilization of peptide samples, 2D LC-MS/MS was performed as described
188 earlier (Ghosh et al. 2013, Das et al. 2019b). We utilized high pH reversed-phase high-
189 performance liquid chromatography (RP-HPLC) (1290 Infinity LC system, Agilent)
190 equipped with a C18 column (WATERS Xbridge C18, 3.5 µm, 3.0 mm×150 mm) to
191 perform first-dimension separation of samples. For gradient preparation, mobile phase
192 A (20 mM ammonium formate in water, pH 10) and mobile phase B (20 mM ammonium
193 formate in 80% ACN, pH 10) were used as follows: mobile phase B 0–10% for 5 min, 10–
194 40% for 60 min, 40–70% for 15 min, 70–100% for 1 min, continued at 100% for 5 min,

and 100–0% for 1 min and subsequently sustained for 10 min at 0% (Suriyanarayanan et al. 2018). The 192 eluted fractions were collected in two 96-well v-bottom plates at a flow rate of 0.5 ml/min. Eluted fractions were pooled into 30 concatenate fractions and lyophilized. The second-dimension separation was carried out as described in the 1D LC-MS/MS section. For MS/MS analysis, 5 µl each of 30 fractions were subjected to online reversed-phase (RP) LC separation on the Ekspert nanoLC-425 system (Eksigent). The RP separation used solvent A (2% ACN and 0.1% formic acid) and solvent B (95% ACN and 0.1% formic acid). Peptide samples were trapped on a precolumn (200 µm × 0.5 mm) before separating on an analytical column (75 µm × 15 cm). Both trap and analytical columns were packed with ChromXP C18CL 3 µm 120 Å phase (Eksigent). Linear gradient of 12-30 % solvent B with a flow rate of 300 nl/min over 90 min were used to elute peptides followed by the analysis with a 5600 TripleTOF system (SCIEX) under positive ionization mode. Mass range of 400–1800 m/z at high-resolution mode (resolution >30,000) with accumulation time of 250 ms per spectrum were used to acquire MS spectra. The 20 most abundant precursors per duty cycle with charges range from +2 to +4 (accumulation time: 100 ms) were selected with 15 s dynamic exclusion for MS/MS analysis in high sensitivity mode (resolution >15,000) with rolling collision energy and iTRAQ reagent collision adjustment settings selected.

Peptide and protein identification

Identification and quantification of iTRAQ-labelled proteins were performed with ProteinPilot 5.0 software Revision 4769 (SCIEX). It utilizes the Paragon database search algorithm (5.0.0.0.4767) and false discovery rate (FDR) analysis function (Shilov et al. 2007, Tang et al. 2008). The search parameters were defined as follows: Sample Type: Identification; Cysteine Alkylation: MMTS; Digestion: Trypsin; Instrument: TripleTOF5600; Special Factors: None; Species: None; ID Focus: Biological Modification; Database:2018_May_uniprot-zebrafish.fasta (total 119356 entries); Search Effort: Thorough; FDR Analysis: Yes. The 1% false discovery rate (FDR) cut-off was applied.

Determination of differentially abundant proteins

The iTRAQ sets contained samples of two types: non-deyolked and deyolked. The former ones were derived from dechorionated embryos containing the whole yolk, while the latter ones were from dechorionated and yolk-depleted (deyolked) embryos (Purushothaman et al. 2019). Therefore, non-deyolked samples were treated as a reference to determine abundance of yolk proteins. Consequently, proteins showing higher abundance in non-deyolked versus deyolked counterparts were considered as putative non-blastodisc proteins (NBPs), whereas proteins with significantly higher abundance in the deyolked samples were considered as putative blastodisc proteins. Differential abundance of proteins against references were determined using paired

232 student's *t*-test with two-tail distribution, where mean $\log_2$ ratio of the replicates were
233 converted into fold change (average ratio) and *p*-value were subsequently calculated for
234 each detected protein. For the selection of differentially abundant proteins, iTRAQ
235 ration >1.3 (*p*-value<0.05) was used as the cut-off threshold for proteins with increased
236 abundance and < 0.76 (*p*-value<0.05) for proteins with decreased abundance (Das et al.
237 2019a).

Exponentially modified protein abundance index (emPAI)-MW deconvolution (EMMOL) for protein quantification

240 We have used a normalization method called exponentially modified protein
241 abundance index (emPAI)-MW deconvolution (EMMOL) to calculate the quantity of
242 individual proteins in each sample (Kim et al. 2012). It uses iTRAQ ratios and the emPAI
243 score of individual proteins to normalize and calculate the protein abundance within and
244 between multiple iTRAQ experiments (Kim et al. 2012). For emPAI score calculation of
245 each protein, MASCOT software (Matrix Science, version 2.6.2) was used to search the
246 MS/MS spectra obtained from the iTRAQ experiments. We used following search
247 parameters: fixed modification-iTRAQ8plex (N-term); iTRAQ8plex (K); variable
248 modifications-Methylthio (C); iTRAQ8plex (Y); protein mass tolerance, 100 ppm;
249 fragment mass tolerance, 0.4 Da; Maximum missed cleavage, 1; and minimum numbers
250 of peptides, 2. The emPAI scores of individual proteins were merged with corresponding
251 iTRAQ ratios (from ProteinPilot 5.0, SCIEX) and the protein contents (weight %) were
252 calculated according to the equation described by Ishihama et al. (2005). The total
253 amount of protein of 800 µg (100 µg/ per iTRAQ channel) was used in each iTRAQ
254 experiment. Therefore, total amount of protein was scaled to 800 µg, and subsequently
255 individual proteins amount in each iTRAQ channel was calculated according to Kim et al.
256 (2012). Total protein amount of each channel was further scaled to 100 µg.

Sequential window acquisition of all theoretical fragment ion spectra mass-spectrometry (SWATH-MS) data acquisition and data processing

259 To generate the sequential window acquisition of all theoretical fragment ion spectra
260 **(**SWATH) spectral library, 2 µg of peptides from pooled deyolked and non-deyolked
261 samples (three technical replicates each) were analysed using the online LC/MS analysis
262 as described in the earlier section with some modifications. Peptides were first trapped
263 on a trap column (100 µm × 25 mm, Reprosil-PUR C18-AQ 3 µm 120 Å, New Objective)
264 before separation on an analytical column (75 µm × 15 cm, ChromXP C18CL 3 µm 120 Å,
265 Eksigent). Peptides were eluted using a two-step gradient composed of 5-18% solvent B
266 over 60 min followed by 18-30% solvent B over 60 min at 300 nl/min. Eluted peptides
267 were analysed using the 6600 TripleTOF system (SCIEX) in the data-dependent analysis
268 mode. Precursor mass range was set at 350-1800 *m/z*, allowing for 250 ms accumulation

269 time per spectrum. A maximum of 50 most abundant precursors were selected for
270 MS/MS fragmentation with 50 ms accumulation time. Generated spectra were searched
271 using the ProteinPilot 5.0 software (SCIEX) against zebrafish UniProt database (2019
272 September release, 54664 entries) using the Paragon search engine (v5.0.0.0) with
273 following parameters: cysteine alkylation by MMTS, common biological modifications
274 specified within the algorithm and detected protein threshold at 0.05. A decoy reversed
275 database was automatically generated using above-mentioned database and searched
276 for FDR analysis.

277 For SWATH data acquisition, 1 µg of peptides from each sample was injected into the
278 LC system as above described and analysed with the 6600 TripleTOF in SWATH-MS mode
279 (DIA). Precursor data were collected from 350-1800 m/z mass range with 50 ms
280 accumulation time. A total of 120 variable SWATH windows were used, ranging from
281 400-1200 m/z with 1 Da window overlaps and minimum window width of 4 Da. Rolling
282 collision energy was used with the spread of 5 eV. Fragment ion spectra for each window
283 were collected in high sensitivity mode with accumulation time of 25 ms over 100–1800
284 m/z mass range, resulting in a total cycle time of 3.1 s.

285 The acquired SWATH data files were analysed using SWATH Acquisition MicroApp 2.0
286 in the PeakView 2.1 software (SCIEX). For peak area extraction, following parameters
287 were used: 25 ppm ion library tolerance, 10 min extracted ion chromatogram (XIC)
288 extraction window, 1% FDR, considering only 99% confident peptides and excluding
289 shared peptides. Up to 10 peptides with 6 transitions for each protein were processed
290 for XIC peak area extraction and exported for analysis in the MarkerView 1.2.1 software
291 (SCIEX). Global normalization was used based on the sum of total area of all proteins
292 detected.

Bioinformatics and statistics

294 For functional analysis, Eukaryotic Orthologous Groups (KOG) classification was used
295 to categorize the identified proteins into 4 broad categories: metabolism, cellular
296 process and signalling, information storage and processing, and poorly characterized
297 (Tatusov et al. 2000). To obtain KOG annotation of NBPs, the corresponding FASTA
298 sequences were submitted into eggNOG-mapper
299 (http://eggnogdb.embl.de/#/app/emapper) and analysed against eggNOG 4.5.1
300 database with the following parameters: a) mapping mode, HMMER; b) Taxonomic
301 Scope, chordata; c) Orthologs, use all orthologs (prioritize coverage); and d) Gene
302 Ontology evidence, use non-electronic terms (prioritize coverage) (Huerta-Cepas et al.
303 2015). NBPs were classified into 25 functional groups according to KOG annotation. For
304 Kyoto Encyclopedia of Genes and Genomes (KEGG) analysis, we subjected FASTA files of
305 identified proteins to online server "KAAS - KEGG Automatic Annotation Server"

306 (https://www.genome.jp/kegg/kaas/) to obtain KEGG Orthology (KO) assignments
307 (Moriya et al. 2007). The list of KO numbers was input into KEGG mapper web server
308 (http://www.genome.jp/kegg/tool/map_pathway2.html) to map KEGG pathways
309 (Kanehisa et al. 2015). For Gene Ontology (GO) analysis, we used UniProt accession
310 numbers to obtain GO annotation and subsequent functional classification using online
311 server "Panther classification system" (http://www.pantherdb.org/geneListAnalysis.do)
312 (Panther14.1, 2019-07-03; (Mi et al. 2017). Venn diagrams were created using the online
313 tool "Bioinformatics & Evolutionary Genomics"
314 (http://bioinformatics.psb.ugent.be/webtools/Venn/). To represent comparative
315 proteomics of deyolked vs non-deyolked zebrafish embryo data graphically, volcano
316 plots were generated using "Instant clue" open-source software
317 (http://www.instantclue.uni-koeln.de) (Nolte et al. 2018).

Immunohistochemistry and imaging

319 Embryos of 1-, 16- and 32- cell stages were fixed in 10% Neutral Buffered Formalin
320 (Sigma) for 24-48 h. They were dehydrated in ascending grades of ethanol, infiltrated
321 with xylene, and impregnated with paraffin. After processing, samples were embedded
322 in paraffin wax and sectioned at 5 μm thick slices and mounted on a glass slide.

323 Immunostaining was performed in Leica Bond III Automated Staining System. The
324 sections were deparaffinised with Bond dewax solution (AR9222) and rehydrated
325 through descending grades of 100% ethanol to 1× Bond wash solution. The samples
326 were treated with Bond epitope retrieval solution (Leica microsystems, cat: ar9640) at
327 pH 9.00 for 40 min at 100°C and cooled to room temperature. Subsequently, specimens
328 were washed four times with 1× Bond wash solution for 5 min. Sections were blocked
329 with endogenous peroxidase for 15 min, then five times washed with 1× Bond wash
330 solution (2 min each) and treated with 10% goat serum for 30 min. Primary antibodies,
331 diluted with Bond antibody diluent 1:50, were applied overnight at 4°C. They were
332 against ribosomal protein S16 (RPS16; Invitrogen, cat: PA5-40733), eukaryotic
333 translation elongation factor 2 (EEF2; Abcam, cat: ab33523), and heat shock protein 90
334 (Hsp90 β; Abcam, cat: ab236282). For negative control, the sections were treated with
335 Bond Antibody Diluent without a primary antibody. The sections were washed five times
336 (2 min each) with 1× Bond wash solution, then incubated with polymer (Leica, DS9800)
337 for five min. The specimens were treated with Bond mixed DAB refine (Leica, DS9800)
338 for 7 min and the DAB reaction was stopped by rinsing in deionized water. Subsequently,
339 sections were stained with haematoxylin (Leica, DS9800) and washed with water
340 deionized and 1× Bond wash solution. Slides were dehydrated and mounted with
341 synthetic mounting media. The presence of positive staining was viewed under Olympus
342 BX51 microscope (Olympus Corporation, Tokyo, Japan). The representative images were

captured at 200x and 600x magnifications using DP71 Camera (Olympus Corporation, Tokyo, Japan).

For immunofluorescence staining, the sections mounted on a glass slide were deparaffinised with xylene and rehydrated through descending grades of ethanol and then placed into milli-Q water. Then, the specimens were treated with EDTA buffer (pH 9.06) for 40 min at 121°C to expose the antigenic determinants in epitopes. Subsequently, they were washed three times with Tris buffered saline (TBS) containing 0.5% Tween 20 (TBS-T) for 5 min. Sections were blocked with 10% goat serum in TBS-T for 30 min. Primary antibodies, the same as in the section above, at dilution of 1:50, were applied overnight at 4°C. For negative control, the sections were treated with goat serum without a primary antibody. The sections were washed with running tap water and TBS-T for 10 and 5 min, respectively, then incubated with secondary antibody Alexa 488-coupled goat-anti-rabbit (Invitrogen, cat: A11034) at 1:500 dilution for 30 min in the dark, followed by washing with running tap water and PBS-T for 10 and 5 min, respectively. All sections were counterstained with DAPI (Vector Laboratories, cat: H-1200). The presence of positive staining was inspected under Confocal laser scanning microscope (Olympus FLUOVIEW FV3000). The DAPI signal was serving as a positive control, while the Alexa flour 488 signal determined locations of primary antibodies.

RNA extraction and determination of presence of rRNA

RNA was extracted from dissected lower halves of yolk cells using QIAzol lysis reagent (Qiagen, Hilden, Germany) following manufacturer's guidelines. Its profile was characterised using the Agilent 2200 tape station (Agilent, Santa Clara, USA) utilizing High Sensitivity RNA screen tape (Agilent).

Results

Vegetal proteins in cleavage stage embryos

We identified 1245 (1-cell stage) and 2549 proteins (16- and 32-cell stages) in the iTRAQ experiment (Table 1). Despite lower number of spectra and identified proteins in comparison with later developmental stages (Supplementary Figure S1), the highest number of differentially abundant proteins (DAPs) showing significant decrease in deyolked samples as compared to their non-deyolked counterparts (DAP-) was found at the 1-cell stage; then, the number of DAPs- was decreasing with the development (Table 1 and Supplementary File S1). In the shotgun experiment, we identified 169, 103 and 111 proteins in the dissected vegetal pole from 1-, 16- and 32-cell stage embryos, respectively (Supplementary File 2). Out of these, 133, 67, and 76 proteins, respectively, were found also in the iTRAQ experiment (Figure 1 and Supplementary File 3). Proteins verified by the shotgun LC-MS/MS were within DAPs identified by iTRAQ, both showing significant increase in deyolked samples as compared to their non-deyolked counterparts DAP+ and DAP- (Figure 2).

Functional classifications of vegetal proteins and associated pathways

The proteins identified independently by both iTRAQ and shotgun MS methods were further considered as verified vegetal proteins, that is present in the vegetal part of an embryo (not implicating whether they are present or absent in the blastodisc). They were subjected to EuKaryotic Orthologous Groups (KOG) and Kyoto Encyclopedia of Genes and Genomes (KEGG) pathways. The KOG analysis showed distribution into four functional categories and further into 20 groups (Figure 3). In all the three developmental stages, *posttranslational modification, protein turnover, chaperones* was the most represented group, followed by *translation, ribosomal structure and biogenesis*. At the 1-cell stage, 133 proteins were annotated and classified into *metabolism*, *cellular processes and signalling*, *information storage and processing*, and *the poorly characterized protein category* (31%, 39%, 20% and 9%, respectively). For 16-cell (67 annotated proteins) and 32-cell (76 annotated proteins) stages, these fractions were 31%, 33%, 18% and 17%, and 32%, 45%, 10% and 13%, respectively (Figure 3).

Vegetal proteins belonged to several major pathways according to the KEGG analysis, with *ribosome*, *carbon metabolism*, *protein processing in endoplasmic reticulum*, and *biosynthesis of amino acids* as the most represented ones (Table 2).

Response to lipid and *response to hormone* were the two biological processes highly enriched in vegetal proteins in all three developmental stages according to GO analysis. Biological processes related to *translation* and *ribonucleoprotein formation* were enriched specifically at 1-cell stage only. Under molecular function category, *structural*

constituent of ribosome and *structural molecule activity* were the most representative terms during early embryogenesis in 1- and 16-cell stages, and *lipid transporter activity* was the only term significantly enriched in all three developmental stages. Under the cellular component category, *ribosomal subunit*, *ribosome*, *cytosolic part* and *lysosome* were significantly enriched at 1- and 16-cell stages, and *cytosol* was the only term significantly enriched in all three developmental stages (Figure 4).

Protein dynamics

We have used the EMMOL method to calculate the quantitative dynamics of proteins belonging to four groups: *ribosome*, *carbon metabolism*, *protein processing in ER and proteasome*, and *translational developmental and nuclear*. Ribosome and carbon metabolism generally showed similar downward trend. The other two groups showed an initial dip at 16-cell stage, followed by upward trend (Figure 5).

Validation of selected proteins using SWATH

We selected 25 proteins from 6 categories; ribosome pathways (10 proteins), carbon metabolism (6), protein processing in endoplasmic reticulum (3), translation (3), nuclear (2) and developmental (1). All these proteins were DAP- in iTRAQ experiment. The results of SWATH analysis were fully concurrent since the abundance of these proteins in deyolked samples was decreased as compared to the non-deyolked counterparts (Table 3).

Localization of selected proteins in early embryos

All the three targeted proteins HSP90, RPS16 and EEF2 showed ubiquitous presence in the cytoplasm across all the developmental stages, both in the blastodisc and vegetal parts of embryos (Figure 6, Supplementary Figure S2). Within the yolk cell area, the proteins localized to the thin layer of ectoplasm (peripheral cytoplasm) surrounding the inner parts of the yolk (Supplementary Figure S3) were decreasing in number and size, or eventually forming vertically oriented stretches, axial streamers (Figure 6). This was also apparent to the clusters of endoplasm among the yolk cell granules. In addition, the immunostained proteins showed localization to membranes of yolk granules (Supplementary Figure S4). Signals were not localized to the yolk cell membrane (Supplementary Figure S3).

Presence of ribosomal RNA in the yolk of cleavage stage embryos

The qualitative analysis of the total RNA extracted from dissected yolk portions showed a distinct presence of nuclear rRNA, both large (28S) and small (18S) subunits (Supplementary Figure S5).

Discussion

A number of studies have been performed on transcriptome dynamics in zebrafish embryos where focus has been given to determining the onset of the zygotic transcription (maternal-to-zygotic transition, MZT), which marks the start of zygotic control over the development (Vesterlund et al. 2011, Harvey et al. 2013, Heyn et al. 2014, White et al. 2017). Despite the fact that pre-MZT phase of the development is driven primarily by maternal proteins, either loaded pre-ovulatory or translated post-fertilization (Tadros & Lipshitz 2009), the reports on zebrafish embryonic proteome (Link et al. 2006, Lucitt et al. 2008) are few, and particularly those of pre-MZT. The main reason is the lack of an appropriate methodology for reliable analyses. In our recent study (Purushothaman et al. 2019), we improved the deyolking procedure in zebrafish embryos, generating a proper coverage of proteins and overcame the problem of highly abundant vitellogenins in early stages of development. The iTRAQ-based comparative quantitative proteomics study represents a first insight into the vegetal proteome, beyond vitellogenins, in zebrafish embryos at cleavage stages. Our results reveal presence of diverse categories proteins representing various functional and structural pathways not characterized previously in the vegetal embryo.

The vegetal proteins are mostly cytoplasmic and ubiquitous

The process of segregation of ooplasm from the yolk begins at stage V oocytes (Fernández et al. 2006) , and is driven by bulk actin polymerization (Shamipour et al. 2019). Some of the initial features persist to the cleavage stage (Fernández et al. 2006). They include: the granular structure of ooplasm due to presence of ribonucleoproteins and organelles, the presence of most peripheral cytoplasmic layer (ectoplasm), inner stretches of endoplasm (axial streamers), and organization of yolk cell granules inwards and outwards of the yolk cell (Figure 6, Supplementary Figures S3 and S4). It is well known that the yolk-containing, vegetal part of zebrafish embryos at the early stages contains essential determinants for the further development (Mizuno et al. 1999, Ober & Schulte-Merker 1999). Most of these essential elements are maternal mRNAs and proteins that are localized in the embryonic vegetal portions (Fuentes et al. 2018). Deyolking procedure results in a considerable reduction of vitellogenins (Purushothaman et al. 2019). Interestingly, the present study revealed that most of the proteome derived from the vegetal parts of embryos (MS shotgun analysis) was not specifically depleted in the deyolked embryos versus their non-deyolked counterparts (iTRAQ analysis; Figure 2). Moreover, vegetal proteins were considerably enriched in cytosolic part (GO, cellular component) at 1- and 16-cell stages (Figure 4), suggesting that the yolk removal (deyolking procedure) has not affected them at most. Consequently, this indicates that the localization of the majority of vegetal part proteins is cytoplasmic (both ecto- and endoplasmic) and not specific to the vegetal part, similarly

476 to maternal transcripts (Lubzens et al. 2017, Winata & Korzh 2018). In line with this, the
477 three proteins confirmed with IHC (HSP90, RPS16 and EEF2) were localized to the whole
478 cytoplasm ubiquitously (Figure 6).

Translational, post-translational, and protein processing activity in the vegetal part of cleavage stage zebrafish embryos

481   To our knowledge, there is no previous data on the translational processes in the
482 vegetal part of early embryos. Our proteomics analysis discovered the presence of
483 components of both small (40S) and large (60S) ribosomal subunits in the vegetal part
484 of cleavage embryos, including proteins (S16, S25, S3, S5, and L11, L24, L14, L4, L6, P2,
485 respectively; Table 3), and rRNA (Supplementary Figure S5). Also, we showed the
486 presence of translation factors, such as eukaryotic translation elongation factor eEF2b
487 and elongation factor eEF1α, and chaperones, such as heat shock protein HSP90β. Most
488 of them were verified with three independent methods (iTRAQ, MS Shotgun, and
489 SWATH; Table 3). Additionally, we confirmed the presence of RPS16, eEF2b and HSP90β
490 in the vegetal cytoplasm by IHC (Figure 6, Supplementary Figure S2). The vegetal
491 proteins were highly enriched in translation and post-translational functional categories
492 (Figure 6). All these results suggest active translational and post-translational processes
493 in the vegetal part of an early embryo.

494   The intriguing question is to what extent this activity is specific to the vegetal part.
495 Anatomically and morphologically, the vegetal cytoplasm, both ecto- and endoplasm,
496 resembles the blastodisc counterpart, both rich in ribonucleoproteins and mitochondria
497 (Fernández et al. 2006). Also, a number of proteins, as those examined by IHC, are
498 ubiquitous. However, a number of determinants of the further development, including
499 axis formation and primordial germ cell formation, is located vegetally and transported
500 to specific functional locations *via* vegetal cortex microtubules within a defined time
501 after the egg activation (Welch & Pelegri 2017, Winata & Korzh 2018). Removal of the
502 vegetal part during the 1-cell stage results in ventralization of the embryos, and the
503 vegetal part of the yolk cell contains determinants of mezoderm induction (Ober &
504 Schulte-Merker 1999). Apart from the developmental determinants, vegetal part of an
505 embryo has other functions, such as those related to metabolism (Fan et al. 2010,
506 Lubzens et al. 2017). However, most of the evidence for "maternal factors" or
507 "maternal-effect genes" is derived from RNA-based analyses, while the information on
508 the corresponding proteome is very scarce if any (Lubzens et al. 2017).

509   Notably, protein processing in endoplasmic reticulum and proteasome is a highly
510 enriched KEGG pathway (Table 2). The transitional endoplasmic reticulum ATPase
511 protein is involved in stress-induced ER-based quality control of newly synthesized
512 proteins (Kadowaki et al. 2015). This ATPase is also required for the clearance of

513 ubiquitinated proteins by autophagy (Papadopoulos et al. 2017), which then are
514 transported to proteasome and deubiquitinated by an ubiquitin carboxyl-terminal
515 hydrolase before degradation (Yeh & Klesius 2010). Protein disulfide-isomerase is an
516 enzyme of ER involved in disulfide bond formation (Wilkinson & Gilbert 2004, Gruber et
517 al. 2006). These activities, important for ER function, were constitutively present among
518 the vegetal proteins (Figure 5 and Table 3).

519 Carbon metabolism in the vegetal part of zebrafish early embryo

520 Carbon metabolism is a central energy metabolism and has an essential role in many
521 biological processes within cell signalling, proliferation and differentiation (Shyh-Chang
522 et al. 2013, Pavlova & Thompson 2016). Zebrafish yolk contains relatively low level of
523 carbohydrates, but is rich in fatty acids and free amino acids (Hoar et al. 1988, Kamler
524 2007). Experimental multiple-fold enrichment of zebrafish yolk with glucose had little
525 effect on carbohydrate metabolic genes (Rocha et al. 2014). Interestingly, our
526 proteomics results showed the presence of multiple glycolytic, citric acid cycle and
527 pentose phosphate pathway enzymes in the vegetal embryo. The KEGG pathway
528 analysis identified several proteins belonging to carbon metabolism pathway at 1-cell
529 (10 proteins), 16-cell (4 proteins) and 32-cell (4 proteins) stages. Glycolytic enzymes,
530 such as phosphoglycerate kinase (F1QXV8), glyceraldehyde-3-phosphate
531 dehydrogenase (A0A0R4IGI1), pyruvate kinase PKM (Q7ZVT2), triosephosphate
532 isomerase A (TPISA), or enolase (Q6TH14E), as well as pentose phosphate pathway
533 enzyme transaldolase (A0A1L1QZF2) were either gradually decreasing in time or showed
534 a slight elevation at the 16-cell stage followed by the decrease at 32-cell stage. Whereas
535 enzymes of citric acid cycle, such as malate dehydrogenase (Q7T334), aspartate
536 aminotransferase (F1QCD4) and isocitrate dehydrogenase 2 (E7F4R9) showed gradual
537 increase throughout the development (Figure 5). This indicate that carbohydrate
538 catabolism is generally decreasing in time, perhaps due to the usage of the stored
539 carbohydrates, being gradually replaced by the acetate catabolism (citric acid cycle).

540

Conclusion

542 The present study investigated proteomic profiles of zygote and cleavage stages of
543 the zebrafish embryos prior to MZT. Quantitative and qualitative proteomics analyses
544 uncovered the enriched abundance of translation, post-translational modifications,
545 protein processing and carbon metabolism processes in the vegetal region of the zygote
546 and cleavage-stage zebrafish embryo. The presence of rRNA in the vegetal pole is
547 consistent with the existence of translational machinery in this part of the embryo. Our
548 results further suggested that most of the vegetal proteome has a cytoplasmic origin,
549 where processes like translation and post-translational and degradation were active

550　during the early stages of development. This study represents a first detailed view of the
551　vegetal proteome of early developing zebrafish embryos.

552

Acknowledgments

560

References

561

562 Allen JD, Pernet B (2007) Intermediate modes of larval development: bridging the gap between
563   planktotrophy and lecithotrophy. Evolution & Development 9:643-653

564 Beams H, Kessel R, Shih C, Tung H (1985) Scanning electron microscope studies on blastodisc formation in
565   the zebrafish, *Brachydanio rerio*. Journal of Morphology 184:41-49

566 Carducci F, Biscotti M, Canapa A (2019) Vitellogenin gene family in vertebrates: evolution and functions.
567   The European Zoological Journal 86:233-240

568 Carnevali O, Carletta R, Cambi A, Vita A, Bromage N (1999) Yolk formation and degradation during oocyte
569   maturation in seabream *Sparus aurata*: involvement of two lysosomal proteinases. Biology of
570   Reproduction 60:140-146

571 Das PP, Chua GM, Lin Q, Wong S-M (2019a) iTRAQ-based analysis of leaf proteome identifies important
572   proteins in secondary metabolite biosynthesis and defence pathways crucial to cross-protection
573   against TMV. Journal of Proteomics 196:42-56

574 Das PP, Lin Q, Wong S-M (2019b) Comparative proteomics of Tobacco mosaic virus-infected Nicotiana
575   tabacum plants identified major host proteins involved in photosystems and plant defence.
576   Journal of Proteomics 194:191-199

577 Dawid IB (2004) Developmental biology of zebrafish. Annals of the New York Academy of Sciences
578   1038:88-93

579 Fan X, Klein M, Flanagan-Steet HR, Steet R (2010) Selective yolk deposition and mannose phosphorylation
580   of lysosomal glycosidases in zebrafish. Journal of Biological Chemistry 285:32946-32953

581 Farinazzo A, Restuccia U, Bachi A, Guerrier L, Fortis F, Boschetti E, Fasoli E, Citterio A, Righetti PG (2009)
582   Chicken egg yolk cytoplasmic proteome, mined via combinatorial peptide ligand libraries. Journal
583   of Chromatography A 1216:1241-1252

584 Fernández J, Valladares M, Fuentes R, Ubilla A (2006) Reorganization of cytoplasm in the zebrafish oocyte
585   and egg during early steps of ooplasmic segregation. Developmental dynamics: an official
586   publication of the American Association of Anatomists 235:656-671

587 Fraher D, Sanigorski A, Mellett NA, Meikle PJ, Sinclair AJ, Gibert Y (2016) Zebrafish embryonic lipidomic
588   analysis reveals that the yolk cell is metabolically active in processing lipid. Cell Reports 14:1317-
589   1329

590 Fuentes R, Mullins MC, Fernández J (2018) Formation and dynamics of cytoplasmic domains and their
591   genetic regulation during the zebrafish oocyte-to-embryo transition. Mechanisms of
592   Development 154:259-269

593 Ghosh D, Li Z, Tan XF, Lim TK, Mao Y, Lin Q (2013) iTRAQ based quantitative proteomics approach validated
594   the role of calcyclin binding protein (CacyBP) in promoting colorectal cancer metastasis*.
595   Molecular & Cellular Proteomics 12:1865-1880

596 Gruber CW, Cemazar M, Heras B, Martin JL, Craik DJ (2006) Protein disulfide isomerase: the structure of
597   oxidative folding. Trends in Biochemical Sciences 31:455-464

598 Harvey SA, Sealy I, Kettleborough R, Fenyes F, White R, Stemple D, Smith JC (2013) Identification of the
599   zebrafish maternal and paternal transcriptomes. Development 140:2703-2710

600 Heyn P, Kircher M, Dahl A, Kelso J, Tomancak P, Kalinka AT, Neugebauer KM (2014) The earliest transcribed
601   zygotic genes are short, newly evolved, and different across species. Cell Reports 6:285-292

602 Hoar WS, Randall DJ, Blaxter JHS, Rombough PJ, Alderdice DF, Von Westernhagen H, Mommsen TP, Walsh
603   PJ, Heming TA, Buddington RK, Yamagami K (1988) Fish physiology, volume xi: The physiology of
604   the developing fish; Part A: eggs and larve, San Diego, Academic Press, Inc

605 Huerta-Cepas J, Szklarczyk D, Forslund K, Cook H, Heller D, Walter MC, Rattei T, Mende DR, Sunagawa S,
606   Kuhn M, Jensen LJ, von Mering C, Bork P (2015) eggNOG 4.5: a hierarchical orthology framework
607   with improved functional annotations for eukaryotic, prokaryotic and viral sequences. Nucleic
608   Acids Research 44:D286-D293

609 Ishihama Y, Oda Y, Tabata T, Sato T, Nagasu T, Rappsilber J, Mann M (2005) Exponentially modified protein
610   abundance index (emPAI) for estimation of absolute protein amount in proteomics by the
611   number of sequenced peptides per protein. Molecular & Cellular Proteomics 4:1265-1272

612 Kadowaki H, Nagai A, Maruyama T, Takami Y, Satrimafitrah P, Kato H, Honda A, Hatta T, Natsume T, Sato
613   T, Kai H, Ichijo H, Nishitoh H (2015) Pre-emptive quality control protects the ER from protein
614   overload via the proximity of ERAD components and SRP. Cell Reports 13:944-956

615 Kamler E (2007) Resource allocation in yolk-feeding fish. Reviews in Fish Biology and Fisheries 18:143

616 Kanehisa M, Sato Y, Kawashima M, Furumichi M, Tanabe M (2015) KEGG as a reference resource for gene
617   and protein annotation. Nucleic Acids Research 44:D457-D462

618 Kim PD, Patel BB, Yeung AT (2012) Isobaric labeling and data normalization without requiring protein
619   quantitation. Journal of Biomolecular Techniques 23:11-23

620 Kimmel CB, Ballard WW, Kimmel SR, Ullmann B, Schilling TF (1995) Stages of embryonic development of
621   the zebrafish. Developmental Dynamics 203:253-310

622 Krigsgaber MR, Neyfakh AA (1972) Investigation of the mode of nuclear control over protein synthesis in
623   early development of loach and sea urchin. Journal of Embryology and Experimental Morphology
624   28:491-509

625 Li H, Zhang S (2017) Functions of vitellogenin in eggs. Results Problems in Cell Differentiation 63:389-401

626 Link V, Shevchenko A, Heisenberg C-P (2006) Proteomics of early zebrafish embryos. BMC Developmental
627   Biology 6:1

628 Lu X, Zhu H (2005) Tube-gel digestion: a novel proteomic approach for high throughput analysis of
629   membrane proteins. Molecular & Cellular Proteomics 4:1948-1958

630 Lubzens E, Bobe J, Young G, Sullivan CV (2017) Maternal investment in fish oocytes and eggs: the
631   molecular cargo and its contributions to fertility and early development. Aquaculture 472:107-
632   143

633 Lucitt MB, Price TS, Pizarro A, Wu W, Yocum AK, Seiler C, Pack MA, Blair IA, Fitzgerald GA, Grosser T (2008)
634   Analysis of the zebrafish proteome during embryonic development. Molecular & Cellular
635   Proteomics 7:981-994

636 Mann K, Mann M (2008) The chicken egg yolk plasma and granule proteomes. Proteomics 8:178-191

637 Mi H, Huang X, Muruganujan A, Tang H, Mills C, Kang D, Thomas PD (2017) PANTHER version 11: expanded
638   annotation data from Gene Ontology and Reactome pathways, and data analysis tool
639   enhancements. Nucleic Acids Research 45:D183-d189

640 Mizuno T, Yamaha E, Kuroiwa A, Takeda H (1999) Removal of vegetal yolk causes dorsal deficencies and
641   impairs dorsal-inducing ability of the yolk cell in zebrafish. Mechanisms of Development 81:51-
642   63

643 Moriya Y, Itoh M, Okuda S, Yoshizawa AC, Kanehisa M (2007) KAAS: an automatic genome annotation and
644   pathway reconstruction server. Nucleic Acids Research 35:W182-185

645 Nolte H, MacVicar TD, Tellkamp F, Krüger M (2018) Instant clue: A software suite for interactive data
646   visualization and analysis. Scientific Reports 8:12648

647 Ober EA, Schulte-Merker S (1999) Signals from the yolk cell induce mesoderm, neuroectoderm, the trunk
648   organizer, and the notochord in zebrafish. Developmental Biology 215:167-181

649 Papadopoulos C, Kirchner P, Bug M, Grum D, Koerver L, Schulze N, Poehler R, Dressler A, Fengler S,
650   Arhzaouy K, Lux V, Ehrmann M, Weihl CC, Meyer H (2017) VCP/p97 cooperates with YOD1,
651   UBXD1 and PLAA to drive clearance of ruptured lysosomes by autophagy. The EMBO Journal
652   36:135-150

653 Pavlova NN, Thompson CB (2016) The emerging hallmarks of cancer metabolism. Cell Metabolism 23:27-
654   47

655 Purushothaman K, Das PP, Presslauer C, Lim TK, Johansen SD, Lin Q, Babiak I (2019) Proteomics analysis
656   of early developmental stages of zebrafish embryos. International Journal of Molecular Sciences
657   20:6359

658 Rauwerda H, Pagano JFB, de Leeuw WC, Ensink W, Nehrdich U, de Jong M, Jonker M, Spaink HP, Breit TM
659   (2017) Transcriptome dynamics in early zebrafish embryogenesis determined by high-resolution
660   time course analysis of 180 successive, individual zebrafish embryos. BMC Genomics 18:287

661 Rocha F, Dias J, Engrola S, Gavaia P, Geurden I, Dinis MT, Panserat S (2014) Glucose overload in yolk has
662   little effect on the long-term modulation of carbohydrate metabolic genes in zebrafish (*Danio*
663   *rerio*). Journal of Experimental Biology 217:1139-1149

664 Shamipour S, Kardos R, Xue S-L, Hof B, Hannezo E, Heisenberg C-P (2019) Bulk actin dynamics drive phase
665   segregation in zebrafish oocytes. Cell 177:1463-1479. e1418

666 Shilov IV, Seymour SL, Patel AA, Loboda A, Tang WH, Keating SP, Hunter CL, Nuwaysir LM, Schaeffer DA
667   (2007) The paragon algorithm, a next generation search engine that uses sequence temperature
668   values and feature probabilities to identify peptides from tandem mass spectra. Molecular &
669   Cellular Proteomics 6:1638-1655

670 Shyh-Chang N, Daley GQ, Cantley LC (2013) Stem cell metabolism in tissue development and aging.
671   Development 140:2535-2547

672 Suriyanarayanan T, Qingsong L, Kwang LT, Mun LY, Truong T, Seneviratne CJ (2018) Quantitative
673   proteomics of strong and weak biofilm formers of *Enterococcus faecalis* reveals novel regulators
674   of biofilm formation. Molecular & Cellular Proteomics 17:643-654

675 Tadros W, Lipshitz HD (2009) The maternal-to-zygotic transition: a play in two acts. Development
676   136:3033-3042

677   Tang WH, Shilov IV, Seymour SL (2008) Nonlinear fitting method for determining local false discovery rates
678   from decoy database searches. Journal of Proteome Research 7:3661-3667

679   Tatusov RL, Galperin MY, Natale DA, Koonin EV (2000) The COG database: a tool for genome-scale analysis
680   of protein functions and evolution. Nucleic Acids Research 28:33-36

681   Thomas RJ (1968) Yolk distribution and utililization during early development of a teleost embryo. Journal
682   of Embryology and Experimental Morphology 19:203-215

683   Vesterlund L, Jiao H, Unneberg P, Hovatta O, Kere J (2011) The zebrafish transcriptome during early
684   development. BMC Developmental Biology 11:30

685   Welch E, Pelegri F (2017) Reorganization of vegetal cortex microtubules and its role in axis induction in
686   the early vertebrate embryo. Cytoskeleton: Structure, Dynamics, Function and Disease:1

687   White RJ, Collins JE, Sealy IM, Wali N, Dooley CM, Digby Z, Stemple DL, Murphy DN, Billis K, Hourlier T
688   (2017) A high-resolution mRNA expression time course of embryonic development in zebrafish.
689   Elife 6:e30860

690   Wilkinson B, Gilbert HF (2004) Protein disulfide isomerase. Biochimica et Biophysica Acta (BBA) - Proteins
691   and Proteomics 1699:35-44

692   Winata CL, Korzh V (2018) The translational regulation of maternal mRNAs in time and space. FEBS Letters
693   592:3007-3023

694   Yeh H-Y, Klesius PH (2010) Characterization and tissue expression of channel catfish (*Ictalurus punctatus*
695   Rafinesque, 1818) ubiquitin carboxyl-terminal hydrolase L5 (UCHL5) cDNA. Molecular Biology
696   Reports 37:1229-1234

697

698

699 **Table 1**. iTRAQ experiment: Total number of proteins and differentially abundant
700 proteins (DAPs) with significant ($P < 0.05$) increase (DAP+) or decrease (DAP-) in quantity
701 in deyolked samples as compared to their non-deyolked counterparts. The criteria for
702 DAPs are given in Material and Methods.

Stages	Total proteins	DAP+		DAP-	
		n	%	n	%
1-cell stage	1245	659	(53%)	203	(16.3%)
16-cell stage	2549	1117	(44%)	154	(6%)
32-cell stage	2549	1094	(43%)	115	(5%)

703

704

705 **Table 2.** List of KEGG pathways and corresponding number of vegetal proteins common

706 for iTRAQ and shotgun experiments from early developmental stages of zebrafish

707 embryo.

Pathways	1-cell	16-cell	32- cell
map01100 Metabolic pathways	29	11	15
map03010 Ribosome	18	6	3
map01200 Carbon metabolism	10	4	4
map04141 Protein processing in endoplasmic reticulum	9	3	5
map01230 Biosynthesis of amino acids	8	1	3
map00010 Glycolysis / Gluconeogenesis	5	1	3
map00071 Fatty acid degradation	4	2	1
map04714 Thermogenesis	4	2	2
map00020 Citrate cycle TCA cycle	4	2	1
map00230 Purine metabolism	3	1	2
map04218 Cellular senescence	3	1	0
map04979 Cholesterol metabolism	3	1	1
map01212 Fatty acid metabolism	3	2	1
map04217 Necroptosis	5	3	2
map03018 RNA degradation	2	1	2
map03050 Proteasome	2	0	0
map04145 Phagosome	4	3	2
map03013 RNA transport	1	1	1
map00500 Starch and sucrose metabolism	2	2	2
map04530 Tight junction	2	1	1
map03060 Protein export	1	0	1
map04210 Apoptosis	1	1	1
map04921 Oxytocin signalling pathway	1	0	0
map04152 AMPK signalling pathway	1	1	1

708

709

710

711

712

713

714

Table 3. Validation of selected proteins found depleted in deyolked samples as
compared to non-deyolked samples (iTRAQ experiment) using SWATH. Values represent
fold-change of vegetal proteins, confirmed with SWATH MS and iTRAQ analyses.

Accession	Name	1-cell		16-cell		32-cell	
		iTRAQ	SWATH	iTRAQ	SWATH	iTRAQ	SWATH
Ribosome							
G1K2N0	40S ribosomal protein S25					-3.25	-1.90
Q6IQI6	60S ribosomal protein L11	-1.29	-3.55	-3.44	-2.40	-3.61	-1.96
A0A0R4IMS3	60S ribosomal protein L24	-2.21	-2.91			-4.79	-2.32
A8E526	Ribosomal protein L14			-5.75	-3.80	-6.78	-1.17
Q7ZW95	60S ribosomal protein L4	-1.12	-1.48			-1.36	-1.03
Q567N5	60S ribosomal protein L6	-1.13	-1.24			-2.11	-1.27
Q1LWH1	40S ribosomal protein S16	-1.17	-3.37	-3.47	-3.21	-4.13	-1.27
Q6TLG8	Ribosomal protein S3			-3.33	-2.06	-1.99	-1.52
Q6PC80	Ribosomal protein S5			-4.55	-3.23	-3.52	-1.13
A7E2K4	60S acidic ribosomal protein P2	-1.81	-5.21	-3.72	-4.95	-5.37	-2.03
Carbon metabolism							
Q6TH14E	Beta-enolase	-3.04	-5.39	-7.96	-4.23	-6.29	-2.70
A0A0R4IGI1	Glyceraldehyde-3-phosphate dehydrogenase			-5.12	-3.76	-5.79	-2.33
F1QXV8	Phosphoglycerate kinase			-7.36	-5.73	-7.59	-3.30
Q7ZVT2	Pyruvate kinase PKM	-1.04	-5.64	-7.80	-4.31	-2.69	-2.33
A0A1L1QZF2	Transaldolase			-8.15	-4.16	-8.22	-2.12
TPISA	Triosephosphate isomerase A	-2.40	-6.73	-5.60	-4.73	-3.66	-3.03

716
717
718
719
720

721 **Table 3**. Continued

722

Accession	Name	1-cell		16-cell		32-cell	
		iTRAQ	SWATH	iTRAQ	SWATH	iTRAQ	SWATH
Protein processing in ER							
Q6YI49	Ubiquitin carboxyl-terminal hydrolase			-9.70	-5.78	-12.47	-4.20
A0A0R4IPV5	Protein disulfide-isomerase precursor	-1.12	-1.42	3.56	2.44		
A0A2R8QNF0	Transitional endoplasmic reticulum ATPase			-8.38	-3.75	-9.27	-2.52
Translation							
Q6P3J5	Eukaryotic translation elongation factor 2b	-1.87	-5.37	-8.83	-3.73	-5.02	-2.69
A0A2R8QSR4	Elongation factor 1-alpha			-4.68	-2.83	-2.59	-2.83
HS90B	Heat shock protein HSP 90-beta	-1.94	-5.21	-6.79	-4.31	-7.24	-2.39
Developmental							
A0A0R4INF8	Nothepsin			-3.86	-4.95	-9.73	-1.23
Nuclear							
Q803X7	Nap1l1 protein			-15.92	-5.62	-11.43	-1.11
F1R606	Importin subunit alpha			-8.45	-3.00	-6.97	-1.49

723

Figure Legends

Figure 1. Proteins identified by iTRAQ (blue field) and shotgun LC-MS/MS (red field).
726 Overlapping proteins were considered as verified vegetal proteins.

727 **Figure 2.** Volcano plot of identified proteins in iTRAQ and shotgun LC-MS/MS
728 experiments. Protein abundance of deyolked vs. non-deyolked sample was represented
729 with p-value as – $\log_{10}$ (p-value) at Y-axis and relative abundance ratio as $\log_2$ (fold
730 change of non-deyolked /deyolked) at X-axis. Each dot represents a single protein. The
731 cut-off criteria for differentially abundant proteins (DAPs) are given in Material and
732 Methods.

733 **Figure 3.** EuKaryotic Orthologous Groups (KOG) functional classification of vegetal
734 proteins from 1-cell, 16-cell and 32-cell stages zebrafish embryos.

735 **Figure 4.** Gene Ontology (GO) Slim analysis of differentially abundant proteins with
736 significantly enriched terms (FDR < 0.05). Analysis for proteins shared between iTRAQ
737 and shotgun experiment grouped under biological process, molecular function, and
738 cellular component. Representation of GO terms containing a minimum 100 reference
739 genes and a fold change ≥ 4 or ≤ 4 is given. X-axis represents fold enrichment and Y-axis
740 shows GO terms.

741

742 **Figure 5**. Quantitative dynamics (EMMOL method; details in Material and Methods) of
743 chosen groups of proteins, functionally related to (A) ribosome; (B) protein processing
744 in ER and proteasome; (C) translation; (D) developmental; (E) nuclear; and (F) carbon
745 metabolism. Y-axis represents relative amount of protein in μg and X-axis shows three
746 different stages of embryogenesis.

747

748 **Figure 6.** Organization of yolk granules and early embryonic cytoplasm in zebrafish,
749 visualized through immunohistochemistry against essential translational proteins.
750 Channels for DAPI and Alexa Fluor 488 are merged. The fluorescence staining was done
751 using DAPI (blue signal) and Alexa Fluor 488 coupled with goat anti-rabbit secondary
752 antibody (green signal) against HSP90 (upper row), RPS16 (second row), and EEFa (third
753 row) primary antibodies. Negative controls (bottom row) have no primary antibodies.
754 At the 1-cell stage, the majority of ooplasm (green fluorescence) is located towards the
755 animal pole forming the blastodisc, while clusters of ooplasm remain within the yolk
756 area; constantly, a thin layer of ooplasm is located toward the yolk membrane. Yolk cell
757 granules (blue fluorescence) are located mainly within the vegetal, yolk cell area, with
758 bigger granules located more inwards and smaller granules outwards; yolk granules of
759 small size are visible within the blastodisc area. At the 16- and 32-cell stages, cytoplasmic
760 clusters in the yolk are in form of stretches ("streamers") and are few, while the layer of

761 cytoplasm surrounding the inner area of the yolk is still prominent. Apart from the yolk
762 cell compartment, small yolk cell granules are present also in the blastodisc area,
763 particularly at the cleavage furrows (white arrows at negative control picture). The
764 details are described in Material and Methods.

765

766
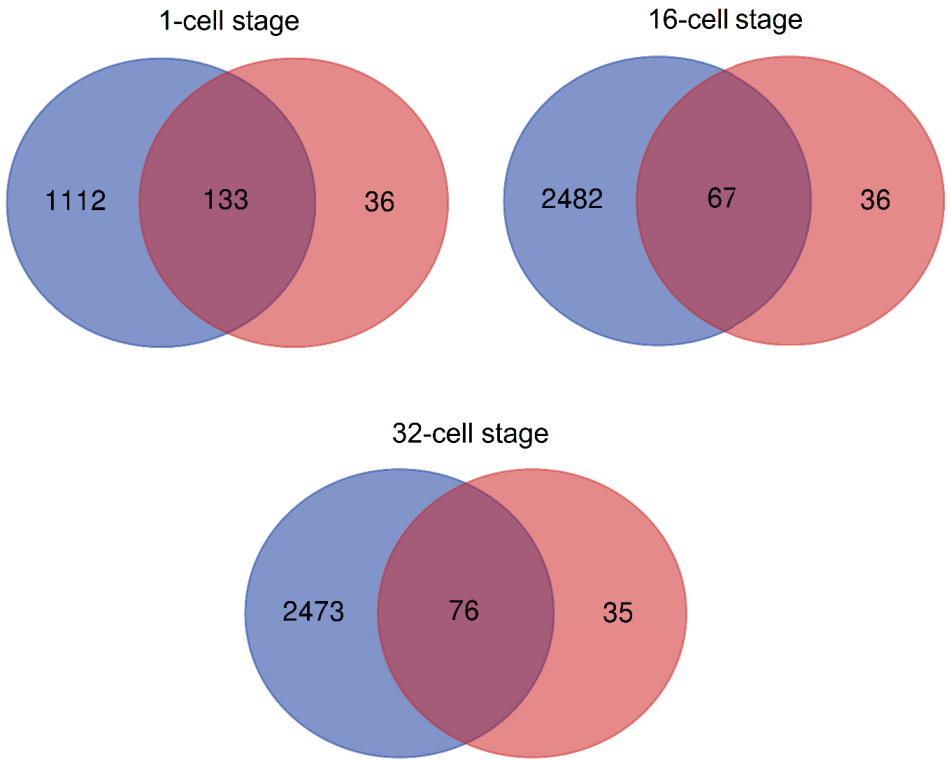
Figure 1

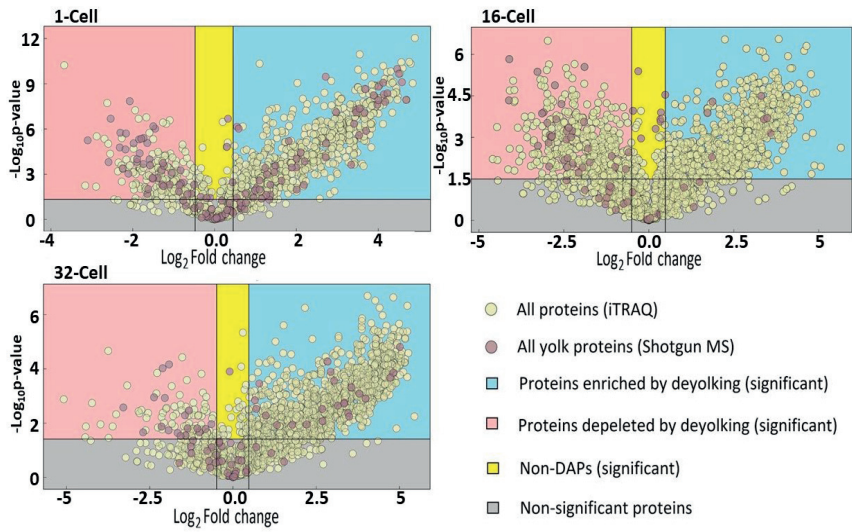772   **Figure 2**

773

774

775
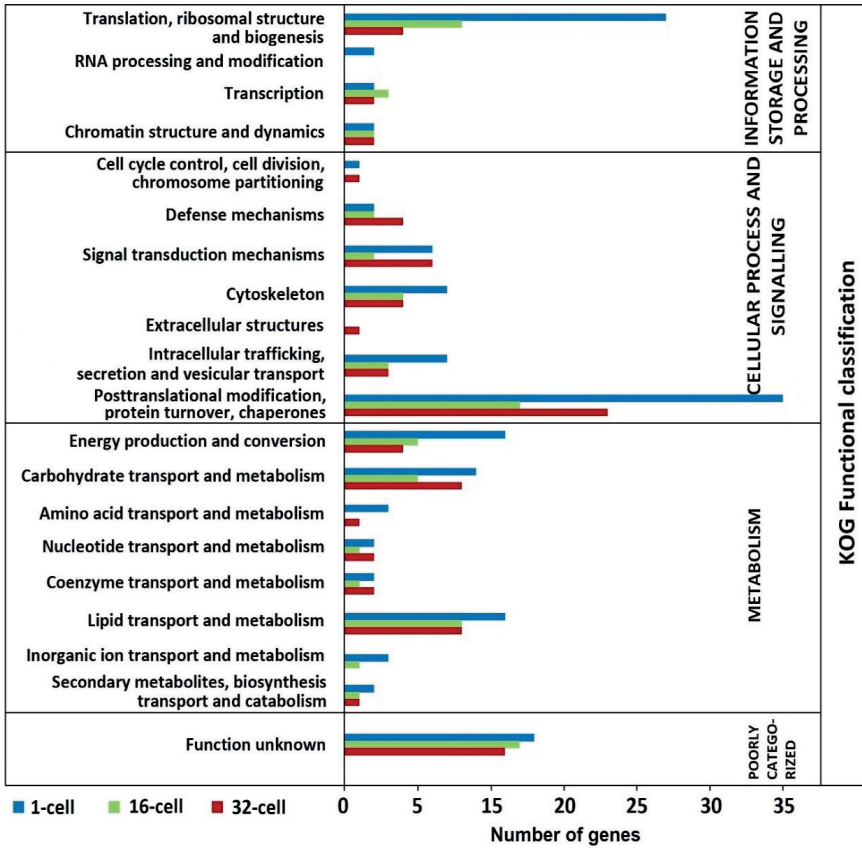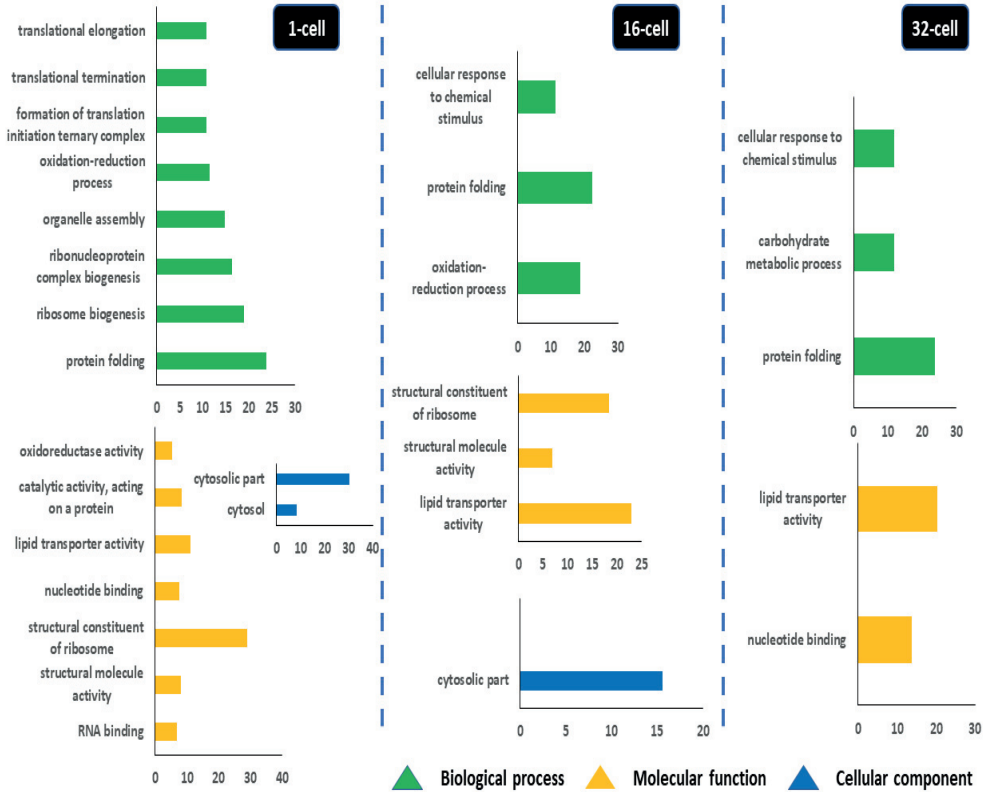
776

Figure 3

781   **Figure 4**

782

783

784

785

786

787

788

789

790

791

792
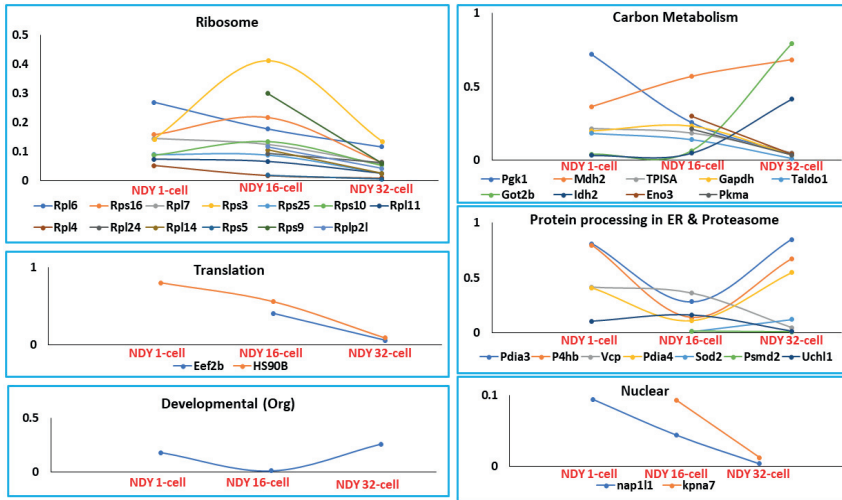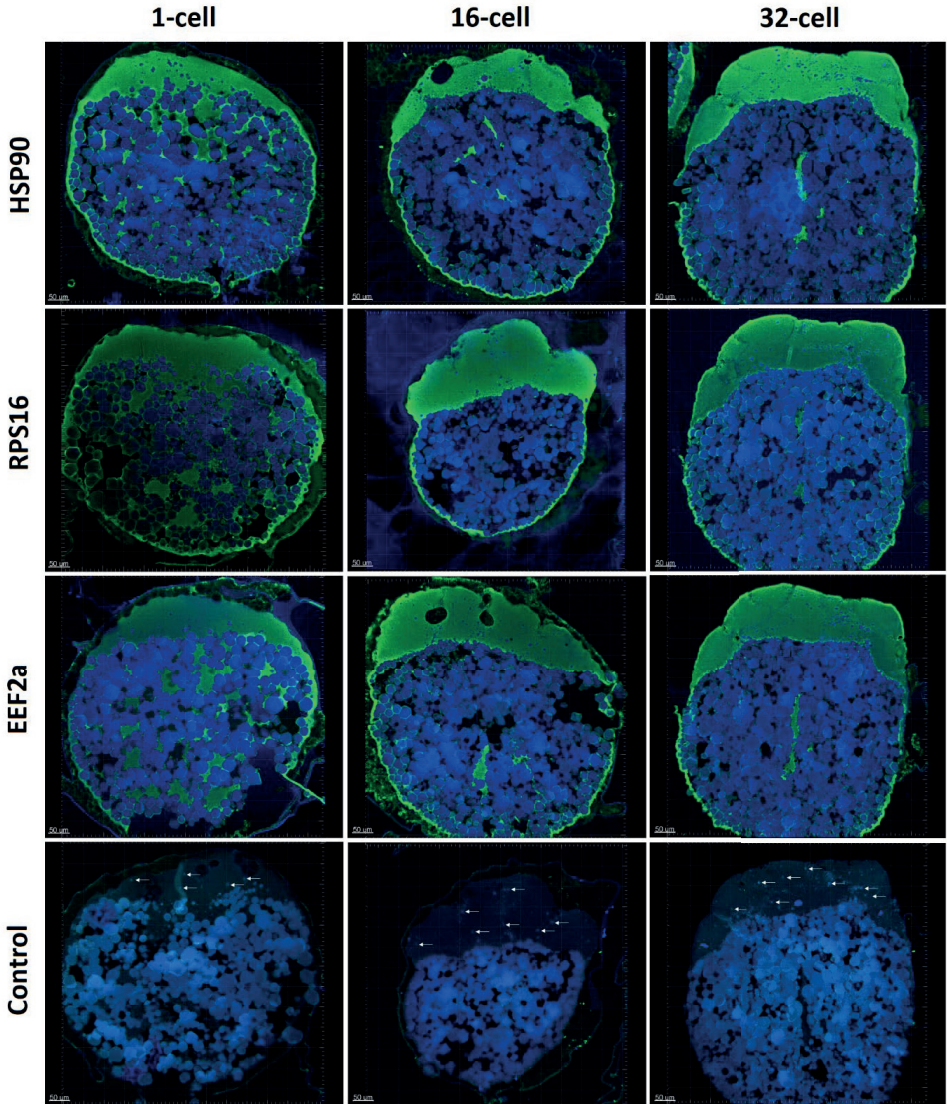
Figure 5

Figure 6

Supplementary Files

Supplementary Figure S1. Spectra, peptides and proteins identified in iTRAQ experiment. Spectra were identified after reverse phase HPLC and LC-MS/MS, whereas proteins with iTRAQ tags were identified from two iTRAQ sets: 1-cell (iTRAQ1) and 16- and 32-cell stages (iTRAQ2) by searching and analysing zebrafish_uniport database. Y-axis represents spectra/peptide/protein number.

Supplementary Figure S2. Organization of yolk granules and early embryonic cytoplasm in zebrafish, visualized through immunohistochemistry against essential translational proteins. The hematoxylin staining was done coupled with Bond™ mixed DAB refine (brown signal) against HSP90 (upper row), RPS16 (second row), and EEFa (third row) primary antibodies. Negative controls (bottom row) have no primary antibodies. At the 1-cell stage, the majority of ooplasm (brown signal) is located towards the animal pole forming the blastodisc, while clusters of ooplasm remain within the yolk area; constantly, a thin layer of ooplasm is located toward the yolk membrane. Yolk cell granules (brown signal) are located mainly within the vegetal, yolk cell area, with bigger granules located more inwards and smaller granules outwards. Yolk granules of small size are visible within the blastodisc area. At the 16- and 32-cell stages, cytoplasmic clusters in the yolk are in form of stretches ("streamers") and are few, while the layer of cytoplasm surrounding the inner area of the yolk is still prominent. Apart from the yolk cell compartment, small yolk cell granules are present also in the blastodisc area, particularly at the cleavage furrows. The details are described in the Material and Methods.

Supplementary Figure S3. Essential translation and post-translation proteins in the yolk of 1-cell stage zebrafish embryo are located in both ectoplasm (ec) and endoplasm (en), but not at the yolk cell membrane (ym). Ribonucleoprotein granular structure of vegetal cytoplasm is clearly visible. The photographs are taken from the location depicted at (A). In panels, left picture: green-fluorescent signal produced by Alexa Fluor 488 coupled with a goat anti-rabbit secondary antibody against primary antibodies for HSP90 (B), RPS16 (C), and EEF2 (D); right picture, bright light structure. ch – chorion; yg – yolk granules.

Supplementary Figure S4. Localization of Eukaryotic translation elongation factor 2 (EEF2), Ribosomal protein S16 (RPS16) and Heat shock protein 90β (Hsp90) proteins to membranes of yolk granules of 16-cell stage zebrafish embryo. Arrows point to representative aggregations of signals in ribonucleoprotein granules seen on the surface of yolk granules. Red rectangulars depict enlarged motifs (x600 magnification). Immunohistochemistry procedure is described in Material and Methods section.

837   **Supplementary Figure S5**. Quality and quantity analysis of total RNA extracted from 1-,
838   16- (A), and 32-cell stages (B) zebrafish embryo using TapeStation. Figures contain three
839   charts (for each stage) of size fraction analysis, with marked peaks corresponding to
840   nuclear rRNA subunits.

841   **Supplementary Table S1**. Number of selected samples labelled with different iTRAQ tags
842   for subsequent iTRAQ analysis.

843   **Supplementary File S1.** List of differentially abundant proteins (DAPs) present in 1-, 16-
844   and 32- cell stages of zebrafish from iTRAQ 1 and iTRAQ 2 dataset.

845   **Supplementary File S2.** List of total yolk proteins identified from 1-, 16- and 32- cell
846   stages zebrafish embryo using Shotgun LC MS/MS.

847   **Supplementary File S3.** List of common proteins identified from 1-, 16- and 32- cell
848   stages zebrafish embryo using both iTRAQ and shotgun LC MS/MS proteomics.

849

1 **Unravelling the proteome dynamics during the early**
2 **developmental stages of zebrafish**

3

4 Purushothaman Kathiresan[1], Prem Prakash Das[2], Su Min Yeoh[2], Lim Teck Kwang[2], Steinar D.
5 Johansen[1], Lin Qingsong[2*], and Igor Babiak[1*]

6

7 [1]Faculty of Biosciences and Aquaculture, Nord University, 8049 Bodø, Norway

8 [2]Department of Biological Sciences, National University of Singapore, 14 Science Drive 4,
9 117543 Singapore

10 *Corresponding authors

11

12 **E-mails:**

13 Purushothaman Kathiresan: kathiresan.purushothaman@nord.no
14 Prem Prakash Das: dbsppd@nus.edu.sg
15 Su Min Yeoh: dbsysm@nus.edu.sg
16 Lim Teck Kwang: dbslimtk@nus.edu.sg
17 Steinar D. Johansen: steinar.d.johansen@nord.no
18 Lin Qingsong: dbslinqs@nus.edu.sg
19 Igor Babiak: igor.s.babiak@nord.no

20

Abstract

The transcriptomics data on zebrafish embryonic development are well established. However, the data on the proteome are limited, particularly those linked to the pre-maternal-to-zygotic transition (pre-MZT) stages. This is predominantly due to the presence of the high-abundant embryonic yolk proteins, which tend to mask the less abundant cell proteins. In this study, we investigated unfertilized and freshly fertilized eggs, zygote, pre-MZT (4-, 16-, 32- and 128- cell), MZT (oblong) and post-MZT (50% epiboly and bud) developmental stages to map the embryonic proteome dynamics. We have applied the Isobaric tags for relative and absolute quantification (iTRAQ)-based quantitative proteomics to quantify the protein abundance. We performed shotgun LC-MS/MS-based qualitative and Sequential window acquisition of all theoretical fragment ion spectra mass spectrometry (SWATH) MS-based quantitative analysis to validate the iTRAQ results. We identified ~1500 to 2100 and ~3500 to 5000 distinct proteins in different stages of both non-deyolked and deyolked samples, respectively. We mapped housekeeping proteins, as well as those that are unique in pre-MZT, those present in both pre-MZT and MZT, and those unique in post-MZT stages, that were associated with various GO terms and KEGG pathways such as carboxylic acid metabolic process, translation, cellular biosynthetic process, cellular component organization, gene expression, fatty acid degradation, lysosome, ubiquitin mediated proteolysis, and Wnt signalling. We also revealed various transcription factors and proteins involved in RNA and DNA methylation. These pathways are likely to be active in the early developmental process. The study provides the first proteome-wide insight into the control of early embryonic development in zebrafish.

Introduction

Zebrafish (*Danio rerio*) is a well-established experimental model organism for studying vertebrate development and human diseases due to its genetic similarity to human (Howe et al. 2013). Understanding zebrafish early embryogenesis could provide insights, among others, into major birth defects and the molecular mechanisms during human early embryogenesis (Tu & Chi 2012, Howe et al. 2013, Zaucker et al. 2020).

Advances in high-throughput sequencing have markedly contributed to the elucidation of transcriptome profiles of early stages of zebrafish development (Mathavan et al. 2005, Aanes et al. 2011, Heyn et al. 2014, White et al. 2017, Nudelman et al. 2018, Mehjabin et al. 2019). However, corresponding information on proteome is scarce. It should be noted that prediction of the protein abundance based on the expression of transcripts is not accurate (Schwanhäusser et al. 2013). Furthermore, it is known that RNA expression and protein abundance in the same stages of both zebrafish (Alli Shaik et al. 2014) and *Xenopus laevis* (Smits et al. 2014) are poorly correlated. Identifying the temporal proteome landscape in early zebrafish embryos would provide direct information about the molecular details governing the embryonic development as well as allow comparative analysis between transcriptomic and proteomic data that disclose the post-transcriptional, maternal and zygotic RNA-based regulation of development.

There are not many proteome studies that have reported the protein profiles in the early developmental stages of zebrafish embryos, particularly in the zygotic and cleavage stages. Most of the proteomic studies have been performed using the late developmental stages of embryos and adult tissues (Zhang et al. 2010, Groh et al. 2011, Rahlouni et al. 2015). In this context, it should be pointed out that identification of low abundant proteins is compromised by the presence of highly abundant yolk proteins. Lack of appropriate deyolking methods resulted in identification of only few proteins (Tay et al. 2006, Lucitt et al. 2008, Rahlouni et al. 2015). Our improved deyolking protocol (Purushothaman et al. 2019) yielded more proteins compared to procedures reported by Link et al. (2006). Most importantly, it allowed for proteome analysis of the earliest developmental stages.

The proteome of "maternal cargo" in the oocyte, especially the non-vitellogenin proteins, is unknown to a great extent. Embryo proteome can be either (i) maternally deposited, (ii) zygotically synthesized from maternal transcripts, or (iii) zygotically synthesized from zygotic transcripts. Global analyses estimate that the maternal transcripts represent around three-quarters of the protein-coding transcriptome in zebrafish embryos (Aanes et al. 2011, Harvey et al. 2013). The maternal-to-zygotic transition (MZT) is a key process characterized

by several simultaneous events such as the onset of zygotic transcription (Newport & Kirschner 1982) and rapid degradation of maternal gene products. Approximately a quarter of the maternal transcripts in zebrafish degrade and this turnover of transcripts/proteins is possible due to the initiation of zygotic transcription/translation (Aanes et al. 2011, Bazzini et al. 2012, Harvey et al. 2013, Mishima & Tomari 2016). Now it is clear that even after the initiation of zygotic transcription, the tenacious maternal products perform critical functions alone or together with other maternal products or through interactions with nascent zygotic products (Pelegri 2003).

In the present study, we have employed three techniques to reveal the housekeeping proteins, unique and shared proteins that are active in the early developmental processes.

Materials and methods

Fish

Embryos were collected from the zebrafish AB line maintained at the zebrafish facility of the Nord University, Bodø, Norway. The fish were reared in Aquatic Habitats Recirculating System (Pentair, Apopka, FL, USA), and fed both SDS zebrafish-specific diet (Special Diet Services, Essex, UK) and newly hatched *Artemia* sp. nauplii (Pentair). The animal husbandry and experimental protocols were according to the Norwegian Regulation on Animal Experimentation (The Norwegian Animal Protection Act, No. 73 of 20 December 1974) and based on the General License for Fish Maintenance and Breeding (Godkjenning av avdeling for forsøksdyr, no. 17) given by the National Animal Research Authority (Utvalg for forsøk med dyr, forsøksdyrutvalget, Norway).

Sample collection

Male and female fish (equal representation) were allowed to spawn naturally, and the newly fertilized embryos were transferred to a Petri dish (100 mm × 15 mm) and incubated at 28.5 °C. The following developmental stages were identified according to Kimmel at al. (1995) and collected: (i) unfertilized eggs; (ii) freshly fertilized eggs (5 min from fertilization); (iii) 1-cell; (iv) 4-cell; (v) 16-cell; (vi) 32-cell; (vii) 128- cell; (viii) oblong; (ix) 50% epiboly; and (x) bud stage. Part of the collected samples from stages iii to x was subjected to deyolking procedure (Purushothaman et al. 2019), hereafter referred to as deyolked samples. The remaining samples were non-deyolked. Both the non-deyolked (stage i to x) and deyolked samples (stage iii to x) were immediately snap-frozen in liquid nitrogen and further stored

112 at -80°C. The exact number of eggs or embryo per sample and replicate is given in
113 Supplementary Table S1.

Total protein extraction

115 Embryos were enzymatically dechorionated with Pronase (Sigma Aldrich, St. Louis, MO,
116 USA) under 37°C with gentle shaking for 5 min. One mL of deyolking buffer (55 mM NaCl,
117 3.6 mM KCl, and 1.25 mM NaHCO$_3$) was added with dechorionated embryos and
118 mechanically disrupted with pipetting repeatedly via 100 μL tip. The disrupted embryos and
119 deyolking buffer were mixed gently by inverting the tube and the mixture was centrifuged
120 at 15,400 x g for 1 min at 4°C. Thereafter the yolk content in supernatant was discarded.
121 The above step was repeated two more times, and after that 10 mM Tris-HCl (pH 7.4) was
122 added to the pellets and centrifuged as described above. The pellets were snap-frozen in
123 liquid nitrogen and stored at −80°C (Purushothaman et al. 2019). Briefly, 100 μL of sodium
124 dodecyl sulphate (SDS) lysis buffer [1% SDS (Sigma-Aldrich, St. Louis, MO, USA), 0.5 M
125 triethylammonium bicarbonate buffer pH 8.5 (TEAB; Sigma Aldrich), and 1×Protease
126 Inhibitor cocktail (Thermo Scientific, Rockford, IL, USA) were added to the frozen samples.
127 The content was thoroughly homogenized and incubated at 90°C for 30 min, followed by 5
128 min incubation on ice. The lysed samples were centrifuged for 20 min at 15,400 X g at 4°C.
129 The supernatant containing total proteins was collected in a new microcentrifuge tube. We
130 used the Qubit® 3.0 Fluorometer (Invitrogen, Eugene, OR, USA) and the Qubit™ Protein
131 Assay Kit (Invitrogen) for protein quantification according to the manufacturer's protocol.
132 The isolated total protein samples lyophilized using a lyophilizer (VirTis BenchTop™ K,
133 Warminster, USA) at -80°C for 18 h were shipped to the Department of Biological Sciences,
134 National University of Singapore, Singapore for proteomics analysis.

Tube-gel-based trypsin digestion and iTRAQ labelling

136 The extracted proteins (100 μg) were used for tube-gel-based trypsin digestion, and the
137 tube gel contained 10% SDS, 1× PBS, 40% acrylamide solution, 10% APS, TEMED, in milliQ
138 water. The tube-gel was fixed with 50% methanol and 12% acetic acid for 30 min at room
139 temperature. The solidified gels were cut into small pieces (~1 mm^3) and washed with 50
140 mM triethylammonium bicarbonate (TEAB). Samples were again washed with 50%
141 acetonitrile (ACN) and dehydrated subsequently with 100% ACN. The washed gels were
142 reduced for 1 h at 57°C with 5 mM tris-(2-carboxyethyl) phosphine (TCEP) in 100 mM TEAB
143 and alkylated at room temperature for 1 h using 10 mM methyl methane-thiosulfonate
144 (MMTS) in 100 mM TEAB. Treated gels were washed and dehydrated by adding 100% ACN.

5

145 The gels were digested at 37°C for 16 h with trypsin (1 µg of trypsin per 20 µg of proteins),
146 and the supernatant containing the digested peptides was collected and dried by a vacuum
147 drier.

148 The dried samples were reconstituted with 30 µL 0.5 M TEAB (pH 8.5). We labelled the
149 total digested peptide samples with iTRAQ reagent 8-Plex kit (ABI-SCIEX) according to the
150 manufacturer's protocol. Four and five sets of 8-plex iTRAQ reagents were used to label the
151 digested total peptides from deyolked and non-deyolked samples, respectively, each in
152 three independent replicates (Supplementary File S1; "iTRAQ setup" tab). The labelled
153 peptide samples of each set of 8-iTRAQ-tags were pooled together and desalted using a
154 Sep-Pak C18 cartridge (Waters). All the eluents were lyophilized before they were subjected
155 to the 2D LC-MS/MS analysis (Das et al. 2019).

SWATH data acquisition and data processing

157 The SWATH spectral library was generated using 2 µg of peptides in three technical
158 replicates from deyolked and non-deyolked samples. SWATH data acquisition was carried
159 out by injecting 1 µg of peptides from sample into the 6600 TripleTOF in SWATH-MS mode
160 (DIA). Mass range of 350-1800 m/z with 50 ms accumulation time was used to collect
161 precursor ion data. A total of 120 variable SWATH windows within the range of 350-1800
162 m/z were used, where minimum window width was of 4 Da with 1 Da window overlaps.
163 Rolling collision energy was used with the spread of 5 eV. Subsequently, for collection of
164 fragment ion spectra for each window, we used mass range of 100–1800 m/z in high
165 sensitivity mode with accumulation time of 25 ms resulting in a total cycle time of 3.1 s.
166 MicroApp 2.0 in the PeakView 2.1 software (SCIEX, Foster city, CA, USA) was used to analyse
167 the acquired SWATH data files. The following parameters were used to extract peak area:
168 ion library tolerance 25 ppm, extracted ion chromatogram (XIC) extraction window 10 min,
169 FDR 1%, considering only 99% confidant peptides and excluded shared peptides. The
170 MarkerView 1.2.1 software (SCIEX) was utilized to process up to 10 peptides with six
171 transitions for each protein for XIC peak area extraction and the peptide data was exported
172 for analysis. Global normalization was performed using the sum of total area of all proteins
173 detected (Lin et al. 2019).

Shotgun and 2D LC-MS/MS analysis

175 The peptide samples were subjected to 2D LC-MS/MS analysis as described previously
176 (Das et al. 2019). The high pH reversed-phase high-performance liquid chromatography (RP-
177 HPLC) equipped with a C18 column (WATERS Xbridge C18, 3.5 µm, 3.0 mm × 150 mm) was
178 used for the first-dimension separation of iTRAQ-labelled peptides. The eluted fractions

179 were pooled together into 10 concatenated fractions (non-deyolked samples) and 30
180 concatenated fractions (deyolked samples), and the pooled fractions were subsequently
181 lyophilized.

182   For shotgun proteomics, the trypsin-digested proteins were separated into 8 fractions
183 using Pierce™ high pH reversed-phase peptide fractionation kit (Thermo Fisher Scientific,
184 USA) according to manufacturer's protocol. All the collected 8 fractions were lyophilized
185 and reconstituted with 2% ACN for LC-MS/MS analysis as described below.

186   The Eksigent nanoLC Ultra and ChiPLC-nanoflex (Eksigent, Dublin, CA) in TrapElute
187 configuration was performed in the second dimension of peptide separation. The
188 lyophilized samples were reconstituted by adding 2% ACN and 98% water and followed by
189 injected on a 200 μm × 0.5 mm column and eluted on an analytical 75 μm × 15 cm column
190 (ChromXP C18-CL, 3 μm). Ten (deyolked samples) and thirty (non-deyolked samples)
191 fractions were injected independently into the 5600 TripleTOF system (SCIEX) under
192 positive ionization mode, respectively.

193 **Peptide and protein identification**

194   ProteinPilot 5.0 software Revision 4769 (AB SCIEX) was utilized for protein identification
195 and relative quantification. The software runs on Paragon database search algorithm
196 (5.0.0.0.4767) and the integrated false discovery rate (FDR) analysis function (Shilov et al.
197 2007, Tang et al. 2008). In ProteinPilot, we have used the following user-defined search
198 parameters for the MS/MS spectra: Sample type: iTRAQ 8-Plex; Cysteine alkylation: MMTS;
199 Digestion: Trypsin; Instrument, TripleTOF5600; Special factors: None; Search effort:
200 Throughout; ID focus: Biological modification; FDR analysis: Yes; Background correction:
201 yes; and User modified parameter files: Yes. The datasets were searched against the protein
202 sequences of *Danio rerio* (zebrafish) which was downloaded from Uniprot database
203 (https://www.uniprot.org/). The FDR was estimated by searching the decoy database which
204 comprises of reverse protein sequences from the above-mentioned database.

205   The presence or absence of proteins in a particular developmental stage was validated
206 by utilizing two criteria (direct validation and indirect prediction). The direct validation was
207 performed using data from independent methods. They were (i) shotgun data produced for
208 our previous publication (Purushothaman et al. 2019); (ii) shotgun data produced for the
209 present study, (iii) shotgun data from other extraction methods described in
210 Purushothaman et al. (2019), (iv) shotgun data from other extraction method described in
211 the present study, and (v) SWATH data. In the indirect prediction, three criteria were
212 considered: (i) average area of the used peptides composing a given protein is significantly

higher (*t*-test for dependent samples at p < 0.05) than average background, (ii) protein is present in parallel stage replicates, and (iii) protein is within 1% FDR for a given iTRAQ. A protein´s presence was considered as validated in a particular developmental stage in a particular iTRAQ set when it was either directly validated with an independent method, or met at least two of the three criteria for the indirect prediction ("Protein validation" tab in Supplementary File S1).

Exponentially modified protein abundance index (emPAI)-MW deconvolution (EMMOL) for protein quantification

Exponentially modified protein abundance index (emPAI)-MW deconvolution (EMMOL) method was used to normalise within and between multiple iTRAQ experiments (Kim et al. 2012). This method utilizes iTRAQ isobaric reporter ratio together with emPAI score (using MASCOT software, Matrix Science, version 2.6.2) of the proteins of known and unknown amounts from within and between iTRAQ sets. MASCOT search with raw MS/MS ions, based on one and more peptides and the following search parameters were used: quantitation-iTRAQ 8plex; enzyme-Trypsin; fixed modification- iTRAQ8plex (N-term), iTRAQ8plex (K); variable modifications-Methylthio (C), iTRAQ8plex (Y); mass value- monoisotopic; protein mass- unrestricted; protein mass tolerance- 100 ppm; fragment mass tolerance- 0.4 Da; maximum missed cleavage- 1 and minimum numbers of peptides- 2. The emPAI score and iTRAQ reporter ratios (from ProteinPilot 5.0, SCIEX) were merged and subsequently employed to calculate the total protein content (weight %) according to the equation described by Ishihama et al. (2005).

Normalization of relative quantification

The total amount of protein per iTRAQ was normalized to 800 μg, with 100 μg/each iTRAQ channel (Kim et al. 2012). Then, a two-step normalization (channel correction and biological correction) was performed. Channel correction was applied to remove false positive proteins. In brief, the list of proteins from each iTRAQ analysis has been verified for each channel separately. Proteins classified as "true" were either confirmed directly (independent method) or predicted indirectly (based on objective quantitative criteria; see "Peptide and protein identification" section). The remaining proteins were classified as "false" (effect of noise from other samples in a given iTRAQ). The details of the procedure are given in "Protein validation" tab of Supplementary File S1. The total number of peptides (95%) from ProteinPilot statistics was corrected for each channel, and the proportion between this number and the number of all Peptides (95%) for a given iTRAQ was calculated. For each iTRAQ, these proportions were scaled to the lowest channel, and each

247 channel´s normalized total protein value (100 µg) was multiplied by the corresponding
248 channel correction factor ("Channel correction" tab in Supplementary File S1).

249   The biological correction was performed to calibrate the analysed samples to the total
250 extracted protein per embryo. It was done upon assumption that embryos in their
251 development have different content and amounts of proteins. In brief, the total amount of
252 extracted protein per embryo was calculated for each replicate within each of the extraction
253 protocols (non-deyolked and deyolked separately). Average amount per developmental
254 stage was calculated and scaled to the earliest developmental stage for each extraction
255 method separately (namely, 1-cell stage for deyolked samples, and unfertilized eggs for
256 non-deyolked samples). Next, the relative values from the previous step (channel
257 correction) were multiplied with the biological correction factors. The details are given in
258 "Biological correction" tab in Supplementary File S1.

Unique or shared proteins, and differentially abundant proteins

260 For both deyolked and non-deyolked samples, stage-by-stage comparisons were
261 conducted, where a preceding stage was used as the reference; for example, 1-cell stage
262 was used as a reference for the 4-cell stage, and 4-cell stage was a reference for 16-cell
263 stage, and so on. The proteins being present in both the compared stages were termed
264 "shared". Statistically significant differences between the abundances of proteins in the two
265 compared stages were calculated using a two-tailed paired Student's t-test. The mean of
266 the log2 ratio was calculated to obtain the fold-change and the p-value was subsequently
267 calculated for each of the proteins. The differentially abundant proteins (DAPs) were the
268 shared proteins with the cut-off threshold fold-change of ≥ 1.3 and p-value of <0.05) for
269 significant increase in abundance (DAP+), or the cut-off threshold of ≤ 0.76 or $\leq$-1.3 (p-value
270 <0.05) for the significant decrease (DAP-) in abundance, in relation to a reference.

271   The remaining (non-shared) proteins in such pairwise comparison were termed
272 "unique", as they were present in either of the compared stages. The unique proteins in the
273 earlier developmental stages of the pairwise comparisons were classified as DAP-, whereas
274 the unique proteins in the later developmental stages were classified as DAP+.

Functional annotations

276   Eukaryotic Orthologous Groups (KOG) classification was used to decipher the functions
277 associated with deyolked and non-deyolked proteins. The classification has 4 categories:
278 metabolism; cellular process and signalling; information storage and processing; and poorly
279 characterized (Tatusov et al. 2000). The FASTA format of the protein list was obtained from

280 the online server uniport (https://www.uniprot.org/) and submitted into eggNOG-mapper
281 (http://eggnogdb.embl.de/#/app/emapper, eggNOG 4.5.1 database) with the following
282 parameters: a) mapping mode- HMMER, b) Taxonomic Scope- chordata, c) Orthologs- use
283 all orthologs (prioritize coverage) Gene Ontology evidence- use non-electronic terms
284 (prioritize coverage). The proteins were classified into 25 functional groups according to
285 KOG annotation (Huerta-Cepas et al. 2015).

286 For Kyoto Encyclopedia of Genes and Genomes (KEGG) analysis, UniProtKB files were first
287 converted to KEGG id using uniprot online server (https://www.uniprot.org/uploadlists/).
288 The converted KEGG id list was submitted to online server "KEGG Mapper – Search & Color
289 Pathway" (https://www.genome.jp/kegg/tool/map_pathway2.html) to map KEGG
290 pathways (Kanehisa et al. 2015).

291 For Gene Ontology (GO) analysis, the input gene list was acquired by converting UniProt
292 using online server (https://www.uniprot.org/uploadlists/). Functional classification of all
293 DAPs was done using PANTHER (Released 2020.07.28) (http://www.pantherdb.org) with
294 the following parameters: analysis type- PANTHER overrepresentation test; reference list-
295 *Danio rerio*; test type- Fisher's exact; and correction- calculate FDR (Mi et al. 2016). We also
296 used http://bioinformatics.sdstate.edu/go/ for the GO analysis of housekeeping proteins,
297 unique proteins in pre-MZT, shared proteins in pre-MZT and MZT and unique proteins in
298 post-MZT. Venn diagrams were created using the online tool "Bioinformatics & Evolutionary
299 Genomics" (http://bioinformatics.psb.ugent.be/webtools/Venn/).

300

Results

302 A complete list of proteins identified with the three methods iTRAQ, Shotgun LC-MS/MS
303 and SWATH MS, is given in Supplementary File S2. iTRAQ method, as expected, yielded the
304 highest number of identified proteins in every investigated developmental stage. Generally,
305 the coverage of identified proteins among the three methods was good, although certain
306 proteins detected by LC-MS/MS shotgun (13 to 24% of proteins from unfertilized eggs to
307 bud stages of the non-deyolked samples and 12 to 19% of proteins from 1-cell to bud stages
308 of deyolked samples) and SWATH (from 22 to 24% and 9 to 10% of proteins from 1-,16 and
309 32-cell stages of both non-deyolked and deyolked samples, respectively) were not detected
310 by iTRAQ (Supplementary Figure 1). Non-deyolked samples yielded ~1500 to 2100 proteins
311 from unfertilized eggs to bud stage, while in deyolked samples we identified ~3500 to 5000
312 proteins across the investigated developmental stages. Regardless of the protein extraction
313 method, the number of identified proteins was approximately stable until the end of

cleavage phase (128-cell) and it has been gradually increasing in the later developmental
stages (Figure 1).

Dynamics of developmental proteins

The quantified proteins from iTRAQ experiment (Supplementary Files S3 and S4) were
analysed for dynamics of their abundance. Stage-by-stage pairwise comparisons identified
DAPs across the development (Supplementary Files S5 and S6). DAP- represented reduced
translation and degradation, while DAP+ represented increased translation and *de novo*
translation, the DAP-/DAP+ dynamics in the deyolked samples showed increased
translational activity at 16-cell stage and then from the oblong stage (MZT) onwards. The
latter trend was also seen in non-deyolked samples (Supplementary Figure S2).

Dynamics of selected proteins, belonging to developmental transcription factors, RNA
polymerase II – related activity m6A RNA and 5mC DNA methylation processes, have been
focused on because of their importance in early developmental regulatory events (Figure
2). While we observed a peak at the 50% epiboly (EB) stage in the proteins associated with
the abovementioned processes, a similar increase in proteins related to m6A RNA occurred
at 4-cell stage.

Annotation and functional classification

A number of proteins was constantly present throughout all the investigated
developmental stages, here termed "housekeeping" (Supplementary Files S7). On the other
hand, some proteins were unique, or were massively enriched at certain developmental
phases, such as pre-MZT (abundantly detected in cleavage stages such as 4-cell to 128-cell
stages), MZT (abundant in the oblong stage) and post-MZT (abundantly identified in the
50% EB and bud stages) (Supplementary Files S7). The KOG analysis revealed the
distribution of the above mentioned shared and unique proteins from these groups into
four functional categories and further division into 23 groups (Figure 3). The most
represented KOG term associated with the housekeeping proteins was "Energy production
and conversion", whereas "Signal transduction mechanisms" was the most common in both
pre-MZT and post-MZT stages. The functional group "Posttranslational modification,
protein turnover, chaperones" was highly represented in the MZT stage. It should be noted
that considerable portion of proteins was under the category "function unknown". Two
hundred and eighty-eight housekeeping proteins were annotated and classified into
metabolism, cellular processes and signalling, information storage and processing, and
poorly characterized category (36%, 26%, 18% and 20%, respectively). For pre-MZT stages
(37 annotated proteins), MZT stages (34 annotated proteins), and post-MZT (231 annotated

348 proteins) stages, the corresponding distribution abundancies were 24%, 33%, 19% and 24%;
349 17%, 44%, 20% and 19%; and 10%, 35%, 24% and 31%, respectively (Figure 3).

350 The GO enrichment and KEGG pathway analyses of the above-mentioned housekeeping
351 and unique and/or highly enriched proteins revealed specific functions relevant for the pre-
352 MZT stage: DNA binding, cellular biosynthetic process, ubiquitin mediated proteolysis and
353 RNA transport pathway. We also detected proteins from the MZT stage that were
354 associated with cellular component organization, regulation of cell cycle, regulation of
355 proteasomal protein -catabolic process, cytoplasmic translation, lysosome, proteasome,
356 and RNA degradation pathway. In addition, proteins linked to gene expression, RNA
357 processing, organelle organization, lysosome, ubiquitin mediated proteolysis and Wnt
358 signalling pathway were identified in the post-MZT stages. Housekeeping proteins were
359 connected to translation, oocyte meiosis, nucleoside binding, fatty acid degradation, cell
360 cycle, lysosome, gap junction, dorso-ventral axis formation, ubiquitin mediated proteolysis,
361 processing in endoplasmic reticulum, cell adhesion and tight junction (Figure 4, Table 1,
362 Supplementary File S8, and Supplementary Table 2).

363 The generated data for the stage-by-stage DAPs and the functional meaning, using KOG
364 (Supplementary File S9), KEGG (Supplementary File S10), and GO (Supplementary Files S11-
365 S114) are provided.

366

Discussion

368 In the present study, we identified and quantified proteins in the eggs and early embryos
369 of zebrafish. We revealed stage-by-stage protein dynamics, and the potential translation of
370 the proteins was inferred based on their depletion or enrichment in the selected stages.
371 Selected proteins, with emphasis on the functions in transcription and translation in early
372 embryonic development (Figure 5), are discussed below.

Pre-MZT proteins vital for DNA replication

374 Proteins enriched in pre-MZT stages (Figure 4, Table 1, Supplementary Files S8 and
375 Supplementary Table 2) were likely either maternally loaded or they were translated from
376 maternal transcripts, suggesting functional roles in pre-MZT stages. DNA replication is an
377 important event during pre-MZT stages. Top3a, a type IA DNA topoisomerase involved in
378 chromosome replication and stability (Heck et al. 1988), was among the unique proteins
379 identified in the pre-MZT stages of the present study. Initially, cell cycles in zebrafish

12

380　embryos occur very fast and they are synchronous. However, during the 10th and 11th
381　division cell cycle slows down, after which occurs a shift in cell cycle, transcription from
382　zygotic products and cell movements (Kermi et al. 2017), and Top3a appears to be essential
383　for zebrafish embryogenesis at pre-MZT stages. We found another protein, SWI/SNF
384　related-matrix-associated actin-dependent regulator of chromatin subfamily C (Smarcc) in
385　the pre-MZT stages. The chromatin remodelling enzyme SWI/SNF has diverse functions and
386　this is likely due to the interactions of the subunits with transcription factors (Kadam &
387　Emerson 2003). These remodelers help transcription factors to bind to chromatin.
388　Furthermore, SWI/SNF-dependent distal enhancers are vital in controlling genes associated
389　with developmental processes (Alver et al. 2017). Our findings corroborate with those of
390　the abovementioned studies (Heck et al. 1988, Kadam & Emerson 2003, Alver et al. 2017)
391　in that the enriched proteins from the pre-MZT phase were involved in cell cycle and
392　chromosome replication and stability.

Proteins involved in maternal product clearance and zygotic translation

394　　Proteins enriched at the oblong stage were associated with, among others, the
395　proteasome, lysosome, RNA degradation, and translation (Figure 4, Table 1, Supplementary
396　File S8 and Supplementary Table S2). Degradation of maternal proteins follows two main
397　pathways: autophagy-mediated lysosomal degradation and ubiquitin-proteasome-
398　mediated degradation. It precedes the translation of new proteins from zygotic transcripts
399　(Ma et al. 2001, DeRenzo & Seydoux 2004, Higuchi et al. 2018). The ubiquitin-proteasome
400　system is responsible for the degradation of damaged or unwanted proteins through
401　proteolysis (Rock et al. 1994). The lysosome degradation process eliminates mRNA and
402　proteins in the cytoplasm (Tsukamoto et al. 2013) and leads to the utilization of the yolk
403　during embryogenesis (Saftig & Klumperman 2009). The translational activation of maternal
404　mRNAs is regulated by cytoplasmic polyadenylation machinery. This translational activation
405　also is initiated during the MZT stage (Winata et al. 2018). Current study identified the
406　proteins related to both proteasomal protein catabolic process and proteasome such as
407　Proteasome activator subunit 3 (Psme3), Proteasome (Prosome, macropain) 26S subunit,
408　ATPase, 1b (Psmc1b), 26S proteasome regulatory subunit T2 (Psmc1) and Proteasome
409　activator subunit 3 (Pa28 gamma); lysosomal pathway-related protein such as V-type H+-
410　transporting ATPase 16kDa proteolipid subunit (ATPeV0c). We also identified the proteins
411　associated with cytoplasmic translation such as 40S ribosomal protein S28 (Rps28) and
412　Eukaryotic translation initiation factor 3 subunit E (Eif3eb). Our findings corroborate with
413　those of the abovementioned reports (Yeh et al. 2013, Higuchi et al. 2018, Winata et al.

13

414   2018) in that the identified proteins were mainly involved in the clearance of maternal
415   products and translation during MZT.

Post-MZT proteins associated with organ development

417   The proteins that are unique and enriched in the post-MZT stages (50% EB and bud
418   stages) are likely translated from zygotic transcripts. Members of Wnt signalling pathway:
419   chromodomain helicase DNA binding protein 8 (Chd8) and receptor tyrosine kinase-like
420   orphan receptor 2 (Ror2), as well as bone morphogenetic protein 7 (Bmp7) were among the
421   unique proteins in the post-MZT stage. The Wnt pathway is conserved and functions in cell
422   proliferation and cell fate regulation, swimbladder development, body-axis determination,
423   microtubule-dependent dorsoventral axis specification, and eye development during early
424   embryogenesis of zebrafish (Yin et al. 2011, Hikasa & Sokol 2013, Fujimura 2016). Chd8
425   which controls Wnt signalling, is involved in chromatin remodelling after binding to β-
426   catenins and is crucial for the normal development of vertebrate neurons and brain (Bernier
427   et al. 2014). Ror2 is activated when it binds to Wnt8a, and the transport of Wnt8a to
428   neighbouring cells induces Wnt/b-catenin-dependent gene transcription and proliferation.
429   All these steps are essential for zebrafish development (Mattes et al. 2018). Bmps are
430   detected after the gastrulation and identified in the ventral and posterior mesoderm (Pyati
431   et al. 2005). Bmp7 is essential for specifying the fates of the ventral cells during early
432   dorsoventral patterning of zebrafish, and it is involved in embryogenesis, hematopoiesis,
433   neurogenesis and skeletal morphogenesis (Dick et al. 2000, Aluganti Narasimhulu & Singla
434   2020). In addition, Bmp7 cooperates with Bmp2b in the ventralization of wildtype zebrafish
435   embryos (Schmid et al. 2000). The results indicate that the identified unique proteins from
436   post-MZT stages are mainly associated with cell fate regulation, axis specification, and
437   development of organs such as eye and swimbladder (Figure 4, Table 1, Supplementary Files
438   S8 and Supplementary Table 2).

Housekeeping proteins of the zebrafish embryonic stages

440   Proteins identified in all the developmental stages and showing little variance in
441   abundance are shown in Figure 4, Table 1, Supplementary File S8 and Supplementary Table
442   S2. They were likely maternally supplied, as well as translated from both maternal and
443   zygotic transcripts. The steady quantity suggests their housekeeping functions. Embryonic
444   development is characterized by events such as cell division, cell differentiation and
445   morphogenesis. The rapid synchronous cell divisions occur until oblong stage, after which
446   lengthening of the cell cycles and asynchronous cell divisions take place (Kimmel et al. 1995,
447   Mendieta-Serrano et al. 2013). Cell division control protein 42 (Cdc42) from both nucleoside

448 binding and junction pathways are known to help the cells in carrying out many functions
449 such as proliferation, apoptosis, and maintaining polarity. The cell cycle and oocyte meiosis
450 pathway-related protein cyclin-dependent kinase 2 (Cdk2) is essential during zebrafish
451 embryonic development (Chu et al. 2012). Both maternal and zygotic products are essential
452 for alignment of dorso-ventral axis. Furthermore, certain pathways such as focal adhesions
453 are crucial in morphogenesis of zebrafish heart valve (Gunawan et al. 2019). Lysosome and
454 ubiquitin-mediated proteolysis are vital during the development because these pathways
455 will help the embryo to reach the appropriate MZT events. The proteins identified in the
456 present study were involved in the clearance of maternal products, regulation of oocyte
457 maturation, cell division, dorso-ventral axis and morphogenesis (Figure 4, Table 1,
458 Supplementary File S8 and Supplementary Table S2).

459 Transcription factors (TFs) are crucial to regulate the ZGA in zebrafish and initiate the MZT
460 (Lee et al. 2013, Langley et al. 2014, Lee et al. 2014, Paranjpe & Veenstra 2015, Onichtchouk
461 & Driever 2016). The onset of zygotic transcription is mediated by specific transcription
462 factors. The three distinct TFs, namely Nanog, SoxB1, and Pou5f1 are involved in the
463 initiation of the first wave of zygotic transcription and control the dorso-ventral patterning
464 (Okuda et al. 2010, Onichtchouk 2012, Lee et al. 2013). Pou5f3, Nanog, and Sox19*b* bind to
465 developmental enhancers to initiate transcription at ZGA of zebrafish embryos (Veil et al.
466 2019). In zebrafish, Pou5f1 controls the temporal gene expression patterns (Onichtchouk et
467 al. 2010). Nanog which is essential for endoderm formation in zebrafish is supplied
468 maternally (Xu et al. 2012). Nanog together with SoxB1 and Pou5f1 regulate miR-430, which
469 is directly associated with maternal RNA degradation. The upregulation of miR-430 by these
470 transcription factors helps the handover of gene expression from maternal RNAs to zygotic
471 RNAs (Lee et al. 2013). Our study revealed that transcription factors such as Nanog and
472 Pou5f3 are present in all the early developmental stages of zebrafish embryos. In addition,
473 another Pou5f, Pou5f1 was identified in the 128-cell, oblong and 50% epiboly stages. The
474 changes in abundance of both Nanog and Pou5f3 followed the same pattern; the
475 abundance peaked at 50% EB stage (Figure 2). This trend confirms that these TFs are
476 maternally supplied and are essential for zygotic transcription. Previous reports support our
477 data and suggest that the maternal Nanog combined with Soxb1 family and Pou5f3 will
478 activate the zygotic transcription during ZGA and they are abundantly translated in the
479 transcriptionally silent period preceding ZGA (Lee et al. 2013).

480 The N6-methyladenosine modification of mRNA is essential in ZGA, MZT and
481 haematopoietic stem cell specification in early zebrafish embryogenesis (Zhang et al. 2017,
482 Zhao et al. 2017a), spermatogenesis and brain development in mouse (Hsu et al. 2017, Lin
483 et al. 2017, Xu et al. 2017, Yoon et al. 2017) and sex determination in *Drosophila*

484 *melanogaster* (Haussmann et al. 2016). The Mettl3 and Mettl14 are the constituents of core
485 methyltransferase complex, and Mettl3 is required for catalytic activities and Mettl14 is
486 essential for promoting Mettl3 activity and substrate recognition (Liu et al. 2014). After the
487 modification of the m^{6}A by methyltransferases, YTH domain-containing proteins will
488 recognize them and instructs the complex to regulate different RNA signalling pathways.
489 Ythdf1 is involved in the translation of these mRNAs in the cytoplasm, and Ythdf2 is essential
490 for the RNA stability (Liu et al. 2020). Xia et al. (2018) reported that the maternally supplied
491 *mettl3* was highly expressed in early embryonic stages, but its expression decreased
492 dramatically at 256-cell stage and was further declined at dome stage of zebrafish. The
493 deficiency of *mettl3* results in ineffective maturation of gametes, which in turn affect the
494 fertility in zebrafish (Xia et al. 2018). Our result showed the high abundance of Mettl3 at
495 cleavage stages followed by a decline from oblong stage onwards. The Ythdf2 is involved in
496 oocyte maturation and early development of embryos (Ivanova et al. 2017). The elimination
497 of *ythdf2* in zebrafish embryos delays the degradation of maternal mRNA, thereby impeding
498 ZGA and embryonic development (Zhao et al. 2017b). Our result identified the presence of
499 Mettl3, Mettl14 Ythdf1 and Ythdf2 in all the stages and their abundance increased as the
500 development progressed. The result suggests that Mettl3, Mettl14, Ythdf1 and Ythdf2 are
501 maternally provided, as well as they are synthesized from maternal and zygotic transcripts
502 (Figure 2).

503 DNA methylation is the most abundant epigenetic modification and achieved during the
504 early embryonic developmental period by utilizing *de novo* DNA methyltransferases (Dnmt)
505 from the maternal transcripts (Goll & Halpern 2011). Dnmt1 is recruited by the ubiquitin-
506 like protein Uhrf1 to methylate cysteine residue of newly synthesized DNA during the
507 replication (Bostick et al. 2007, Arita et al. 2008, Avvakumov et al. 2008). Tittle et al. (2011)
508 reported that Uhrf1 and Dnmt1 function together to perform DNA methylation during the
509 lens development and maintenance in zebrafish embryogenesis. The *uhrf1* and *dnmt1*
510 knockout mice were prone to early lethality (Li et al. 1992, Lei et al. 1996, Muto et al. 2002,
511 Sharif et al. 2007). The *dnmt1* knock-down leads to ~40% embryonic lethality in zebrafish
512 and unreliable terminal differentiation in the pancreas, retina and intestine (Rai et al. 2006).
513 Uhrf1 and Dnmt1, have also important roles during zebrafish gastrulation period (Kent et
514 al. 2016). The role of Dnmt1 is well studied but there is limited knowledge about abundance
515 of this protein before and during MZT in zebrafish. Our study shows a constant presence of
516 Dnmt1 up to 128-cell stage and a constant increase during the MZT and post-MZT stages
517 (Figure 2).

518

Conclusions

In conclusion, the present study provides an insight into the proteome dynamics during early embryogenesis of zebrafish. The presence of maternally provided proteins, as well as those transcribed in the embryo from maternal and zygotic transcripts has been demonstrated. They enriched processes such as DNA replication, degradation of maternal products, cell fate regulation, morphogenesis, axis specification, mesoderm patterning and organ development. We also identified development-related proteins such as transcription factors, and proteins connected to DNA and RNA methylation. Our study indicated quantitative proteome dynamics and major regulatory elements and pathways throughout the early embryonic development. This is the first report that provides a proteomics background into maternal and zygotic control and developmental regulation of transcription and translation in early embryogenesis of zebrafish.

Acknowledgments

References

539 Aanes H, Winata CL, Lin CH, Chen JP, Srinivasan KG, Lee SG, Lim AY, Hajan HS, Collas P, Bourque G (2011) Zebrafish mRNA sequencing deciphers novelties in transcriptome dynamics during maternal to zygotic transition. Genome Research 21:1328-1338

543 Alli Shaik A, Wee S, Li RHX, Li Z, Carney TJ, Mathavan S, Gunaratne J (2014) Functional mapping of the zebrafish early embryo proteome and transcriptome. Journal of Proteome Research 13:5536-5550

545 Aluganti Narasimhulu C, Singla DK (2020) The role of Bone morphogenetic protein 7 (BMP-7) in inflammation in heart diseases. Cells 9:280

547 Alver BH, Kim KH, Lu P, Wang X, Manchester HE, Wang W, Haswell JR, Park PJ, Roberts CWM (2017) The SWI/SNF chromatin remodelling complex is required for maintenance of lineage specific enhancers. Nature Communications 8:14648

550 Arita K, Ariyoshi M, Tochio H, Nakamura Y, Shirakawa M (2008) Recognition of hemi-methylated DNA by the SRA protein UHRF1 by a base-flipping mechanism. Nature 455:818-821

552 Avvakumov GV, Walker JR, Xue S, Li Y, Duan S, Bronner C, Arrowsmith CH, Dhe-Paganon S (2008) Structural basis for recognition of hemi-methylated DNA by the SRA domain of human UHRF1. Nature 455:822-825

555 Bazzini AA, Lee MT, Giraldez AJ (2012) Ribosome profiling shows that miR-430 reduces translation before causing mRNA decay in zebrafish. Science 336:233-237

557 Bernier R, Golzio C, Xiong B, Stessman HA, Coe BP, Penn O, Witherspoon K, Gerdts J, Baker C, Vulto-van Silfhout AT, Schuurs-Hoeijmakers JH, Fichera M, Bosco P, Buono S, Alberti A *et al.* (2014) Disruptive CHD8 mutations define a subtype of autism early in development. Cell 158:263-276

560 Bostick M, Kim JK, Estève P-O, Clark A, Pradhan S, Jacobsen SE (2007) UHRF1 plays a role in maintaining DNA methylation in mammalian cells. Science 317:1760-1764

562 Chu J, Loughlin EA, Gaur NA, SenBanerjee S, Jacob V, Monson C, Kent B, Oranu A, Ding Y, Ukomadu C, Sadler KC (2012) UHRF1 phosphorylation by cyclin A2/cyclin-dependent kinase 2 is required for zebrafish embryogenesis. Molecular Biology of the Cell 23:59-70

565 Das PP, Chua GM, Lin Q, Wong S-M (2019) iTRAQ-based analysis of leaf proteome identifies important proteins in secondary metabolite biosynthesis and defence pathways crucial to cross-protection against TMV. Journal of Proteomics 196:42-56

568 DeRenzo C, Seydoux G (2004) A clean start: degradation of maternal proteins at the oocyte-to-embryo transition. Trends in Cell Biology 14:420-426

570 Dick A, Hild M, Bauer H, Imai Y, Maifeld H, Schier AF, Talbot WS, Bouwmeester T, Hammerschmidt M (2000) Essential role of Bmp7 (snailhouse) and its prodomain in dorsoventral patterning of the zebrafish embryo. Development 127:343-354

573 Fujimura N (2016) WNT/β-catenin signaling in vertebrate eye development. Frontiers in Cell and Developmental Biology 4:138

575 Goll MG, Halpern ME (2011) DNA methylation in zebrafish. Progress in Molecular Biology and Translational
576 Science 101:193-218

577 Groh KJ, Nesatyy VJ, Segner H, Eggen RI, Suter MJ-F (2011) Global proteomics analysis of testis and ovary in
578 adult zebrafish (*Danio rerio*). Fish Physiology and Biochemistry 37:619-647

579 Gunawan F, Gentile A, Fukuda R, Tsedeke AT, Jiménez-Amilburu V, Ramadass R, Iida A, Sehara-Fujisawa A,
580 Stainier DYR (2019) Focal adhesions are essential to drive zebrafish heart valve morphogenesis.
581 Journal of Cell Biology 218:1039-1054

582 Harvey SA, Sealy I, Kettleborough R, Fenyes F, White R, Stemple D, Smith JC (2013) Identification of the
583 zebrafish maternal and paternal transcriptomes. Development 140:2703-2710

584 Haussmann IU, Bodi Z, Sanchez-Moran E, Mongan NP, Archer N, Fray RG, Soller M (2016) m 6 A potentiates
585 Sxl alternative pre-mRNA splicing for robust *Drosophila* sex determination. Nature 540:301-304

586 Heck MM, Hittelman WN, Earnshaw WC (1988) Differential expression of DNA topoisomerases I and II during
587 the eukaryotic cell cycle. Proceedings of the National Academy of Sciences of the United States of
588 America 85:1086-1090

589 Heyn P, Kircher M, Dahl A, Kelso J, Tomancak P, Kalinka AT, Neugebauer KM (2014) The earliest transcribed
590 zygotic genes are short, newly evolved, and different across species. Cell Reports 6:285-292

591 Higuchi C, Shimizu N, Shin S-W, Morita K, Nagai K, Anzai M, Kato H, Mitani T, Yamagata K, Hosoi Y, Miyamoto
592 K, Matsumoto K (2018) Ubiquitin-proteasome system modulates zygotic genome activation in early
593 mouse embryos and influences full-term development. The Journal of Reproduction and
594 Development 64:65-74

595 Hikasa H, Sokol SY (2013) Wnt signaling in vertebrate axis specification. Cold Spring Harbor Perspectives in
596 Biology 5:a007955

597 Howe K, Clark MD, Torroja CF, Torrance J, Berthelot C, Muffato M, Collins JE, Humphray S, McLaren K,
598 Matthews L (2013) The zebrafish reference genome sequence and its relationship to the human
599 genome. Nature 496:498-503

600 Hsu PJ, Zhu Y, Ma H, Guo Y, Shi X, Liu Y, Qi M, Lu Z, Shi H, Wang J (2017) Ythdc2 is an N 6-methyladenosine
601 binding protein that regulates mammalian spermatogenesis. Cell Research 27:1115-1127

602 Huerta-Cepas J, Szklarczyk D, Forslund K, Cook H, Heller D, Walter MC, Rattei T, Mende DR, Sunagawa S, Kuhn
603 M, Jensen LJ, von Mering C, Bork P (2015) eggNOG 4.5: a hierarchical orthology framework with
604 improved functional annotations for eukaryotic, prokaryotic and viral sequences. Nucleic Acids
605 Research 44:D286-D293

606 Ishihama Y, Oda Y, Tabata T, Sato T, Nagasu T, Rappsilber J, Mann M (2005) Exponentially modified protein
607 abundance index (emPAI) for estimation of absolute protein amount in proteomics by the number of
608 sequenced peptides per protein. Molecular & Cellular Proteomics 4:1265-1272

609 Ivanova I, Much C, Di Giacomo M, Azzi C, Morgan M, Moreira PN, Monahan J, Carrieri C, Enright AJ, O'Carroll
610 D (2017) The RNA m6A reader YTHDF2 is essential for the post-transcriptional regulation of the
611 maternal transcriptome and oocyte competence. Molecular Cell 67:1059-1067. e1054

612   Kadam S, Emerson BM (2003) Transcriptional specificity of human SWI/SNF BRG1 and BRM chromatin
613   remodeling complexes. Molecular Cell 11:377-389

614   Kanehisa M, Sato Y, Kawashima M, Furumichi M, Tanabe M (2015) KEGG as a reference resource for gene and
615   protein annotation. Nucleic Acids Research 44:D457-D462

616   Kent B, Magnani E, Walsh MJ, Sadler KC (2016) UHRF1 regulation of Dnmt1 is required for pre-gastrula
617   zebrafish development. Developmental Biology 412:99-113

618   Kermi C, Lo Furno E, Maiorano D (2017) Regulation of DNA replication in early embryonic cleavages. Genes
619   8:42

620   Kim PD, Patel BB, Yeung AT (2012) Isobaric labeling and data normalization without requiring protein
621   quantitation. Journal of Biomolecular Techniques 23:11-23

622   Kimmel CB, Ballard WW, Kimmel SR, Ullmann B, Schilling TF (1995) Stages of embryonic development of the
623   zebrafish. Developmental Dynamics 203:253-310

624   Langley AR, Smith JC, Stemple DL, Harvey SA (2014) New insights into the maternal to zygotic transition.
625   Development 141:3834-3841

626   Lee MT, Bonneau AR, Takacs CM, Bazzini AA, DiVito KR, Fleming ES, Giraldez AJ (2013) Nanog, Pou5f1 and
627   SoxB1 activate zygotic gene expression during the maternal-to-zygotic transition. Nature 503:360-
628   364

629   Lee MT, Bonneau AR, Giraldez AJ (2014) Zygotic genome activation during the maternal-to-zygotic transition.
630   Annual review of Cell and Developmental Biology 30:581-613

631   Lei H, Oh SP, Okano M, Juttermann R, Goss KA, Jaenisch R, Li E (1996) De novo DNA cytosine methyltransferase
632   activities in mouse embryonic stem cells. Development 122:3195-3205

633   Li E, Bestor TH, Jaenisch R (1992) Targeted mutation of the DNA methyltransferase gene results in embryonic
634   lethality. Cell 69:915-926

635   Lin Q, Tan HT, Chung MCM (2019) Next generation proteomics for clinical biomarker detection using SWATH-
636   MS. In: Evans CA, Wright PC, Noirel J (eds) Mass Spectrometry of Proteins: Methods and Protocols.
637   Springer New York, New York, NY, p 3-15

638   Lin Z, Hsu PJ, Xing X, Fang J, Lu Z, Zou Q, Zhang K-J, Zhang X, Zhou Y, Zhang T (2017) Mettl3-/Mettl14-mediated
639   mRNA N 6-methyladenosine modulates murine spermatogenesis. Cell Research 27:1216-1230

640   Link V, Shevchenko A, Heisenberg C-P (2006) Proteomics of early zebrafish embryos. BMC Developmental
641   Biology 6:1-9

642   Liu J, Yue Y, Han D, Wang X, Fu Y, Zhang L, Jia G, Yu M, Lu Z, Deng X (2014) A METTL3–METTL14 complex
643   mediates mammalian nuclear RNA N 6-adenosine methylation. Nature Chemical Biology 10:93-95

644   Liu S, Li G, Li Q, Zhang Q, Zhuo L, Chen X, Zhai B, Sui X, Chen K, Xie T (2020) The roles and mechanisms of YTH
645   domain-containing proteins in cancer development and progression. American Journal of Cancer
646   Research 10:1068-1084

647 Lucitt MB, Price TS, Pizarro A, Wu W, Yocum AK, Seiler C, Pack MA, Blair IA, FitzGerald GA, Grosser T (2008)
648   Analysis of the zebrafish proteome during embryonic development. Molecular & Cellular Proteomics
649   7:981-994

650 Ma J, Svoboda P, Schultz RM, Stein P (2001) Regulation of zygotic gene activation in the preimplantation
651   mouse embryo: global activation and repression of gene expression. Biology of Reproduction
652   64:1713-1721

653 Mathavan S, Lee SG, Mak A, Miller LD, Murthy KRK, Govindarajan KR, Tong Y, Wu YL, Lam SH, Yang H (2005)
654   Transcriptome analysis of zebrafish embryogenesis using microarrays. PLoS Genetics 1:e29

655 Mattes B, Dang Y, Greicius G, Kaufmann LT, Prunsche B, Rosenbauer J, Stegmaier J, Mikut R, Özbek S, Nienhaus
656   GU, Schug A, Virshup DM, Scholpp S (2018) Wnt/PCP controls spreading of Wnt/β-catenin signals by
657   cytonemes in vertebrates. Elife 7:e36953

658 Mehjabin R, Xiong L, Huang R, Yang C, Chen G, He L, Liao L, Zhu Z, Wang Y (2019) Full-length transcriptome
659   sequencing and the discovery of new transcripts in the unfertilized eggs of zebrafish (*Danio rerio*).
660   G3: Genes, Genomes, Genetics 9:1831-1838

661 Mendieta-Serrano MA, Schnabel D, Lomelí H, Salas-Vidal E (2013) Cell proliferation patterns in early zebrafish
662   development. The Anatomical Record 296:759-773

663 Mi H, Huang X, Muruganujan A, Tang H, Mills C, Kang D, Thomas PD (2016) PANTHER version 11: expanded
664   annotation data from Gene Ontology and Reactome pathways, and data analysis tool enhancements.
665   Nucleic Acid Research 45:D183-D189

666 Mishima Y, Tomari Y (2016) Codon usage and 3′ UTR length determine maternal mRNA stability in zebrafish.
667   Molecular Cell 61:874-885

668 Muto M, Kanari Y, Kubo E, Takabe T, Kurihara T, Fujimori A, Tatsumi K (2002) Targeted disruption of Np95
669   gene renders murine embryonic stem cells hypersensitive to DNA damaging agents and DNA
670   replication blocks. Journal of Biological Chemistry 277:34549-34555

671 Newport J, Kirschner M (1982) A major developmental transition in early *Xenopus* embryos: II. Control of the
672   onset of transcription. Cell 30:687-696

673 Nudelman G, Frasca A, Kent B, Sadler KC, Sealfon SC, Walsh MJ, Zaslavsky E (2018) High resolution annotation
674   of zebrafish transcriptome using long-read sequencing. Genome Research 28:1415-1425

675 Okuda Y, Ogura E, Kondoh H, Kamachi Y (2010) B1 SOX coordinate cell specification with patterning and
676   morphogenesis in the early zebrafish embryo. PLoS Genetics 6:e1000936

677 Onichtchouk D, Geier F, Polok B, Messerschmidt DM, Mössner R, Wendik B, Song S, Taylor V, Timmer J, Driever
678   W (2010) Zebrafish Pou5f1-dependent transcriptional networks in temporal control of early
679   development. Molecular Systems Biology 6:354

680 Onichtchouk D (2012) Pou5f1/oct4 in pluripotency control: Insights from zebrafish. Genesis 50:75-85

681 Onichtchouk D, Driever W (2016) Zygotic genome activators, developmental timing, and pluripotency. Current
682   Topics in Developmental Biology 116:273-297

683   Paranjpe SS, Veenstra GJC (2015) Establishing pluripotency in early development. Biochimica et Biophysica
684   Acta (BBA)-Gene Regulatory Mechanisms 1849:626-636

685   Pelegri F (2003) Maternal factors in zebrafish development. Developmental dynamics: an official publication
686   of the American Association of Anatomists 228:535-554

687   Purushothaman K, Das PP, Presslauer C, Lim TK, Johansen SD, Lin Q, Babiak I (2019) Proteomics analysis of
688   early developmental stages of zebrafish embryos. International Journal of Molecular Sciences
689   20:6359

690   Pyati UJ, Webb AE, Kimelman D (2005) Transgenic zebrafish reveal stage-specific roles for Bmp signaling in
691   ventral and posterior mesoderm development. Development 132:2333-2343

692   Rahlouni F, Szarka S, Shulaev V, Prokai L (2015) A survey of the impact of deyolking on biological processes
693   covered by shotgun proteomic analyses of zebrafish embryos. Zebrafish 12:398-407

694   Rai K, Nadauld LD, Chidester S, Manos EJ, James SR, Karpf AR, Cairns BR, Jones DA (2006) Zebra fish Dnmt1
695   and Suv39h1 regulate organ-specific terminal differentiation during development. Molecular and
696   Cellular Biology 26:7077-7085

697   Rock KL, Gramm C, Rothstein L, Clark K, Stein R, Dick L, Hwang D, Goldberg AL (1994) Inhibitors of the
698   proteasome block the degradation of most cell proteins and the generation of peptides presented
699   on MHC class I molecules. Cell 78:761-771

700   Saftig P, Klumperman J (2009) Lysosome biogenesis and lysosomal membrane proteins: trafficking meets
701   function. Nature Reviews Molecular Cell Biology 10:623-635

702   Schmid B, Fürthauer M, Connors SA, Trout J, Thisse B, Thisse C, Mullins MC (2000) Equivalent genetic roles for
703   bmp7/snailhouse and bmp2b/swirl in dorsoventral pattern formation. Development 127:957-967

704   Schwanhäusser B, Wolf J, Selbach M, Busse D (2013) Synthesis and degradation jointly determine the
705   responsiveness of the cellular proteome. Bioessays 35:597-601

706   Sharif J, Muto M, Takebayashi S-i, Suetake I, Iwamatsu A, Endo TA, Shinga J, Mizutani-Koseki Y, Toyoda T,
707   Okamura K (2007) The SRA protein Np95 mediates epigenetic inheritance by recruiting Dnmt1 to
708   methylated DNA. Nature 450:908-912

709   Shilov IV, Seymour SL, Patel AA, Loboda A, Tang WH, Keating SP, Hunter CL, Nuwaysir LM, Schaeffer DA (2007)
710   The paragon algorithm, a next generation search engine that uses sequence temperature values and
711   feature probabilities to identify peptides from tandem mass spectra. Molecular & Cellular Proteomics
712   6:1638-1655

713   Smits AH, Lindeboom RG, Perino M, van Heeringen SJ, Veenstra GJ, Vermeulen M (2014) Global absolute
714   quantification reveals tight regulation of protein expression in single Xenopus eggs. Nucleic Acids Res
715   42:9880-9891

716   Tang WH, Shilov IV, Seymour SL (2008) Nonlinear Fitting Method for Determining Local False Discovery Rates
717   from Decoy Database Searches. Journal of Proteome Research 7:3661-3667

718   Tatusov RL, Galperin MY, Natale DA, Koonin EV (2000) The COG database: a tool for genome-scale analysis of
719   protein functions and evolution. Nucleic Acids Research 28:33-36

720 Tay TL, Lin Q, Seow TK, Tan KH, Hew CL, Gong Z (2006) Proteomic analysis of protein profiles during early
721   development of the zebrafish, *Danio rerio*. Proteomics 6:3176-3188

722 Tittle RK, Sze R, Ng A, Nuckels RJ, Swartz ME, Anderson RM, Bosch J, Stainier DY, Eberhart JK, Gross JM (2011)
723   Uhrf1 and Dnmt1 are required for development and maintenance of the zebrafish lens.
724   Developmental Biology 350:50-63

725 Tsukamoto S, Hara T, Yamamoto A, Ohta Y, Wada A, Ishida Y, Kito S, Nishikawa T, Minami N, Sato K, Kokubo T
726   (2013) Functional analysis of lysosomes during mouse preimplantation embryo development. The
727   Journal of Reproduction and Development 59:33-39

728 Tu S, Chi NC (2012) Zebrafish models in cardiac development and congenital heart birth defects.
729   Differentiation 84:4-16

730 Veil M, Yampolsky LY, Grüning B, Onichtchouk D (2019) Pou5f3, SoxB1, and Nanog remodel chromatin on high
731   nucleosome affinity regions at zygotic genome activation. Genome Research 29:383-395

732 White RJ, Collins JE, Sealy IM, Wali N, Dooley CM, Digby Z, Stemple DL, Murphy DN, Billis K, Hourlier T (2017)
733   A high-resolution mRNA expression time course of embryonic development in zebrafish. Elife
734   6:e30860

735 Winata CL, Łapiński M, Pryszcz L, Vaz C, bin Ismail MH, Nama S, Hajan HS, Lee SGP, Korzh V, Sampath P (2018)
736   Cytoplasmic polyadenylation-mediated translational control of maternal mRNAs directs maternal-to-
737   zygotic transition. Development 145

738 Xia H, Zhong C, Wu X, Chen J, Tao B, Xia X, Shi M, Zhu Z, Trudeau VL, Hu W (2018) Mettl3 mutation disrupts
739   gamete maturation and reduces fertility in zebrafish. Genetics 208:729-743

740 Xu C, Fan ZP, Müller P, Fogley R, DiBiase A, Trompouki E, Unternaehrer J, Xiong F, Torregroza I, Evans T (2012)
741   Nanog-like regulates endoderm formation through the Mxtx2-Nodal pathway. Developmental Cell
742   22:625-638

743 Xu K, Yang Y, Feng G-H, Sun B-F, Chen J-Q, Li Y-F, Chen Y-S, Zhang X-X, Wang C-X, Jiang L-Y (2017) Mettl3-
744   mediated m 6 A regulates spermatogonial differentiation and meiosis initiation. Cell Research
745   27:1100-1114

746 Yeh CW, Kao SH, Cheng YC, Hsu LS (2013) Knockdown of cyclin-dependent kinase 10 (cdk10) gene impairs
747   neural progenitor survival via modulation of raf1a gene expression. Journal of Biological Chemistry
748   288:27927-27939

749 Yin A, Korzh S, Winata CL, Korzh V, Gong Z (2011) Wnt signaling is required for early development of zebrafish
750   swimbladder. PloS One 6:e18431

751 Yoon K-J, Ringeling FR, Vissers C, Jacob F, Pokrass M, Jimenez-Cyrus D, Su Y, Kim N-S, Zhu Y, Zheng L (2017)
752   Temporal control of mammalian cortical neurogenesis by m6A methylation. Cell 171:877-889. e817

753 Zaucker A, Kumari P, Sampath K (2020) Zebrafish embryogenesis – A framework to study regulatory RNA
754   elements in development and disease. Developmental Biology 457:172-180

755 Zhang C, Chen Y, Sun B, Wang L, Yang Y, Ma D, Lv J, Heng J, Ding Y, Xue Y (2017) m 6 A modulates
756   haematopoietic stem and progenitor cell specification. Nature 549:273-276

757   Zhang J, Lanham KA, Peterson RE, Heideman W, Li L (2010) Characterization of the adult zebrafish cardiac
758   proteome using online pH gradient strong cation exchange‐RP 2D LC coupled with ESI MS/MS.
759   Journal of Separation Science 33:1462-1471

760   Zhao BS, Roundtree IA, He C (2017a) Post-transcriptional gene regulation by mRNA modifications. Nature
761   reviews Molecular Cell Biology 18:31

762   Zhao BS, Wang X, Beadell AV, Lu Z, Shi H, Kuuspalu A, Ho RK, He C (2017b) m 6 A-dependent maternal mRNA
763   clearance facilitates zebrafish maternal-to-zygotic transition. Nature 542:475-478

764

765

766 **Table 1. List of KEGG pathways of enriched proteins in deyolked zebrafish embryos.**

Pathway Name	House-keeping	pre-MZT	MZT	post-MZT
map01100 Metabolic pathways	75	5	5	18
map04714 Thermogenesis	27	1	0	0
map03010 Ribosome	12	0	1	1
map00071 Fatty acid degradation	10	0	0	1
map04218 Cellular senescence	4	0	0	1
map04142 Lysosome	4	0	1	4
map03060 Protein export	3	0	0	1
map04110 Cell cycle	3	0	0	2
map04510 Focal adhesion	2	0	0	3
map03018 RNA degradation	2	0	1	1
map04141 Protein processing in endoplasmic reticulum	2	0	0	0
map04114 Oocyte meiosis	2	0	0	0
map04915 Estrogen signaling pathway	2	0	0	0
map04540 Gap junction	2	0	0	0
map04520 Adherens junction	2	0	0	0
map04514 Cell adhesion molecules	1	0	0	0
map04320 Dorso-ventral axis formation	1	0	0	0
map04120 Ubiquitin mediated proteolysis	1	1	0	5
map03013 RNA transport	1	1	1	4
map04530 Tight junction	1	0	0	0
map03020 RNA polymerase	1	0	0	0
map03050 Proteasome	0	0	2	0
map00982 - cytochrome P450	0	0	1	0
map03040 Spliceosome	0	0	0	6
map04621 NOD-like receptor signaling pathway	0	0	0	1
map04668 TNF signaling pathway	0	0	0	1
map04310 Wnt signaling pathway	0	0	0	2

767

768

Figure Legends

Figure 1. Total number of proteins identified in non-deyolked and deyolked zebrafish embryos across the developmental stages.

Figure 2. Protein dynamics linked to the early stages of zebrafish embryos. The samples were deyolked and the proteins were quantified using EMMOL method. The six functional groups of proteins were listed such as transcription factors, RNA polymerase II – related activity, m6A RNA, and 5mC DNA methylation. X-axis label indicated the developmental stages and y-axis shows the associated protein content.

Figure 3. EuKaryotic Orthologous Groups (KOG) functional classification of both the housekeeping and developmental phase-enriched proteins of zebrafish embryos. The results are from deyolked samples.

Figure 4. Significantly enriched Gene Ontology (GO) terms of the housekeeping proteins and phase-enriched proteins of zebrafish embryos. The results are from deyolked samples. Top five GO terms based on the protein numbers are shown. $P < 0.05$, and a false discovery rate (FDR) of <0.3**.** X-axis labels display the number of proteins linked to the GO terms shown in the Y-axis.

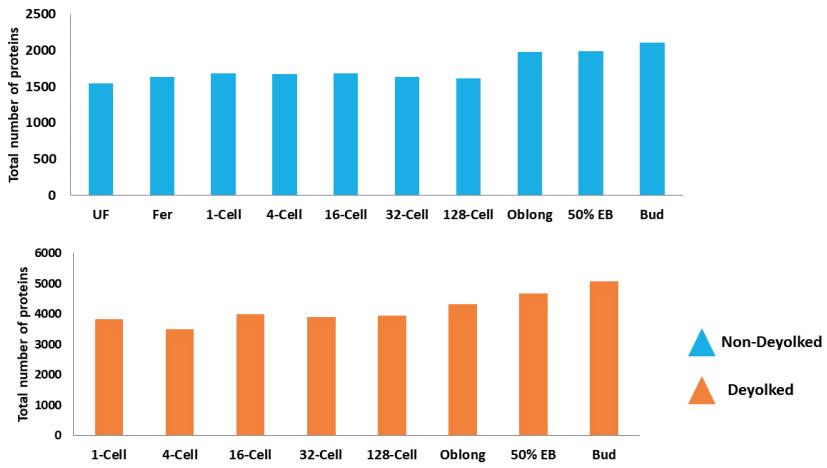**Figure 5**. **The summary of the selected functions of housekeeping proteins and phase-enriched proteins in zebrafish embryonic development.**   MZT: maternal-to-zygotic transition.

790   Figure 1

791

792

793

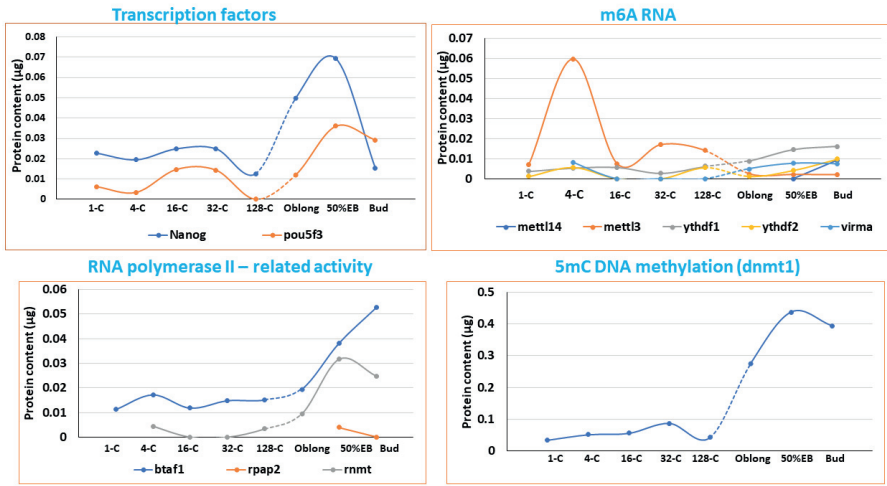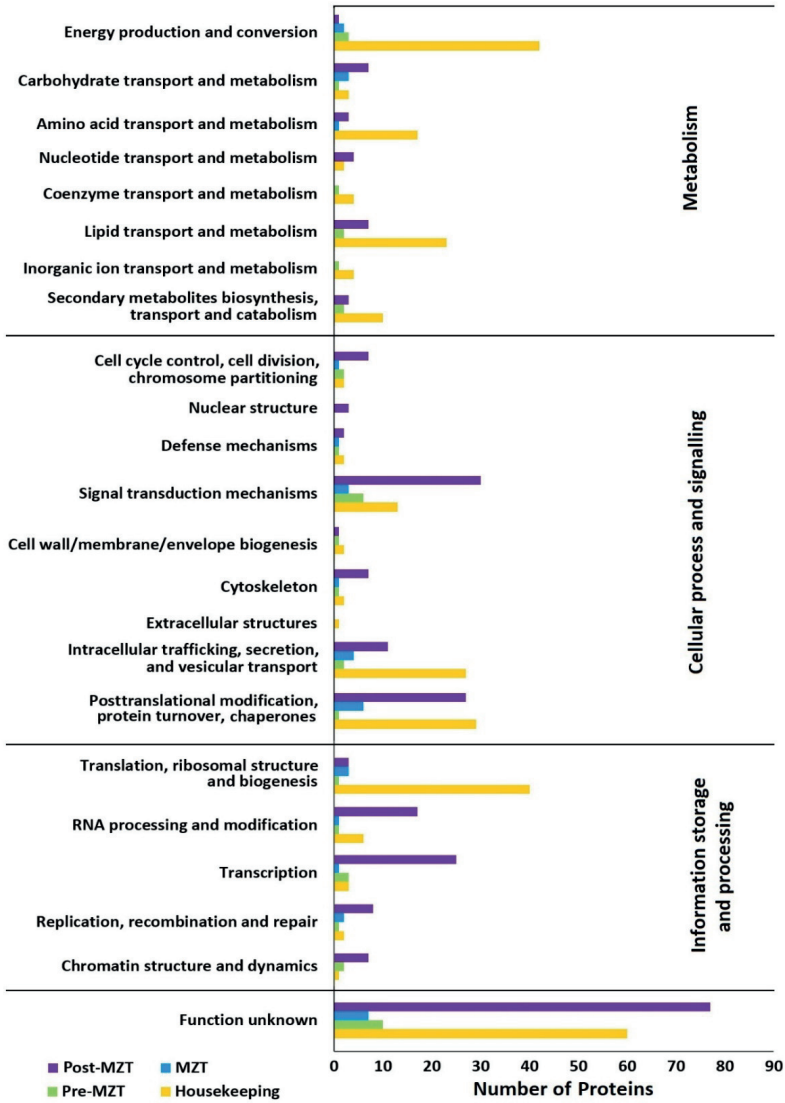794   Figure 2

795

796

797

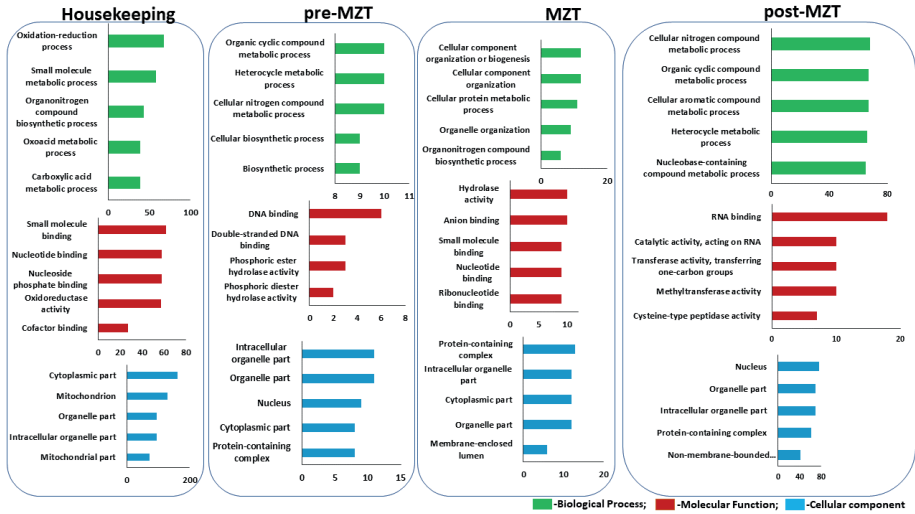　Figure 3

804

805

806

807

808

809

810

811

812

813

814
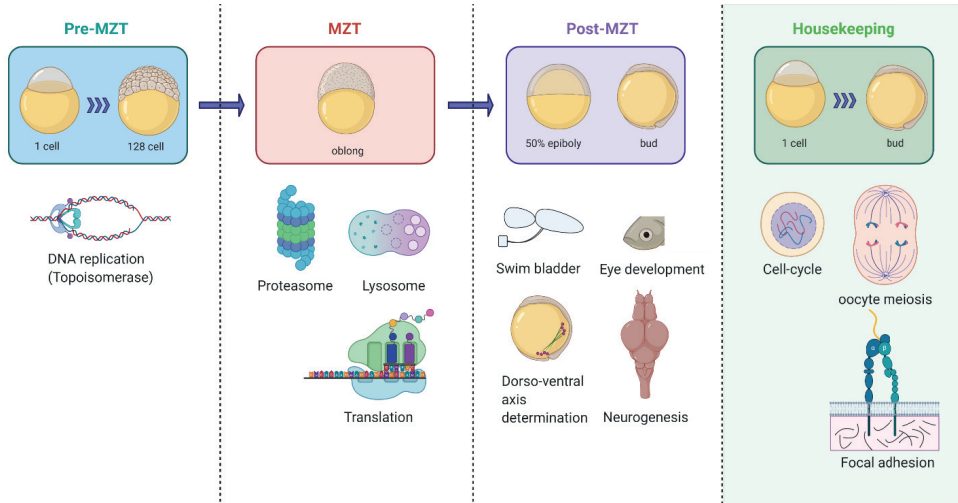
815

816

817

30

818   Figure 5

819

820

821

Supplementary Files

Supplementary Figure S1. Specificity and overlap of the identified proteins across the three detection methods. iTRAQ, shotgun and SWATH were the employed detection methods. Identified number of proteins from early embryonic development stages of both non-deyolked (ND) and deyolked (DY) samples.

Supplementary Figure S2. Overview of the number of differentially abundant proteins (DAPs) in stage-to-stage pairwise comparisons. DAP-: abundance significantly decreased, as compared to the preceding developmental stage (shared), or present only in the earlier of the two compared stages (unique). DAP+: abundance significantly increased, as compared to the preceding developmental stage (shared), or present only in the later of the two compared stages (unique). UF: unfertilized eggs; Fer: fertilized eggs; (explain other symbols related to developmental stages according to this pattern). The details are given in Material and Methods, "Unique or shared proteins, and differentially abundant proteins" section.

Supplementary Table S1. The amount of protein extracted from each stage of both non-deyolked and deyolked embryos.

Supplementary Table S2. List of functions linked to housekeeping proteins and proteins of the pre-MZT, MZT and post-MZT stages of zebrafish deyolked embryos.

Supplementary File S1. Information of iTRAQ tags employed for the different samples and the details of methodology used for protein validation in iTRAQ experiment.

Supplementary File S2. Complete list of proteins identified in the study. DY, deyolked samples; ND, non-deyolked samples; X, present; 0, absent; SG, shotgun. A, B and C indicate the replicates; 0 (zero) before A, B and C indicates the non-deyolked samples.

Supplementary File S3. The list of quantified proteins in the non-deyolked samples.

Supplementary File S4. The list of quantified proteins in the deyolked samples.

Supplementary File S5. The list of differentially abundant proteins (DAPs) in non-deyolked samples, stage-by stage pairwise comparisons. DAP-: abundance significantly decreased, as compared to the preceding developmental stage (shared), or present only in the earlier of the two compared stages (unique). DAP+: abundance significantly increased, as compared to the preceding developmental stage (shared), or present only in the later of the two compared stages (unique).

32

Supplementary File S6. The list of differentially abundant proteins (DAPs) in deyolked samples, stage-by stage pairwise comparisons. DAP-: abundance significantly decreased, as compared to the preceding developmental stage (shared), or present only in the earlier of the two compared stages (unique). DAP+: abundance significantly increased, as compared to the preceding developmental stage (shared), or present only in the later of the two compared stages (unique).

Supplementary File S7. The list of quantified proteins enriched in each developmental stage of deyolked samples such as housekeeping (proteins in all stages), pre-MZT, MZT and post-MZT stage.

Supplementary File S8. Gene ontology analyses of proteins from housekeeping, pre-MZT, MZT and post-MZT stage zebrafish deyolked embryos

Supplementary File S9. KOG functional classification of differentially abundant proteins (DAPs) across the development.

Supplementary File S10. KEGG pathways of differentially abundant proteins (DAPs) across the development.

Supplementary File S11. Gene ontology analyses of proteins with either significant decrease in abundance or absent in the later of the compared stages (DAP-); non-deyolked samples.

Supplementary File S12. Gene ontology analyses of proteins with either significant increase in abundance, or present only in the later of the compared stages (DAP+); non-deyolked samples.

Supplementary File S13. Gene ontology analyses of proteins with either significant decrease in abundance or absent in the later of the compared stages (DAP-); deyolked samples.

Supplementary File S14. Gene ontology analyses of proteins with either significant increase in abundance, or present only in the later of the compared stages (DAP+); deyolked samples.

Supplementary research data from the thesis of Purushothaman Kathiresan that could not be included in the thesis because of its large size can be made available upon request by contacting the PhD administration of the Faculty of Biosciences and Aquaculture.

List of previously published theses for PhD in Aquaculture / PhD in Aquatic Biosciences, Nord University

No. 1 (2011)
PhD in Aquaculture
Chris André Johnsen
Flesh quality and growth of farmed Atlantic salmon (*Salmo salar* L.) in relation to feed, feeding, smolt type and season
ISBN: 978-82-93165-00-2

No. 2 (2012)
PhD in Aquaculture
Jareeporn Ruangsri
Characterization of antimicrobial peptides in Atlantic cod
ISBN: 978-82-93165-01-9

No. 3 (2012)
PhD in Aquaculture
Muhammad Naveed Yousaf
Characterization of the cardiac pacemaker and pathological responses to cardiac diseases in Atlantic salmon (*Salmo salar* L.)
ISBN: 978-82-93165-02-6

No. 4 (2012)
PhD in Aquaculture
Carlos Frederico Ceccon Lanes
Comparative Studies on the quality of eggs and larvae from broodstocks of farmed and wild Atlantic cod
ISBN: 978-82-93165-03-3

No. 5 (2012)
PhD in Aquaculture
Arvind Sundaram
Understanding the specificity of the innate immune response in teleosts: Characterisation and differential expression of teleost-specific Toll-like receptors and microRNAs
ISBN: 978-82-93165-04-0

No. 6 (2012)
PhD in Aquaculture
Teshome Tilahun Bizuayehu
Characterization of microRNA during early ontogeny and sexual development of Atlantic halibut (*Hippoglossus hippoglossus* L.)
ISBN: 978-82-93165-05-7

No. 7 (2013)
PhD in Aquaculture
Binoy Rajan
Proteomic characterization of Atlantic cod skin mucosa – Emphasis on innate immunity and lectins
ISBN: 978-82-93165-06-04

No. 8 (2013)
PhD in Aquaculture
Anusha Krishanthi Shyamali Dhanasiri
Transport related stress in zebrafish: physiological responses and bioremediation
ISBN: 978-82-93165-07-1

No. 9 (2013)
PhD in Aquaculture
Martin Haugmo Iversen
Stress and its impact on animal welfare during commercial production of Atlantic salmon (*Salmo salar* L.)
ISBN: 978-82-93165-08-8

No. 10 (2013)
PhD in Aquatic Biosciences
Alexander Jüterbock
Climate change impact on the seaweed *Fucus serratus*, a key foundational species on North Atlantic rocky shores
ISBN: 978-82-93165-09-5

No. 11 (2014)
PhD in Aquatic Biosciences
Amod Kulkarni
Responses in the gut of black tiger shrimp *Penaeus monodon* to oral vaccine candidates against white spot disease
ISBN: 978-82-93165-10-1

No. 12 (2014)
PhD in Aquatic Biosciences
Carlo C. Lazado
Molecular basis of daily rhythmicity in fast skeletal muscle of Atlantic cod *(Gadus morhua)*
ISBN: 978-82-93165-11-8

No. 13 (2014)
PhD in Aquaculture
Joanna Babiak
Induced masculinization of Atlantic halibut (*Hippoglossus hippoglossus* L.): towards the goal of all-female production
ISBN: 978-82-93165-12-5

No. 14 (2015)
PhD in Aquaculture
Cecilia Campos Vargas
Production of triploid Atlantic cod: A comparative study of muscle growth dynamics and gut morphology
ISBN: 978-82-93165-13-2

No. 15 (2015)
PhD in Aquatic Biosciences
Irina Smolina
Calanus in the North Atlantic: species identification, stress response, and population genetic structure
ISBN: 978-82-93165-14-9

No. 16 (2016)
PhD in Aquatic Biosciences
Lokesh Jeppinamogeru
Microbiota of Atlantic salmon (*Salmo salar L.*), during their early and adult life
ISBN: 978-82-93165-15-6

No. 17 (2017)
PhD in Aquatic Biosciences
Christopher Edward Presslauer
Comparative and functional analysis of microRNAs during zebrafish gonadal development
ISBN: 978-82-93165-16-3

No. 18 (2017)
PhD in Aquatic Biosciences
Marc Jürgen Silberberger
Spatial scales of benthic ecosystems in the sub-Arctic Lofoten-Vesterålen region
ISBN: 978-82-93165-17-0

No. 19 (2017)
PhD in Aquatic Biosciences
Marvin Choquet
Combining ecological and molecular approaches to redefine the baseline knowledge of the genus Calanus in the North Atlantic and the Arctic Oceans
ISBN: 978-82-93165-18-7

No. 20 (2017)
PhD in Aquatic Biosciences
Torvald B. Egeland
Reproduction in Arctic charr – timing and the need for speed
ISBN: 978-82-93165-19-4

No. 21 (2017)
PhD in Aquatic Biosciences
Marina Espinasse
Interannual variability in key zooplankton species in the North-East Atlantic: an analysis based on abundance and phenology
ISBN: 978-82-93165-20-0

No. 22 (2018)
PhD in Aquatic Biosciences
Kanchana Bandara
Diel and seasonal vertical migrations of high-latitude zooplankton: knowledge gaps and a high-resolution bridge
ISBN: 978-82-93165-21-7

No. 23 (2018)
PhD in Aquatic Biosciences
Deepti Manjari Patel
Characterization of skin immune and stress factors of lumpfish, *Cyclopterus lumpus*
ISBN: 978-82-93165-21-7

No. 24 (2018)
PhD in Aquatic Biosciences
Prabhugouda Siriyappagouder
The intestinal mycobiota of zebrafish – community profiling and exploration of the impact of yeast exposure early in life
ISBN: 978-82-93165-23-1

No. 25 (2018)
PhD in Aquatic Biosciences
Tor Erik Jørgensen
Molecular and evolutionary characterization of the Atlantic cod mitochondrial genome
ISBN: 978-82-93165-24-8

No. 26 (2018)
PhD in Aquatic Biosciences
Yangyang Gong
Microalgae as feed ingredients for Atlantic salmon
ISBN: 978-82-93165-25-5

No. 27 (2018)
PhD in Aquatic Biosciences
Ove Nicolaisen
Approaches to optimize marine larvae production
ISBN: 978-82-93165-26-2

No. 28 (2019)
PhD in Aquatic Biosciences
Qirui Zhang
The effect of embryonic incubation temperature on the immune response of larval and adult zebrafish (*Danio rerio*)
ISBN: 978-82-93165-27-9

No. 29 (2019)
PhD in Aquatic Biosciences
Andrea Bozman
The structuring effects of light on the deep-water scyphozoan *Periphylla periphylla*
ISBN: 978-82-93165-28-6

No. 30 (2019)
PhD in Aquatic Biosciences
Helene Rønquist Knutsen
Growth and development of juvenile spotted wolffish (*Anarhichas minor*) fed microalgae incorporated diets
ISBN: 978-82-93165-29-3

No. 31 (2019)
PhD in Aquatic Biosciences
Shruti Gupta
Feed additives elicit changes in the structure of the intestinal bacterial community of Atlantic salmon
ISBN: 978-82-93165-30-9

No. 32 (2019)
PhD in Aquatic Biosciences
Peter Simon Claus Schulze
Phototrophic microalgal cultivation in cold and light-limited environments
ISBN: 978-82-93165-31-6

No. 33 (2019)
PhD in Aquatic Biosciences
Maja Karoline Viddal Hatlebakk
New insights into Calanus glacialis and C. finmarchicus distribution, life histories and physiology in high-latitude seas
ISBN: 978-82-93165-32-3

No. 34 (2019)
PhD in Aquatic Biosciences
Arseny Dubin
Exploration of an anglerfish genome
ISBN: 978-82-93165-33-0

No. 35 (2020)
PhD in Aquatic Biosciences
Florence Chandima Perera Willora Arachchilage
The potential of plant ingredients in diets of juvenile lumpfish (*Cyclopterus lumpus*)
ISBN: 978-82-93165-35-4

No. 36 (2020)
PhD in Aquatic Biosciences
Ioannis Konstantinidis
DNA hydroxymethylation and improved growth of Nile tilapia (*Oreochromis niloticus*) during domestication
ISBN: 978-82-93165-36-1

No. 37 (2021)
PhD in Aquatic Biosciences
Youngjin Park
Transcriptomic and cellular studies on the intestine of Atlantic salmon
Discovering intestinal macrophages using omic tools
ISBN: 978-82-93165-34-7

Zebrafish (*Danio rerio*) is a freshwater fish and an attractive model for human biology-related research. Set of proteins (proteome) in zebrafish is highly similar to that of human. Early embryonic development of zebrafish is driven by maternally provided factors, including proteins and RNA. However, there is a scarce information on this early embryonic proteome. The general objective of this PhD study was to identify and characterize the proteome of zebrafish embryos. We have employed various proteomic techniques, such as liquid chromatography mass spectrometry-based proteomics, isobaric tag for relative and absolute quantitation, shotgun, liquid chromatography–mass spectrometry, and sequential window acquisition of all theoretical mass spectra. We have developed an efficient procedure for reducing the amount of yolk in early zebrafish embryos to enable the effective identification of proteins. This is the first report on the successful identification and quantification of substantial number of proteins in very early stages of development (pre-maternal-to-zygotic transition stage) as well as proteins from the vegetal part of zebrafish embryos. Our analysis of developmental dynamics of proteins indicates that the maternal control of the early development is executed not only through translation of transcripts of maternal-effect genes but also by native maternal proteome. This study contributes to the understanding of the regulation of vertebrate early embryogenesis.